THESIS/
REPORTS
White,
J.D.

Application of Remote Sensing and Ecological Modeling Technolgies for Assessing Change in Landscapes Due to the Red Bench Fire

FINAL REPORT FOR RESEARCH AGREEMENT
#INT-89440-RJVA
The University of Montana
FS Contact: Kevin Ryan
Co-op Contact: Joseph White

FINAL REPORT

RESEARCH JOINT VENTURE AGREEMENT NO. INT-89440-RJVA

Application of Remote Sensing and Ecological Modeling Technologies for Assessing Change in Landscapes Due to the Red Bench Fire

by

Joseph D. White
Research Assistant, University of Montana

Kevin C. Ryan
Intermountain Fire Sciences Laboratory

and

Steven W. Running
Professor of Forestry, University of Montana

January 18, 1994

INTRODUCTION

During the 1988 fire season, wildfires burned thousands of forests throughout the western United States. Many of the fires burned large tracts of relatively inaccessible wilderness land administered by the National Park Service and the United States Forest Service. These fires burned through several vegetation types growing on a variety of sites. They left a mosaic of forest and meadow with varying severity of burn. Given the diversity of sites and fire treatment, there was a considerable range of effects on vegetation, soil, water, and wildlife. A considerable range of recovery rates can be expected for various resources on different sites. Managers are interested in the spatial distribution of these fires and their potential impacts on and off site. The size and remoteness of the 1988 fires make it difficult to assess effects on resource values using traditional methods.

Administration of wilderness fire management programs requires current knowledge of fuels and vegetation. Managers also need baseline data on the status of various wilderness resources and how these resources affect off-site values (e.g., water quality and quantity). When large-scale disturbances such as fire occur, managers need new techniques to rapidly assess resource changes, update resource inventories, and project future resource conditions. For example, during and after the 1988 fires, questions were raised about the affect of the fires on wildlife habitat, forest recovery, and water quality. Overall, managers lacked methods to quickly provide answers to these questions.

The 1988 fires provide us with an opportunity to develop techniques to map wilderness fire severity and assess its effects on the landscape. Given the return frequency of such fires, it is appropriate to develop technology that can be used on future fires. Remotely sensed data, geographical information systems (GIS), and ecological modeling are particularly useful for maintaining and updating data bases and understanding the role and outcome of large fires.

The 1988 Red Bench Fire in Glacier National Park and the Flathead National Forest provided

us with an ideal situation to study the use of satellite digital data and ecological models in fire research. In this paper, we outline the use of remote sensing data for 1) determining pre-fire vegetation communities, 2) developing a spectral model that differentiates burn severity classes, 3) input into an ecosystem model for understanding the effects of a fire on regional estimates of net primary productivity (NPP) and hydrologic outflow.

Background

Vegetation Mapping

Computer-aided classification of remote sensing information has become a standard tool for mapping vegetation across large areas (Iverson *et al.* 1989). Data from Landsat and airborne radiometers have been used to identify the species composition of various deciduous and coniferous forest ecosystems (Likens *et al.* 1982, Khorram and Katibah 1984, Benson and DeGloria 1985, Hughes *et al.* 1986, Skidmore 1989). Mayer and Fox (1981) discriminated lodgepole pine, ponderosa pine, and fir at a rate of 91% using Multispectral Scanner (MSS) data at the McCloud Ranger District near Mt. Shasta, California. Walsh (1980) mapped forests composed of lodgepole pine, ponderosa pine, white fir, shasta red fir, and mountain hemlock at Crater Lake National Park using classification of MSS data with an overall accuracy level of 88.8 percent. Moore and Bauer (1990) reported accuracies of 63-67% mapping various Minnesota conifer species such as red pine, jack pine, black spruce, white pine, and tamarack using the Landsat Thematic Mapper (TM). Shen *et al.* (1985) mapped the same species using TM simulator at 68 percent. The higher mapping performance of the studies using MSS over TM sensors is notable considering the refined spectral and spatial resolution of the TM sensors, however, this may be function of both the environmental conditions and spectral characteristics of those particular forest species.

Unsupervised classification of spectral data may be preferable when mapping large areas with a rugged terrain (Fleming *et al*, 1975). Terrain effects, expressed as topographic data, may be used to modify remote sensing classifications to map forested areas in which species are not easily distinguished spectrally (Skidmore 1989, Richards *et al.*, 1982, Cibula and Nyquist 1987). Bolstad and Lillesand (1992) mapped forest species between 73 and 89% by coupling TM data with soil and topographic data. Individual forest species were mapped at Lassen Volcanic National Park using a combination of Landsat TM data and topographic data to an overall accuracy level of 60 percent (White *et al. in press*).

Fire Severity

Ryan and Noste (1985) developed a classification system for qualifying fire severity, or the level of fire treatment, in wildland fires. The classification system provides physical descriptions for assessing the heat impact on over- and understory vegetation and soils within quadrat-type survey plots. They also provide guidelines for extending plot data to stand level areas. A body of research is emerging that indicates that short-term successional responses are related to stand species attributes and fire severity (c.f., Morgan 1984, Fischer, 1989). Dutton and Cooper (1988) used similar criteria to develop preliminary classification of fire severity in the 1988 Red Bench Fire. Sirucek and Shovic (Shovik 1988) used similar methods for mapping the severity of the 1988 fires in the Greater Yellowstone Area.

There are a number of significant questions to answer while investigating the use of satellite data for fire severity mapping. First, what variation exists in spectral reflectance between burn severity and vegetative lifeforms? Jakubauskas *et al.* (1990) found that burn severity was detected differently among conifers, deciduous trees, and shrubs based on the Landsat MSS spectral data as fire caused differences in re-vegetation patterns among these communities. The re-establishment of

vegetation is also very important as it relates to fire severity because in post-fire years, more severely burned areas have less vegetation cover and therefore different radiation budgets (Hall *et al.* 1980). Jakubauskas (1988) also used GIS technology to assess changes in spectral responses and vegetation classifications for three time periods. As expected, vegetative recovery was retarded on severely burned sites. Also, fire can have a significant effect on the reflective properties of the land surface due to vegetation removal, soil exposure, and soil color alteration making the observation of fire severity by spectral data possible (Jakubauskas *et al.* 1990, Milne, 1986).

Ecological Modeling

Ecological models provide a means of testing various assumptions about the effects of climate, topography, and disturbance on the ecological processing of carbon and water. Systems have been developed which incorporate models of climate, soil hydrology, and biogeochemical cycling in a geographical information system (Nemani *et al.* 1993). These types of systems provide a plausible alternative for investigating watershed and regional-scale ecosystem processes. These regional ecosystems models have been used for non-disturbed systems to determine the sensitivity of the models to various parameters associated with climate and hydrology (Running *et al.* 1989, Running and Nemani 1991, Band 1993). In a disturbed landscape, such as those affected by fire, models must incorporate landcover changes as these occur over space and time. Simulation of individual biomes have been done in which same biogeochemical process models are used with biome-specific parameters (Running and Hunt, 1993), but these have not been incorporated into regional models.

METHODOLOGY

Study Area

The Red Bench Fire of 1988 covered approximately 15,400 ha of Glacier National Park and the Flathead National Forest. Roughly three-fourths of the fire was in Glacier Park (Dutton and Cooper 1988). The fire burned from the river bottom at 1,100 m elevation to area in excess of 1,500 m. Vegetation types affected by the fire include riparian shrubs, sedge meadows, and various conifer forest types. The burned area is located on the west side of the park (T35N R20 & 21W) adjacent to the North Fork of the Flathead River. This area is included in the data for Landsat-5 Path 41, Row 26.

Pre-Fire Vegetation Map

Vegetation Classification

Different approaches were considered for devising a classification scheme which best characterized the North Fork vegetation. ECODATA plot data for the study area were obtained from the Region 1 Office of the Forest Service which were summarized into major environmental and vegetation components (Appendix 1). These data were subjected to a series of analyses such as hierarchical canonical classification and principal component analyses (Wilkinson, 1986). While these efforts provided an abundance of information regarding the diversity of communities, no simple unifying classification was derived. The original objectives of the project stated that a Küchler-type classification would be used, i.e. species groups such as mixed conifer, fire-spruce, etc. Küchler (1988) describes the purpose of vegetation mapping as a basis for scientific discovery. The map becomes the object for understanding the phenomena of organization of vegetation communities. In this study, we were interested in broadly describing the plant communities which existed before the Red Bench fire. A floristic classification was derived from the Glacier View

Ranger District of the Flathead National Forest forest type map. The level of specific description of this map corresponds well with Küchler's (1967b) map of the vegetation of the U.S. These floristic categories were *Abla lasiocarpa* - *Picea spp.* mix (subalpine fir - spruce, ABLA-PIEN), *Pinus albicaulis* (white-bark pine, PIAL), *Pseudotsuga menziesii* - *Larix occidentalis* mix (Douglas fir - western larch, PSME-LAOC), *P. contorta* (lodgepole pine, PICO), deciduous mix (*Populus spp.*, *Betula paperifera*), and shrub-meadow. Other landscape features such as bare ground, water, and ice were also included in this classification.

Spectral Classification

An August 28, 1988, Landsat TM scene was obtained which included the North Fork drainage (Path 41, Row 26). A subset of the spectral data were georectified into Zone 12 UTM coordinates with 30 by 30m pixels using 20 ground control points (GCP) selected from landmarks on USGS 7½′ topographic maps. These GCPs were positioned towards the edge of the subset data to diminish errors associated with calculating the transformation matrix from GCPs that are too centrally located (ERDAS, 1991). A nearest-neighbor georectification procedure was used to maintain the integrity of the spectral data.

The reflective spectral bands of the TM data were converted into radiance values given by using the following:

$$L_i = G \cdot DN + O$$

where L_i is the radiance value in $W \cdot m^{2\,-1} \cdot sr^{-1}$, G is the gain, DN is the digital number from the satellite sensor, and O is the offset. The following gain and offset values were used for this calculation (Table 1). Atmospheric haze effects which decrease the spectral contrast due to brightening, especially in the shorter wavelength bands, were reduced using the "clear-lake" strategy

(Jensen, 1986). Band 6, the thermal IR band, was not processed and not used in any spectral analysis because of the 120 by 120m spatial resolution of this band and because the information of this band is redundant, where vegetation is concerned, with other TM spectral bands such as band 5 (Nemani and Running 1991).

Table 1 - Gain and offset values used for TM digital number conversion into radiance values (from Kleman and Alm 1989).

TM Band	Gain	Offset
1	0.041974	-0.0666
2	0.130451	-0.1573
3	0.064997	-0.1127
4	0.117052	-0.2329
5	0.027265	-0.0864
7	0.016922	-0.0511

Early in the study, we found that the pre-determined floristic categories were not separable by simple classification of the processed TM data. Also, we found that the overall, spectral separability of the forest species groups was limited (Figure 1). We reasoned that some spectral differentiation of the forest groups might be possible if the number of floristic groups were limited by the spatial distribution of these groups. The ECODATA plot data were graphed based on elevation, aspect, and slope (Figures 2 and 3) to show trends in topographic organization of the species groups. This analysis revealed that the North Fork forests show some sensitivity to these topographic variables. For instance, *Picea* and *P. contorta* forests tend to dominate low to mid-elevation sites which are flat. *P. albicualis* stands occur more frequently above an elevation of 1980 m. *P. menziesii* stands are unlikely to occur on northwest facing aspects, rather, they are more

likely to be found on southeast facing slopes in an elevation ranging from 1450 to 1830 m in which the elevation limit increases with slope. *L. occidentalis* type forests are found in similar topographically-defined habitats as *P. menziesii* except that larch also occurs in moderate frequency on northwest facing slopes below 1450 m on any slope.

Based on this information, we designed a spectral classification in which we: a) identified the natural spectral centers of the entire dataset, b) partitioned the spectral data into topographic zones, and c) used the spectral center information to drive a classification of each of the topographic regions. ISODATA (Iterative Self-Organizing Data Analysis Technique) is a multispectral classification algorithm offered in the ERDAS series of image processing programs which can be used to identify inherent clusters in a multi-band dataset (ERDAS 1991). The ISODATA program operates by randomly selecting cluster centers from multi-channel data and assigning members to the clusters based on the vector distance from these centers. As the name implies, this process is repeated over a number of trials until a user specified convergence level is achieved. The number of clusters identified can also be specified to increase or decrease the inclusiveness of the classification. In addition, the program outputs statistical information about each cluster which can be used as input into other classification procedures.

We ran the ISODATA classification on the entire 1988 TM data, setting the maximum number of clusters at 50 and the convergence level at 99 percent. The program only identified 33 individual clusters from this data. Based on this result, we argued that these 33 clusters represented the maximum separability of the spectral data. Any further division might be either artificial or random noise. This is important because we believe that maximum separability of vegetation types is present in these clusters. However, this differentiation is not adequate for our objectives. We conclude that we can use these clusters as training statistics for classification of topographically defined subsets of the spectral data to obtain some extra degree of vegetation type

differentiation.

Using the information derived from the topographic analysis of the ECODATA plot data, we defined five topographic regions to divide the spectral data. We described these areas as bottomland (B), north-west-low (NL), south-east-low (SL), north-south-mid-high (NSMH), and north-south-high (NSH). The elevation, slope, and aspect limits of these areas can be found in Table 2. Data are from the Flathead National Forest Supervisor's Office and were used to subdivide the spectral data into the defined regions based on the Table 2 criteria. The result was five separate spectral data sets.

The spectral clusters derived from the ISODATA cluster algorithm were used as statistical input for the second classification of the different subsets. MAXCLAS, an ERDAS maximum likelihood classifier, was used to classify each topographic spectral subset into 33 classes. In total,

Table 2 - Definition of topographic regions used to separate spectral data.

Topographic region	Elevation (m)	Aspect (deg)	Slope (deg)
B	$\leq$ 1450	any	$\leq$ 10
NL	$\leq$ 1450	$\leq$ 45 and $\geq$ 225	> 10
SL	$\leq$ 1450 to $\leq$ 1830*	> 45 and < 225	> 10
NSMH	> 1450 to < 1980	any	any
MH	$\geq$ 1980	any	any

* Upper limit of elevation increases linearly with slope.

165 different classes were defined, first based on spectral information and second on topography. The ECODATA plot data were compared with the classification data to ascertain whether or not the classes could be interpreted into the pre-determined vegetation categories. We determined that they could not. The total classification procedure did increase the potential for separability based on the number of different vegetation groups within each spectral class. An index of class to class

confusion was calculated using the following:

$$ARCE = \frac{1}{n_c} \sum \frac{| 1-a |}{n_p}$$

where *ARCE* is the average relative confusion error, n_c is the total number of classes, a is the number of vegetation groups per class, and n_p is total number of plots per class. The simple ISODATA classification had and ARCE score of 29% versus the topographically separated spectral classification with a score of 19%. This index is slightly biased because the average score will ultimately decrease if the number of classes increase while the number of plots remain constant. This process did, however, increase the number of classes from 33 to 165 while decreasing the number of possible groups that are represented by these spectral classes. This demonstrated that the overall classification separability increased when using the 165 topographic-spectral classes versus the 33 classes derived solely from the ISODATA classification.

Kessell's Topographic Gradient Model

As the spectral classification was shown to be insufficient for mapping the floristic classes, we chose to explore using a gradient model developed by Kessell (1979) as part of the classification. This model is an ordination of field data onto three axes: topographic moisture, elevation, and time since last burn. The benefits of using this model are that it is derived from an independent field sampling, the axis variables can be easily derived or input from available data in a GIS, and Kessell summarized his results in a series of nomograms which show gradations of relative cover for individual plant species for the North Fork area. Our strategy was to develop Kessell's model in a GIS environment in order to merge it with the spectral classification. The exact merger process will be described more fully later.

As we have stated, the Kessell model was based on three basic parameters: topographic

moisture, elevation, and time since last burn. The GIS derivation of these variables was easy for elevation and burn because these data were readily available from the Flathead National Forest and from the geographic data library of Glacier National Park. Building the topographic moisture data layer proved to be more of a challenge because Kessell never fully defined this variable in his writings on the model (Kessell 1979). On the x-axis of the nomograms, Kessell described 9 basic topographic positions which are bottomlands, ravines, draws, northeast and southwest sheltered slopes, northeast and southwest open slopes, and northeast and southwest ridges, peaks, and xeric flats. Translation of these positions into a GIS required that we consider defining these areas much in the same way a person would in the field. That is that we assimilated the decision making process that occurs in a field sampling situation into a digital representation of this process.

Bottomlands, ravines, and draws were defined by first deciding what stream order would best describe these three categories. Arbitrarily, we decided that stream orders of one were similar to the definition of a draw. Likewise, streams of orders two or three were considered ravines, and streams with orders equal to or greater than four were considered bottomland type streams. This first step was realized by organizing digitized hydrologic data from the Flathead National Forest and Glacier National Park into these three categories. Recognizing that the stream channel itself does not comprise the entire draw, ravine, or bottomland habitat, we developed a set of rules to define the explicit spatial extent of these topographic regions. We assumed that the stream habitat extends beyond the confines of the stream channel relative to the effect that the water table associated with the stream has on the water availability of the surrounding vegetation community (Gregory *et al.* 1991). We formalized this definition using the following equation:

$$\tan\alpha = \frac{2m}{d}$$

where α is the slope of the area around the stream, 2 m is the effective rooting depth, and d is the

distance from the stream. By substituting various slope values, we calculated the maximum distance from the stream where water would potentially penetrate the vadose zone as a result of the water table. We determined that at a constant 0° slope, water would inundate the vadose zone up to 700 m from the stream channel. At 1°, the stream would influence the water availability up to 200 m and at 2° the effects would be limited to 50 m from the stream. We did not calculate any slope values above 2° because of the 50 by 50 m spatial resolution of the topographic data. This means that if the slope next to the stream channel is greater than 2° then the pixel associated with this slope is not part of the stream habitat. The assumptions used in this calculation are only valid for a gaining stream as the water table for a losing stream could only be predicted from observation wells (Fetter 1988). In moist mountainous terrains such as the North Fork area, it is reasonable to assume that the streams are gaining. Finally, using the digitized stream data, slope data and the rules developed here, we defined the potential bottomland, ravine, and draw habitats.

The sheltered and open slopes were delineated using a combination of digital elevation and aspect data. Sheltered versus open slopes were defined as slope configurations of concave versus convex. In-house GRASS programs were used to derive the slope configuration from the digital elevation data. Then, aspect data were used to divide the resultant concave and convex slopes into northeast and southwest slopes. North-east aspects were defined as slopes with aspects $< 135°$ and $\geq 315°$.

The stream habitat layer and the slope layer were combined in which the stream habitats took precedence over the slopes. This process revealed that large areas were not defined by either layer. This is due to the presence of large flat areas with no aspect in the data and which are not in close proximity to stream channels. We reasoned by deduction that these areas could be defined as the xeric flats Kessell described. However, Kessell also defined peaks and ridges which are included in this drier topographic category. These areas did not become apparent as a result of the data layer

merger. Peaks and ridges were defined by digitizing the ridge lines using the digital elevation data. No underlying principle about the extent of the ridge habitat could be derived, therefore, we decided to arbitrarily assign the spatial extent of the ridge as 200 m from either side of the crest. Aspect data were used to divide the ridge habitats into north-east and south-west aspects. Xeric flats, which were defined as no aspect areas by default were redefined within the model as north-east aspects. By placing the xeric flat areas in the wetter class, we hoped to conservatively estimate the extent of the driest topographic moisture gradients.

All three layers, stream, slope, and ridge habitats, were merged to define the Kessell topographic moisture gradients. The elevation data were aggregated into 6 classes in which upper elevation limits were set at 1250, 1500, 1750, 2000, 2500, and 3000 m. The time since last burn geographic data were organized into four time intervals which consisted of 50, 90, 150, and > 150 years as designated by the Kessell model. Finally, the moisture gradient, elevation, and time since last burn data were combined to form a GIS file with 216 classes which increase in moisture, elevation, and burn time, respectively (Appendix 2).

Merger of the Spectral Classification and the Kessell Model

Merger of the classified Landsat data with the topographic gradient model was accomplished using a fuzzy logic approach (Schumucker 1984). In fuzzy logic, objects are assigned to a set in partial quantities. The "fraction of membership" to which an object belongs to a set can be based on some *a priori* relationship that the object has with the set. In our model, we used relative cover as a measure of the degree to which our spectral classes and topographic gradient classes belonged to the pre-determined vegetation categories.

Relative cover values were derived separately for the ECODATA and for Kessell's topographic gradient data. Cover values for forest and non-forest species in ECODATA were found

using the STRATA program of the ECOPAC series of programs (Keane *et al.* 1990). Cover values were summed for species in species groups (e.g. fir and spruce in the ABLA-PIEN group) and divided by the total cover of all species for each individual EDODATA plot. Then, the final relative cover value for each spectra class was found by taking the average relative cover of all ECODATA plots representing the respective spectral classes. Relative cover values for the topographic gradient data were taken directly from the nomograms (Kessell 1979) based on the specified moisture, elevation and time since burn for each species (Appendix 3). We discovered that the total relative cover for each topographic class was often either greater than or less than 100. This is due to our inaccurate interpretation of the gradient lines and the values we should have associated with each moisture/elevation/burn class. As we could not find a better way to interpret the nomograms, we accepted this inaccuracy. Relative cover was calculated for each floristic group by dividing the total relative cover for the members of the floristic group by the total relative cover for the topographic class. These calculations resulted in the production of two tables in which the floristic groups (objects) had relative cover values (set membership) for both spectral and Kessell's topographic classes (sets). For the spectral classification, this was a 165 by 5 matrix of cover values versus a 216 by 5 matrix for the Kessell model data.

The final vegetation map was produced by joining the spectral classification and topographic gradient maps as a function of the intersection of these two maps. An intersection of two groups in a fuzzy operation can be defined as the minimum value of membership of an object in either set (Schumucker 1984). An example of this operation is:

$$VegetationClass = SPEC \cap TOPO = MIN(SPEC,TOPO)$$

where the final set membership value for the vegetation group is based on the minimum relative cover value from the spectral (SPEC) and Kessell's topographic (TOPO) data. This operation was

calculated for each of the 6 vegetation groups for the entire drainage using a c-language program which we developed (Appendix 4). Dominant vegetation was assigned for 50 by 50m polygons based on the maximum final set membership between the six vegetation categories. Where no maximum occurred, i.e. the final membership value between two groups was equal, the polygon was assigned as mixed. Non-vegetation categories such as water, bare ground, etc., and the shrub-meadow category were derived exclusively from the spectral classification.

During the process of accumulating the relative cover values for the spectral and topographic classes, we recognized that some floristic groups tended to have greater representation than other groups. This tendency was especially true for ABLA-PIEN. As a result, when the fuzzy merger was calculated, the landscape was dominated heavily by this group. When field observations were compared with the fuzzy classification, the accuracy results showed high predictability only for the ABLA-PIEN group. Our own observations of the vegetation in the North Fork led us to believe that in fact the ABLA-PIEN group was over-represented in both the ECODATA and the Kessell model. We analyzed the ECODATA plot data and found that 44% of all plots were dominated by the ABLA-PIEN type. Of the 216 classes characterized by the Kessell model, 71% of these classes had higher relative cover for the ABLA-PIEN class than any other vegetation class. To ameliorate this discrepancy, we developed coefficients with which we reduced the overall cover values of the ABLA-PIEN type and increased the cover values for the PSME-LAOC and PICO groups within the merger calculation. We did not change the cover values for the PIAL and DECID groups as we assumed these groups to be a nominal component of all the North Fork forests.

The coefficients used to modify the cover values for the selected vegetation categories were found by selecting starting values which represented how much the cover values were over- or underestimated. Values were found by first taking the average relative cover value for all classes in the spectral and Kessell models for the ABLA-PIEN, PSME-LAOC, and PICO groups. Next, the

group with the highest cover value was divided by the values of the other two groups, thereby giving a ratio of representation of the various groups within the data used to develop both models. These values were then used as the starting coefficients. The rationale for this process was that all three forest groups were potentially equally distributed in the landscape but not in the field data used for the models. We then ran the merger process using the initialized coefficient values. Classification accuracy was tested using field data collected by Joseph D. White and Rick Ringleb during the summers of 1991-92 (Appendices 5 and 6). We then changed the coefficient values to increase model accuracy levels for the three selected categories (Table 3). This process resulted in reduction of classification accuracy of the ABLA-PIEN and PSME-LAOC groups in some instances but improved the accuracy level of the PICO group. Also, overall accuracy levels increased using this method.

The final pre-fire vegetation map was produced by using the coefficients which produced the best accuracy results for the three forest categories. This map was overlain with the non-vegetation and shrub-meadow classes derived from the spectral classification (Figure 4). These latter categories were considered static in the model/mapping scheme and, therefore, replaced the forest categories where overlap occurred. A final accuracy assessment was tallied including some shrub-meadow samples. The following map classes were not included in the final accuracy assessment due to lack of field information: PIAL, DECID, mix, bare ground, water, and snow/ice. Non-vegetation validation data may be acquired using aerial photo interpretation, however, the mapping of these classes appears to be fairly reasonable and the objectives of the study do not necessitate this level of detail.

Post-Fire Spectral Analysis

Satellite Data Processing

Table 3 - Example of coefficients used to modify the relative cover values for the spectral and Kessell models and the outcome in map accuracy.

Trial (#) (Species Group)	Spectral Model	Kessell Model	Accuracy (%)	Overall Accuracy
1				42.62
ABLA-PIEN	1.00	1.00	97.7	
PSME-LAOC	1.00	1.00	20.9	
PICO	1.00	1.00	0.0	
2				63.93
ABLA-PIEN	0.50	0.66	65.9	
PSME-LAOC	1.50	2.00	79.1	
PICO	1.50	2.00	42.9	
3				66.39
ABLA-PIEN	0.75	0.80	72.7	
PSME-LAOC	1.55	2.22	69.8	
PICO	1.75	4.00	54.3	
4				68.36
ABLA-PIEN	0.81	0.85	73.8	
PSME-LAOC	1.58	2.35	72.5	
PICO	1.80	5.00	57.1	

Landsat TM data from September 20, 1989 were obtained for investigating the effects, thermodynamic and ecological, of the fire on the vegetated landscape. These data were subsetted so as to include the Red Bench Fire area and a periphery of area outside the fire. These data were georectified using UTM control points from the 1988 TM data to help ensure image-to-image registration. The data were georectified using a nearest-neighbor technique with 30 by 30m pixel output. Data were converted to reflectance values using the following:

where R_i is reflectance, Es_i is the exoatmospheric solar irradiance values integrated for each TM bandwidth (Markham and Barker 1985), and θs is the incident solar zenith angle. This reflectance

$$R_i = \frac{\pi \cdot L_i}{Es_i \cdot \cos \theta_s}$$

term has been described as an "apparent reflectance" because it does not take into account atmospheric radiation contribution (Leprieur *et al.* 1988). Atmospheric haze was minimized using the "clear-lake" method as with the 1988 data after the reflectance values were calculated.

The 1989 data contained a large horizontal stripe with 10 lines of missing data. Unfortunately, this stripe passed through the northern section of the burn area. A c-program was written (Appendix 7) to help "fill-in" the missing data using data from the northern and southern lines adjacent to the stripe. Data were interpolated into the striped lines using an inverse distance weighted average technique (Isaaks and Srivastava 1989):

$$R_n = \frac{\sum_{i=0}^{n} \frac{1}{d_i} R_i}{\sum_{i=0}^{n} \frac{1}{d_i}}$$

where the radiance values within the stripe (R_n) were calculated by multiplying the inverse distance from the missing pixel to the reference pixel (d_i) times the radiance value of the reference pixel (R_i). Three pixels north and three south were used as reference to the missing pixel. This process created a pattern of radiance values across the stripe which maintained the general spatial pattern of the area in the north-south direction.

A September, 3, 1990 Landsat dataset were obtained to assess the changes in reflectance associated with regeneration following the fire. These data were processed in the same manner as the other satellite data. The 1989 and 1990 data were "normalized" to the 1988 data. This process was done to reduce differences between scenes due to atmospheric radiance contribution and sun angle differences. The "normalization" process consisted of building linear regression models with

reflectance values from each scene by band (Coppin and Bauer 1992). Fifteen points were chosen from outside the burn area which represented a range of reflectance values and landcover types encompassing water, bare ground, forests, and meadows. Regression coefficients (Table 4) from these models were used to calculate "normalized" reflectance values for 1989 and 1990. These new reflectance values were used to calculate percent changes between years by fire severity class. Percent change was calculated by the subtracting the reflectance value of the previous year minus the reflectance of the following year. This was divided by the reflectance value of the previous year to calculate percent change in reflectance of the following year. This analysis was done to emphasize trends in reflectance changes associated with differing fire effects.

Table 4 - Regression coefficients used to calculate reflectance values "normalized" to 1988 values using the linear regression model $y = mx + b$.

	1989			**1990**		
TM Band	m	b	r^2	m	b	r^2
1	1.993	-0.317	0.80	1.107	-0.020	0.95
2	1.675	-0.247	0.98	1.033	-0.011	0.90
3	1.419	-0.146	0.98	1.001	-0.000	0.88
4	0.735	-0.056	0.86	0.920	0.006	0.99
5	0.851	-0.086	0.98	1.079	-0.001	0.87
7	0.914	-0.048	0.93	1.171	-0.024	0.97

Fire Severity Map

A map of fire severity was produced by using field plots within the burn area as a reference to understand the relationship between fire effects on landcover characteristics and satellite spectral data.

In October of 1988, Barry Dutton and Steve Cooper were contracted by Glacier National

Table 5 - Dutton and Cooper fire severity classification scheme (after Ryan and Noste 1983).

Burn Severity	Litter	Soil	Fuel	Vegetation
light	not consumed	not altered	few small fuels consumed	some scorch, esp. shrubs
moderate	completely consumed	darkened w/ white ash	small fuels consumed	small diameter trees and shrubs killed
high	completely consumed	stability lost, reddish w/ white ash	small and medium fuels consumed	all vegetation killed, incl. rhizomes

Park to establish plots within the burn area. They established 36 permanent plots, sampling for pre-fire vegetation, habitat type, age class, and burn severity. Burn severity was derived from Ryan and Noste (1985) which Dutton and Cooper condensed into three main categories: light, moderate, and high (Table 5). Dutton and Cooper produced a map of burn severity by interpolating the results of their field sampling and some aerial photographic interpretation onto USGS 7½′ topographic maps.

We extracted the reflectance values of the pixels representing the location of the Dutton and Cooper sample sites. Also, four pixels, one from the adjacent north-south east-west directions were extracted for analysis. The adjacent reflectance values were used as a "windowing" technique to account for random errors associated with the satellite data (Conese *et al.* 1988). The reflectance values were compiled in a QuattroPro worksheet where we separated the values into populations based on Dutton and Cooper's burn designation.

Statistical analysis of the reflectance values were performed to determine which TM bands contained the most information regarding burn severity. Student's *t*-tests were used to determine the significant difference in reflectance values between burn severity classes (Table 6). This table demonstrates that only Band 7 has significantly different reflectance values between all severity classes. We found that by taking the maximum reflectance value of Band 5 and 7, we were able to

achieve greater *t* values which we interpreted as better separability between burn classes.

The maximum reflectance value of TM bands 5 and 7 were used in a spectral classification

Table 6 - Student's *t*-test for the TM Bands and band combinations by burn severity and vegetation community.

	TM Bands								
Test	**1**	**2**	**3**	**4**	**5**	**6**	**7**	**AVG 5,7**	**MAX 5,7**
Forest									
low v mod									
t	0.87	0.45	1.26	0.83	2.11	4.66	2.62	2.50	2.51
n = 88						*	*	*	*
low v hi									
t	3.98	7.41	5.65	4.91	5.98	5.43	5.34	5.73	6.09
n = 43	*	*	*	*	*	*	*	*	*
mod v hi									
t	4.32	3.13	1.98	3.54	3.23	2.37	3.21	3.33	3.53
n = 93	*	*		*	*		*	*	*
Riparian									
low v mod									
t	1.81	4.14	6.63	0.15	4.14	1.26	2.65	3.45	3.50
n = 33		*	*		*		*	*	*

* - Signifies statically significant difference in populations ($P<0.01$).

(ERDAS CLUSTR program) to map severity in the burn area. In an initial classification, we found that we were unable to identify the burn perimeter in the total image scene. Instead, the classification mapped burn areas in the same categories as bare ground, meadow, and clouds outside of the burn (Figure 5). Carl Key, Geographer for Glacier National Park, produced a burn severity map of the park side of the burn using aerial photos obtained shortly after the fire in 1988. Key interpreted severity similar to Dutton and Cooper with the exception that severity was determined based solely on fire effects in the vegetation canopy. For mapping purposes, we isolated digital TM data within the burn area by using the perimeter produced by the Key map. We then classified this

data to map burn severity classes only within the burn area.

Table 7. Euclidean distances between spectral classes and Dutton and Cooper fire severity classes for forested areas. (*-Indicates that classes changed to moderate fire severity class in final classification).

		Euclidean Distance			
		Severity			
Spectral Class	Spectral Class Reflectance	Low	Moderate	High	Severity Class
1	0.506	0.256	0.428	0.667	low
2	0.623	0.139	0.311	0.550	low
3	0.731	0.031	0.203	0.442	low
4	0.867	0.105	0.067	0.306	moderate
5	0.556	0.206	0.378	0.617	low
6	0.690	0.073	0.245	0.484	low
7	0.946	0.184	0.012	0.227	moderate
8	0.797	0.035	0.137	0.376	low
9	1.025	0.263	0.091	0.148	moderate
10	0.447	0.315	0.487	0.726	low
11*	1.163	0.040	0.229	0.010	high
12*	1.085	0.323	0.151	0.088	high
13	0.374	0.388	0.560	0.799	low
14	0.302	0.460	0.632	0.871	low
15	1.366	0.604	0.432	0.193	high
16	1.278	0.516	0.344	0.105	high
17	1.320	0.558	0.386	0.147	high
18	1.227	0.465	0.293	0.054	high
19	1.434	0.672	0.500	0.261	high
20	1.555	0.793	0.621	0.382	high
21	1.486	0.724	0.552	0.313	high
22	1.610	0.848	0.676	0.437	high
23	1.651	0.889	0.717	0.478	high
24	1.810	1.048	0.876	0.637	high
25	1.697	0.935	0.763	0.524	high
26	1.760	0.998	0.826	0.587	high
27	2.060	1.298	1.126	0.887	high
28	0.246	0.516	0.688	0.927	low
29	0.113	0.649	0.821	1.060	low
30	0.169	0.593	0.765	1.004	low

* Indicates that class changed to moderate in final classification.

The data were classified using the CLUSTR algorithm into 30 classes. The classes were initially interpreted into severity classes by calculating the Euclidean distance between the class mean reflectance and the mean reflectance of the Dutton and Cooper plots (Table 7). The Euclidean distance is the distance in spectral space between two vector values:

$$D_{ci} = \sqrt{\sum_{i=1}^{n} (s_c - \mu_i)^2}$$

where D_{ci} is the Euclidean distance between each spectral class and mean severity class reflectance value, s_c is the mean spectral class reflectance value, and μ_i is the mean severity class reflectance value (ERDAS 1991). Spectral classes were assigned to severity classes based on which class had the lowest Euclidean distance value. We modified these class interpretations by comparing our severity map to both the Dutton and Cooper and the Key maps. Agreement between Dutton and Cooper's, Key's, and our fire severity map was assessed by comparing 100 randomly selected points between their maps and our's to assess overall percent map-to-map correspondence. We changed different spectral class assignments iteratively to increase the map-to-map agreement until a maximum correspondence level was found and produced a digital burn severity map of the Red Bench Fire (Figure 6).

Ecological Modeling

Ecosystem Model

The Regional Hydro-Ecological Simulation System (RHESSys) (Nemani *et al.* 1992) was used to simulate NPP and hydrologic outflow for the area centered around the Red Bench Fire. RHESSys is a process model which simulates climate, hydrologic balance, and biogeochemical cycling within a GIS. Calculation of water and carbon fluxes occurs within the RHESSys framework using three models: 1) an ecological process model FOREST-BGC (Running and Coughlan 1988),

2) a terrain-sensitive, micro-climatological model MT-CLIM (Running *et al.* 1987), and 3) a topographically derived hydrologic model TOPMODEL (Bevin and Kirkby 1979). The RESSys paradigm is a simple linkage of these vegetation and climate models within a temporal context which is then applied to multiple landscape units (Running *et al.* 1989). The definition of these units is based on some geographic organizing principle which is an arbitrary decision on how the modeler wishes to arrange the landscape. In this study, we used hillslope partitions whose areal dimensions and arrangement were derived from a topographic analysis system, r.watershed in the GIS GRASS. The hillslope system reduces data variance and redundancy and promotes model computation efficiency.

To briefly describe RHESSys operation, daily climate is extrapolated to each partition unit from a base weather station. Maximum, minimum, and dewpoint temperatures are computed based on adiabatic lapse rates determined for the region. Partition temperatures are calculated by finding the difference between the partition mean elevation and the elevation of a known climate station and applying the lapse rate calculation. Minimum temperature is assumed to be equivalent with dewpoint temperature based on climatological observations in mountainous terrain (Glassy and Running *in press*). Precipitation is derived from an isohyet derived from area climatological observations. Incoming shortwave radiation is calculated using partition slope, aspect, and latitude (Garnier and Ohmura 1968) attenuated by atmospheric transmissivity calculated from the diurnal temperature amplitude (Bristow and Campbell 1984) to give site-specific incident solar radiation. Incoming partition precipitation becomes snowpack or soil water as a function of daily average temperature. RESSys utilizes a simple bucket-type model for the soil water compartment. The size of this bucket is determined by the mean soil water holding capacity (WHC) of the land unit.

Transpiration of available soil water is calculated using the Penman-Monteith equation. In this equation, plant-related evaporation is a function of vapor pressure deficit (VPD) and solar

radiation. Canopy conductance of water flux from canopy to atmosphere is derived from partition air temperature, incident radiation, VPD, and leaf water potential. Under these conditions, canopy conductance is reduced to cuticular conductance when either a) VPD is greater than 1.6 KPa, b) leaf water potential decreases below -1.65 MPa, or c) air temperatures are $< 0°C$. Leaf water potential is derived from a simple ratio of available soil water to WHC (Running and Coughlan 1988).

Photosynthesis is calculated by multiplying the atmosphere to mesophyll diffusion gradient of CO_2 times the canopy and mesophyll conductances. As canopy conductances are calculated based on water, a weighting factor of 1.6 is used to account for the difference in molecular weight between water and carbon dioxide. Mesophyll conductance is a function of temperature and radiation. There is an inverse parabolic relationship between mesophyll conductance and temperature with an optimum of 20°C, and high and low compensation points of 0°C and 40°C, respectively. Canopy radiation is calculated from Beers attenuation law using the term:

$$Q_c = Q_i(1 - e^{(-0.5 \cdot LAI)})$$

where Q_c ($kJ \cdot m^{-2} \cdot d^{-1}$) is canopy radiation, Q_i ($kJ \cdot m^{-2} \cdot d^{-1}$) is incident radiation, and LAI is projected or single-sided leaf area (dimensionless). The response of mesophyll conductance to light is asymptotic with half maximum photosynthesis at 9720 $kJ \cdot m^{-2} \cdot d^{-1}$. Plant maintenance respiration is calculated as an exponential function of average daily air temperature with a $Q_{10} = 2.3$ for stem and root biomass. Growth respiration is computed by taking 32% of photosynthate minus maintenance respiration costs (Running and Gower 1991). Carbon stores remaining are considered net primary productivity (NPP).

Hydrologic processes are modelled in Beven and Kirkby's (1979) TOPMODEL using topography and hydraulic properties of soils. In TOPMODEL, hydrologic processes are considered to be 'quasi-distributed' based on the following equation which aggregates areas into zones of a

hydrological similarity (topographic soils index, TSI):

$$TSI = \ln\left(\frac{a \cdot T_e}{\tan B \cdot T_i}\right)$$

where a is the area contributing to a downslope point by upslope points, T_e is the mean soil transmissivity of the hillslope or sub-catchment, T is the transmissivity of the downslope point, and β is the point slope value. Areas defined by this equation are considered to have similar hydrologic characteristics, thereby reducing the number of simulations per hillslope.

Outflow is calculated in TOPMODEL based on the following:

$$q_b = T_e \, e^{-\lambda} \, e^{-\frac{\bar{S}}{m}}$$

where q_b is outflow, λ is the hillslope mean TSI value, $\bar{S}$ is the deficit of soil water below saturation, and m is a term to describe the resistance of water flow with increasing soil depth. All terms of this equation are physically based except for the m-parameter which is difficult to derive in the field.

The "true" value of m is best approximated by running the model with different values. Modeled hydrograph data can be compared with observed hydrograph data for the same time period to determine which m value gives the better representation of timing and magnitude of outflow. However, parmaterization of the m value is difficult when disturbances such as fire affect sub-catchments. Observed outflow data used must be specific to the affected sub-catchments as these disturbances may cause localized effects in hydrologic outflow. Due to scarcity of hydrologic data for the North Fork watershed, we only had data from the USGS Columbia Falls gauging station (i.d.# 12355500, CD-ROM, Hydroshere, Inc., Boulder, CO) which is 30km downstream from the fire area. This station collects water outflow data for the entire North Fork of the Flathead, of

which, the Red Bench Fire affected approximately 4% of the watershed's entire area. Based on this information, we found the Columbia Falls data insufficient for determining the appropriate *m* value as hydrologic surges and descensions modeled for the fire-affected area were more extreme than those found in the data for the entire watershed due to the buffering effect of the relative area of the fire versus the watershed. Consequently, an *m* value of 0.05 was selected based on previous studies in nearby watersheds (Band 1993, White and Running *in press*).

The TOPMODEL component of RHESSys enhances the hydrologic process function of the model by maintaining baseflow during dry weather periods, buffering the effect on outflow by large precipitation events, and increasing the available soil water for PSN and ET. The available soil water is increased by dividing the soil compartment into saturated and unsaturated zones. This reduces the effect of losing soil water to outflow derived from meltwater or precipitation. Primary geographic database inputs for RHESSys are climate, vegetation, soils, and topography. Remote sensing data is used for determining regional vegetation characteristics, especially, lifeform and leaf area index (LAI). Lifeform, e.g. needle-leaf evergreen, needle-leaf deciduous, etc. is important for parameterizing the certain plant physiological variables, while LAI is important for modeling the rate of plant processes such as evapotranspiration, photosynthesis, and respiration.

Leaf Area Index

LAI may be derived from satellite data by correlating ground measurements of LAI with a ratio of near infrared to red wavelengths referred to as the normalized difference vegetation index (NDVI). The 1988 Landsat data were used to derive LAI values for forested areas using correlation coefficients previously derived for the area (Spanner *et al.* 1990). As a best guess, LAI for 1989 in the burned area was derived from correlating 1990 NDVI data with 1991 field estimates of LAI converted from biomass (Appendix 6). Biomass values were converted into LAI by converting

biomass values into units of carbon then calculating LAI by assuming a specific leaf area (SLA) for grasses (Running and Hunt 1993):

$$LAI = \left(Aboveground\ Dry\ Wieght\ Biomass \frac{kg\ CH_2O}{m^2} \cdot 0.4\ \frac{kg\ C}{1.0\ kg\ CH_2O} \right) \cdot 25.0\ \frac{m^2}{kg\ C}$$

where carbon is calculated from the ratio of C to CH_2O. A least-squares regression was performed with the 1991 LAI values and the 1990 TM-derived NDVI data (Figure 7). While it is generally not acceptable to develop least-squares regression models from non-paired data such as the non-synoptic NDVI-LAI data, the model was simply used to help scale the 1989 NDVI data into LAI estimates. The resultant range of LAI from this model was 0 to 2 which are reasonable LAI values for grasses (Weiser *et al.* 1986). LAI outside the burn area, which is primarily forest LAI, was assumed to have remained constant or changed very little, therefore, 1988 LAI values were re-used for 1989 simulations of forested areas.

Database Construction and Model Implementation

To simulate the occurrence of the fire during 1988, a fire progression map produced by Carl Key of Glacier National Park was used to remove LAI over the days of burning. We aggregated the burning time into five major periods to reduce computational complexity. These periods were: 1) the 6th and 7th, 2) the 8th, 3) the 9th, 4) the 10th through the 14th, and 5) the 16th and the 17th. In terms of modeling, this meant that LAI had to be dynamically removed during these time periods to simulate the effects on ecosystem processes as fire moves across the landscape. After the fire, LAI for the burn area was assumed to be near zero.

In 1989, the burn areas were assumed to have converted from a forested lifeform to a grassland. The modeling implications of this assumption were that LAI must be "turned on and off" to approximate the phenology of grass. We defined these on and off periods based on a 10-day

Table 8 - Comparison of physiological parameters changed for simulation of conifers versus grasses.

Variable	conifer	grass
Stem Carbon ($kg \cdot m^2$)	5.000	0.005
Maximum Canopy Conductance (m $H_2O \cdot s^{-1}$)	0.0016	0.0050
Critical Leaf Water Potential (-MPa)	1.65	3.5
Maximum Mesophyll Conductance (m $CO_2 \cdot s^{-1}$)	0.0008	0.0016
Leaf Respiration Coefficient (kg $C \cdot day^{-1} \cdot kg^{-1}$)	0.00015	0.003
Root Respiration Coefficient (kg $C \cdot day^{-1} \cdot kg^{-1}$)	0.0002	0.0003
Q_{10} Constant for Exponential Respiration	0.085	0.083
Leaf N Concentration Fraction	0.015	0.044

average minimum night temperature. If the average night temperatures over 10 days was greater than 0° C leaves were on and vice versa. By this definition, it was possible for leaves to suddenly appear during winter, however, water and radiation limitations would reduce any photosynthesis to a nominal amount. Also, several physiological variables in the FOREST-BGC model had to be adjusted to better simulate the grass physiology (Running and Hunt 1993) (Table 8).

Digital elevation data at 50 m and 1.1 km scales were analyzed to derive slope and aspect values. The 50 m data were obtained from a sub-sampling of Defense Mapping Agency (DMA). The 50 m data were used to derive 18 unique hillslopes using the terrain analysis algorithm.

The 50 m data were combined with soils data were also used to create a map of the TSI for the hydrologic sub-model for RHESSys. Soils data were derived from the STATSGO database, a digital form of a 1:250,000 scale map of the major soils units of the state of Montana. Seven soil units were represented in the STATSGO data for the Red Bench Fire area. Water holding capacities were found for these units ranging from 5 to 21 cm. Soil surface texture was used to approximate soil hydraulic conductivity. Transmissivity values were estimated using soil depth values from a soils map of the Red Bench Fire area (Dutton 1990). Transmissivity values ranged from 0.1 to 13.5

cm^2/s which are reasonable values for glacial outwash soils (Fetter, 1988).

Climate data for 1988 and 1989 were obtained for the National Weather Service (NWS) station at Polebridge, Montana. This data contained daily minimum and maximum temperatures (°C) and precipitation (cm).

Spherical means of elevation, slope, aspect, soil WHC, LAI, and area of each hillslope were assembled into a summary file. These variables are important for the climate and physiology portions of both models. As most of the hillslopes defined for the study area had topographic gradients ranging from valley bottom to ridge, we adjusted the mean elevation for each hillslope by an increase of 10 percent. This was done because we found that from early simulations the study area had much less available water relative to the entire watershed. Mean TSI values were also calculated for the 18 hillslopes as part of the specialized RHESSys hydrologic sub-model. These files were then used as input for the process models.

NPP values for the region were calculated from the model outputs of photosynthesis and respiration. Also, hydrologic outflow was calculated by the model. The outflow data were compared with USGS North Fork stream gauge data from Columbia Falls (i.d. # 12355500, CD-ROM, Hydroshere, Inc., Boulder, CO) and Tuchuck Creek near Flathead, British Columbia international station (i.d. # 12355150, CD-ROM, Hydroshere, Inc., Boulder, CO) to determine possible hydrologic consequences of the fire and post-fire recovery on the water balances of the disturbed landscape. The Tuchuck Station is located 30 km north and upstream of the burn area. Residual error values ($\hat{E}$) (Kleinbaum *et al.* 1988):

$$\hat{E} = observed - modeled$$

of observed versus modeled outflow and Columbia Falls and Tuchuck stations and the Columbia Falls versus Tuchuck stations were calculated to discriminate fire-caused disturbance influence in

hydrologic outflow from climatological differences.

RESULTS AND DISCUSSION

Pre-fire Vegetation Map

The methodology we've presented in this study on how these data were integrated is unique because we have demonstrated the applied use of mapping through fuzzy set theory using our understanding of the limitations of satellite and geographic-based data models. In the development of this mapping process, we have seen how both the satellite data and the Kessell model provided partial information regarding the distribution of forest types in the North Fork area. The satellite data were useful for understanding the limited radiometric differences between forest types. The Kessell model, alternatively, was important for understanding the theoretical spatial definition of the forest types. The intersection logic used in the fuzzy merger of these data was an attempt to emphasize the strengths of the combination of the two data models. We experimented with other logic operators such as the set union where, for example:

$$ABLA\text{-}PIEN = SPEC \cup TOPO = MAX(SPEC,TOPO)$$

in which the mapping value for the ABLA-PIEN group is based on the maximum relative cover value between the spectral and Kessell model. This type of operation tended to over-emphasize mapping of certain forest groups despite the weighting coefficients. The overall mapping proficiency of this type of operation was low compared to the intersection method. We believe this is a result of the mapping process being influenced by the individual strengths of the spectral and Kessell models rather than the combined information resulting from the overlap of both models. This is a rational conclusion given that we found that neither model provided sufficient mapping information for the defined forest groups.

The results of our analysis of the pre-fire vegetation map indicate an overall mapping

accuracy of 70% percent of selected communities. Table 9 illustrates that a wide range of accuracy exists among different communities. These communities were selected over others because of limited field information available on other communities in the area. For instance, a sizeable stand of *P. ponderosa* existed in the pre-fire vegetation near the Polebridge Range Station in Glacier National Park. We could not find ready field data on this stand, so it was excluded from our analysis. Kessell (1979) mentions the occurrence of such stands in his descriptions but considers them nominal components of the North Fork landscape. Also, stands of alpine larch, *L. lyallii*, are also found in the North Fork drainage, but again, no data were found and Kessell describes these stands as highly localized. The objective of this study was to provide a general map of the forest communities in the North Fork. Detailed mapping of vegetation communities with limited spatial distribution may require more detailed ecological and digital information.

Table 9 - Error matrix with ground versus classified data for pre-fire vegetation map.

	GROUND DATA			
CLASSIFIED DATA	A-P	P-L	P	S/m
ABLA-PIEN (**A-P**)	31	5	4	1
PSME-LAOC (**P-L**)	11	29	11	0
PICO (**P**)	0	6	20	1
Shrub/meadow (**S/m**)	1	2	0	16
Accuracy (%)	72	69	57	89

The tradeoff between accuracy levels for individual categories over overall accuracy demonstrated in the development of the merger coefficients brings up the question of representative sampling. The rationale for using the coefficients was prompted by the observation that the ABLA-PIEN group excessively dominates Kessell's and the ECODATA data. This judgement was based

on a) the fact that the realization of Kessell's model in the present landscape would result in forests dominated by the ABLA-PIEN group which are not supported by b) current observation of the North Fork forests. However, what we imply by "observation" is that several people have the same notion about the overall composition of the forests which is not supported by empirical data. Therefore, we can not say for certain whether the data we used to assess accuracy and help develop the coefficients were representative. If, for instance, we over-sampled the PICO community, then classification errors associated with this group would influence the overall accuracy. We could increase the overall accuracy by moderating the number of points used for the accuracy assessment. That is to say, by making the number of points used per category relative to some assumed distribution of the areal extent of the forests, the influence of inaccurately mapped categories such as PICO becomes minimized in the assessment of overall accuracy. This is important to consider if the objective of the mapping process is to identify trends of the spatially dominating features of the landscape or to map unique land cover classes. In this study, we found that mapping the PICO communities to any degree of accuracy required a reduction in accuracy of the ABLA-PIEN and PSME-LAOC groups.

The purpose of this study was to identify spatial trends which are important to the fire ecology of this landscape. Based on this objective, we believe the adjustments made in mapping accuracy were justified. This is a presumption that increased mapping knowledge of certain forest types such as the PICO stand are important enough to reduce the mapping resolution of the other forest categories. PICO stands below 2300 m are adapted for high-frequency (50-100 yrs), stand-replacing fires (Fischer and Bradley 1987). Also, the degree of Mountain pine beetle, *Dendroctonus ponderosae*, infestation may be linked to the role of fire where PICO stands are either seral or climax. As fire is a significant function in lodgepole pine ecology, mapping these stands accurately is important for understanding the role of fire in the North Fork landscape.

The 70% map accuracy achieved in this study can be improved by understanding of the assumptions of the Kessell model and translating these assumptions into the digital database. The return interval of fire in Kessell's model is an important aspect in modeling succession of vegetation communities over time. Kessell does not, however, address the effects of varying types of fire on successional pathways. In Kessell's model, a singular non-specific fire event will have a probabilistic successional outcome. In reality, different types of fire will determine the communities development. The consequence of low versus a high severity fire may be completely different in terms of stand structure and composition (Fischer and Bradley 1987). Kessell's model may be improved by stratifying the fire return interval into fire severity types which in turn would better reflect current understanding of fire's role in forest succession.

The topographic moisture gradient presented in Kessell's model is difficult to interpret empirically as it is only described qualitatively by Kessell (1979). As a result, errors in applying the model result due this interpretative process. In an effort to reduce these errors, we used Beven and Kirkby's (1979) TOPMODEL as a surrogate for Kessell's definition of potential soil moisture. This resulted in map accuracies which were < 60 percent. We concluded that while our digital representation of the topographic moisture gradient was inaccurate, it maintained the intent of Kessell's interpretation of topographic features.

Post-Fire Spectral Analysis

Satellite data are useful for understanding what effect fire has on a forest because mid- and far-IR spectral wavelengths are more sensitive to the degree of landcover changes outlined in Table 5. The relationship we established between TM bands 5 and 7 and fire severity was expected given that these bands have been shown to be sensitive to sparse vegetation cover (Butera 1986), soil

exposure (Ezra *et al.* 1984), and geochemical alteration of soils (Jensen 1986). We anticipated that this relationship was based solely on the immediate effects of the fire on the vegetation communities, however, a full year passed between the fire and the date of the satellite data used for this analysis. During this period, vegetative regeneration occurred which must be included in our evaluation of the relationship between the spectral and severity data. Fire severity greatly influenced the plant communities ability to re-sprout or seed, degree of canopy degeneration due to cambium and crown scorch, and biophysical environment for plants to re-establish. As a result, the spectral response to fire severity is partly based on the effect of the fire on plant regeneration. The spectral response is related to the fire effects on fuels, soils, litter, and vegetation in as much as these characteristics relate to post-fire regeneration.

We explored the relationship between spectral reflectance, fire effects, and vegetation regeneration by comparing the differences in spectral response by fire severity class between 1988-1990 (Figure 8). We limited analysis of the spectral bands to 4, 5, and 7 because a) bands 1-3, and 6 yielded redundant information, b) band 4 is sensitive to vegetation regeneration and cover (Butera 1986, Fiorella and Ripple 1993), and c) bands 5 and 7 were shown to sensitive to fire effects. In this analysis, we looked at the changes in reflectance values from 1988 to 1989 and 1989 to 1990. If the percent change value is positive, this indicated that the previous year had more absorption relative to the succeeding year. If the value was positive, this indicated more reflectance. Figure 8 illustrates several trends. More absorption occurred in the near-IR channel in 1988 relative to 1989 and more reflectance occurred in the mid and far-IR channels. These responses are related to the occurrence of the fire which removed most of the vegetation cover between these two years. Also, there is a trend for increasing reflectance in bands 5 and 7 between 1988 and 1989 by fire severity class. This relates to the degree which the fire removed the vegetation cover, exposing bare soil and rock. This may also relate to the vegetation communities

ability to re-vegetate during this year period as a function of fire severity.

Between 1989 and 1990, there is more reflectance of near-IR energy and more absorption of far-IR energy. There is less reflectance in the high severity class compared to the other fire classes during this time period. There is an increasing trend in absorption in both bands 5 and 7 with increasing fire severity. The reflectance in near-IR in the 1989-1990 period is related to re-vegetation where more vegetation results in greater band 4 reflectance. The smaller reflectance in band 4 of the high severity class is a function of these areas having less vegetation cover regenerate relative to the other fire severity classes. This is consistent with field observations where post-fire vegetation cover was inversely related to increasing fire severity in the following two post-fire years (Earl Williard *pers. comm.*). Alternatively, the high severity class also had lower absorptance during the 1988-1989 period. This indicates that less vegetation existed before the fire in the high burn areas relative to the lower severity classes. Dutton and Cooper (1988) observed that most of the severely burned forests were dense *P. contorta* stands. These forests often have less leaf area relative to other forest types due to this dense stocking and competition (Kaufmann *et al.* 1982). These thick, monoculture stands of *P. contorta* burned the most severe leaving open areas with minimal re-generating vegetation. In a future study, we will use to the pre-fire vegetation map to investigate the differences in radiometric response before and after the fire as it relates to the vegetation composition and the fire ecology of different species.

The increase in absorption increasing fire severity of mid- and far-IR energy with between 1989 and 1990 is related the relative amount of disturbance between burn classes. Areas having high fire severity had major removal of live vegetation. Increases in reflection of near-IR energy between 1989 and 1990 are caused by growth of replacement vegetation destroyed by fire. Increases in absorption in mid- and far-IR energy are caused by vegetation covering exposed rock and soil. The trend for increasing absorption in the longer IR wavelengths is a function of the

amount of exposed non-vegetated surface left after the fire. Low severity burn areas had little exposed surface and therefore less to recover following the fire. Higher severity burns had more exposed surface to re-vegetate. The changes in absorption in the mid- and far-IR wavelengths is a measure of the relative amount of un-vegetated area due to different fire severities.

A comparison of randomly selected points from the Dutton and Cooper and Key fire severity maps with our classified map produced from the MAX(band 5,7) data indicate that there is a 68% percent agreement among the fire severity classification of our map and Dutton and Cooper's and a 70% agreement between our map and Key's map. This map was produced by changing two of the Euclidean Distance-based classes which improved the map-to-map correspondence to the above level. The classes changed were 11 and 12 (Table 7) which we changed from high to a moderate fire classification. Initially, these classes were chosen because changing them to moderate classes made the map "look" more like the Dutton and Cooper and Key maps. A *post-hoc* rationale for changing these classes is that the Euclidean Distances were calculated from reflectance data for forested areas only. Using the pre-fire map, we determined that the burn area is composed of approximately 93% forest, 6% shrub/meadow, and 1% non-vegetation. Dutton and Cooper sampled meadow and riparian shrub areas which we extracted reflectance values. Dutton and Cooper noted that grass dominated areas had only low severity burns while the riparian areas had both low and moderate burns. The mean MAX(band 5,7) reflectance for the grass/low severity was 1.032 compared with 0.969 for the riparian/low and 1.252 for the riparian/moderate severity. Euclidean distances were calculated from these reflectance values and the signature values of classes 11 and 12 (Table 10). Table 10 demonstrates that the riparian/moderate burn area had the lowest Euclidean Distance value of 0.088 for class 11 compared with the other groups on that table and the grass/low burn area had the lowest for class 12 at 0.053. Comparing these values with those calculated in the forested areas (Table 7) we found that for class 11, the riparian/moderate was the third lowest. For

class 12, the grass/low burn had the lowest distance value when compared with the forest values.

Table 10 - Euclidean Distances for grass and riparian areas for spectral classes 11 and 12.

		Euclidean Distance		
Spectral Class	Spectral Class Reflectance	*Grass* Low	*Riparian* Low	Moderate
11	1.163	0.131	0.194	0.088
12	1.085	0.053	0.116	0.167

Classes 11 and 12 are composed of pixels of low and moderately burned grass, riparian communities and high severity burned forest communities. Using the pre-fire classification, we found that class 11 and 12 contain approximately 80% forest, 18% shrub/meadow, and 2% non-vegetated. Also, classes 11 and 12 contain 29% of all shrub/meadow classified pixels in the burn area. These classes constitute a disproportionate number of shrub/meadow pixels relative to the other classes. This indicates that the spectral signature of these classes is highly influenced by the reflectance of low and moderate burned grasses and riparian shrubs. A better fire severity classification may be produced by pre-stratifying the spectral using a pre-fire vegetation classification to understand the radiometric response of differing lifeforms to fire severity.

The correspondence of the different fire severity maps demonstrates that the spectral mapping procedure presented here is a valuable tool for post-fire analysis of fire severity. The mapping process is an important step for understanding the size and distribution of fire effects. The real significance of this information is realized when it is integrated with other information sources such as the pre-fire vegetation map. This integration reveals broader ecological implications of the fire (Figure 9). This illustrates that most of the forested communities were lightly or moderately burned. The PICO community appears to have more light burn than the other forested areas (65%) which is inconsistent with field observations by Dutton and Cooper. They observed that PICO

communities dominated the burn area and that these communities had the most severe burn. The low mapping accuracy of PICO stands (57%) in our pre-fire classification may indicate that we have underestimated the extent of these communities in the burn area. Likewise, the moderate agreement between fire severity maps (68-70%) indicates that size of severely burned forest may be misrepresented. Alternatively, Dutton and Cooper sampled a limited area of the entire burn which could have biased their perception of the overall characteristic of the burn. In this case, the map integration refutes the field observation. In reality, the effect of fire on the Red Bench Fire forests may be represented by the combination of the remotely sensed and field information.

Ecological Modeling

Hydrologic Outflow

We used an ecosystem model to assess what effects fire has on the processing of carbon and water within the landscape. As evapotranspiration is in part directly correlated with LAI (McNaughton and Jarvis 1983), hydrologic outflow is inversely related to LAI. By comparing the outflow data from the model with the North Fork stream gauging data, it is possible to understand what effect fire has on the water balance of the burned area as a function of removal of LAI.

As we have previously stated, the Columbia Falls gauging station did not correlate well to the modeled outflow data, especially during peak flow events (Figure 10). Near Julian Day (JD) 150 of 1988, a large flow event was modeled with a maximum water equivalent value of 1.5 cm versus 0.5 cm for the Columbia Falls station. Likewise, between JD 110 and 165 of 1989, three large surge events occurred in the Columbia Falls data but were not in the modeled data with a maximum difference of 0.5 cm between the observed and modeled data.

The discrepancy between the observed and modeled outflow data during spring melt could represent a climatological or hydrologic parameterization problem with the model. On the contrary,

this difference could be a function of the contributing area of the outflow measured by the Columbia Falls station, the location of the study area within the entire watershed, and the disturbance of vegetation within a limited area of the watershed. The calculated residual error between the model and gauging stations shows a distinct spring seasonality as described above (Figure 11). Analysis of Figure 11 showing the residual errors between the gauging stations and model and between the gauging stations over 1988 and 1989 illustrates five possible scenarios:

1) all three $\hat{E} = 0$; hydrologic conditions are homogeneous throughout basin; condition occurs most frequently under base flow conditions, especially at the beginning of the year,

2) all three $\hat{E} < 0$; a complex hydrologic scenario exists where the burn area (middle of watershed) is "contributing" the most water on an area basis, followed by the upper watershed; this condition may occur during spring melt where lower elevations such as the lower watershed are melting faster than upper reaches as demonstrated between JD 115-130 of 1988,

3) $\hat{E}$ between gauging stations and model > 0 and error between gauging stations < 0; the upper watershed is contributing large quantities of water (melt or precipitation) relative to the lower watershed; this occurs during major melt period of upper elevation which is seen as a surge of water through entire watershed; occurs in both 1988 and 1989 during peak flow between JD 130 to 165,

4) $\hat{E}$ between Columbia Falls and either the model or the Tuchuck station < 0, and $\hat{E}$ of Tuchuck versus the model > 0; a gradation of contribution of water exists from top to

bottom of watershed with upper watershed contributing most; occurs occasionally between JD 130 and 165 of 1988 only,

5) $\hat{E}$ between both gauging stations and model < 0, residual between gauging stations $= 0$; "contribution" of water from modeled area is greatest with equal contribution from top to outlet of the watershed; occurs mostly when either model is not matched with descending limb of peak flow (JD 170-190, 1988 and 1989) or during non-peak flow events such as between JD 270 and 350, 1988 and between JD 200 and 275, 1989.

The first four scenarios demonstrate a reasonable assumption that there is a gradient of more water being contributed from the top of the watershed. Figure 11 demonstrates that the residual error between the Columbia Falls and Tuchuck stations is negative mostly during peak flow meaning more water was being measured by the Tuchuck station than the Columbia Falls station on an area basis. Moreover, the lower end of the watershed has been described as being in the rainshadow of the Whitefish Range which forms the western boundary of the watershed (Finklin 1986).

The fifth scenario is the most important for understanding the effects of the fire on the hydrologic balance. The fire began on JD 250 of 1988 and burned for 11 days after which three precipitation events occurred between JD 270 and 350 (Figure 10). The modeled outflow during these flow events were "contributing" on the average < 0.1 cm $\cdot$ day^{-1} of water or 13.5 m$^3 \cdot$ s^{-1} to the watershed. We cannot determine if the model is representative of the "true" outflow event using our limited observed data. We can assume, however, that the model best represents the change in the landscape and that differences between the model and gauging data are due to scale differences. The total area measured by the Columbia Falls gauge is 400,932 ha which is the size of the entire total. The area of the burn is only 3% of the total watershed which means that the Columbia Falls

station may not be sensitive to increases in outflow due to reduction in evapotranspiring vegetation on such a limited scale. While causality for the differences between the modeled and observed data cannot be assigned, it is enough to say that differences do exist.

These differences are further demonstrated in 1989. In 1989, we made three basic assumptions about the study area which were: a) the burned area converted to a grassland in 1989, b) LAI for the grassland could be derived from NDVI, c) LAI outside the burn area remained constant between 1988 and 1989. Hypothetically, the sparsely vegetated burned area would result in larger outflow of water. As we have previously explained, the differences in modeled and observed data between JD 110 and 165 are caused by high influx rates of water from the upper watershed influencing the hydrograph at the Columbia Falls station (Figure 10). The difference in modeled and observed values between JD 170 and 190 is due to differences in soil water release. The *m* parameter used in TOPMODEL defines the rate at which water will be available for sub-surface flow. Smaller values of this parameter increase soil water reservoir and slows soil water release (Band 1993). The melt recessional limb may be better approximated by either increasing the value of *m* or decreasing the depth at which overflow occurs which was set at 23.5 cm in our simulations. Also, this modeled recessional limb is sensitive to the definition of climate for each modeled hillslope. Climate variables for each hillslope are calculated from mean elevations, aspect and slope. If hillslopes encompass topographical relief ranging from the valley to ridge, as the ones presented in this simulation, this will moderate the timing of events such as spring melting of snow. This process may be better modeled by adjusting snowmelt coefficients to slow melting, changing the definition of the hillslope environment, or reducing the elevational range of each hillslope to represent a more homogeneous climate, the latter being one of the premises on which this simulation system was developed (Band *et al.* 1991).

Differences in the observed and modeled outflow values between JD 200 and 275 are partly

due to changes in landcover from the fire resulting in greater outflow. Climatic records show precipitation in the form of rain occurring during this time. The average difference between the Columbia Falls station and the modeled value during this period was 0.05 $cm \cdot day^{-1}$ or 7.3 $m^3 \cdot s^{-1}$ with the modeled area producing more water than the watershed on an area basis. Localized weather such as afternoon thunderstorms (Finklin 1986) may partly account for this difference by increasing precipitation for small areas while influencing total watershed outflow minimally. However, landcover variation also increases outflow and exaggerates the difference between the model and gauging station to some extent. Figure 12 illustrates the $\hat{E}$ between the model with grass in the burn area and a simulation with full forest cover. The full forest model represents baseline conditions where the fire did not occur in the landscape. In this analysis, we found that the average difference in outflow between JD 200 and 275, 1989, where either grasses or forests were present in the burn area to be > 0.01 $cm \cdot day^{-1}$ or > 1.0 $m^3 \cdot s^{-1}$. Similarly, we found that the amount of water produced by the fire-affected landscape over the amount produced by the forested landscape to be 0.35 $cm \cdot yr^{-1}$ or 3400 $m^3 \cdot yr^{-1}$. Clearly, these are small differences.

Our analysis of the modeled hydrologic balance of the Red Bench Fire area leads us to conclude that a) site-specific stream gauging data are important to discriminate local phenomena rather than total watershed patterns, b) model parameterization is important, especially soil conductive properties and climate definition, and c) the effect of fire on the hydrologic budget of the landscape ecosystems is limited. The last conclusion is based on the small difference in modeled yearly, hydrologic outflow described above. Re-vegetation of the burn area by grasses and herbaceous species reduces water loss by the system. This occurs despite large decreases in LAI because the water use of these lifeforms is efficient in terms of stomatal conductance, critical xylem potential, and maximum photosynthetic rates (Knapp *et al* 1993). A combination of these characteristics allows grasses to make use of water at rates similar to conifers during wet periods as

well as utilize soil water at potentials twice those of conifers during drought. In winter, however, conifers may utilize water when temperature and light conditions are conducive whereas grasses are dormant, but, photosynthesis reactions are limited due to light and water during this time. We conclude that fire affects hydrologic cycling in landscape ecosystems only when the severity and size of the fire reduces the capacity of the systems to re-vegetate.

Net Primary Productivity

The overall ecosystem productivity, measured as annual NPP, differed very little between 1988 and 1989. Average ANPP for 1988 was 1.66 Mg C $\cdot$ ha^{-1} and 1.65 Mg C $\cdot$ ha^{-1} for 1989. This was unanticipated given that 13% of the modeled area had a reduction in LAI by an average of four between these years due to the fire. The relative constancy of production between the two years can be accounted for by the fact that 1989 had more precipitation during the growing season than 1988 (Figure 13). The combination of higher precipitation and lower LAI in 1989 equate to ANPP values which should be similar between the two years. The presence of grasses in the 1989 simulation do not affect ANPP calculation significantly because grasses tend to be as water efficient as conifers where water use efficiency (WUE) is calculated by:

$$WUE = \frac{ANPP}{TotalTranspiration}$$

(Running and Hunt 1993). In simulations where we excluded fire and landcover change from the landscape for 1988 and 1989, the average ANPP values were 1.68 and 1.70 Mg C $\cdot$ ha^{-1}, respectively. These small differences indicate that ecosystem productivity in these environments is more sensitive to climate rather than lifeform.

The areal distribution of ANPP between years is also similar (Figure 14). The bi-modal distribution of this figure is a function of the difference between simulations on the slopes and

simulation in the bottomland. Consistently, the bottomlands have the highest ANPP due to available soil water. In the hydrologic model of RHESSys, no connection is made between hillslope partition water routing. This means that water flowing from the slopes are not influencing the soil water balance of the bottomland areas. The flat, broad valleys of the North Fork were not considered in the original conceptualization of RHESSys, rather, valley bottoms were regarded as the connection between two opposing hillslopes. This logic is appropriate for small tributaries but not for large, sub-basin watershed such as the North Fork of the Flathead River. Improvements in this discontinuity will further increase water availability for valley communities and lead to higher, and possibly more accurate, predictions of productivity.

Although both the average study area estimates and the distribution of area of ANPP are similar between years, the spatial arrangement on the landscape show some differences (Figure 15). In both years, there is a spatial gradient for higher productivity at the north-northwest end of the study area. This is consistent with possible water availability trends given that the northern end has the higher elevation. The bottomlands productivity are consistently the highest in both years. In 1989, the effect of higher precipitation and the fire become evident. The upper northwest watershed, known as the Whale Butte watershed, increases in productivity. The burn area can be seen in the center of the image where productivity is less relative to the surrounding areas. The lowest production in both images occurred in 1989 on the east side of the valley in Glacier Park. This was caused primarily by the lack of LAI in this area as calculated from the satellite derived NDVI estimates. This area also had the severest burn based on the satellite and ground maps of burn severity. This reinforces the conclusion that burn severity is inversely related to re-vegetation and further, that severity is also inversely related to post-fire productivity.

CONCLUSIONS

Coupling remote sensing data and modeling can be used to understand the dynamic relationship between fire and ecological function in this landscape. The minor changes in modeled NPP from 1988 to 1989 despite major changes in vegetation cover demonstrate just how adapted these communities are to fire. Historical records indicate that parts of the Red Bench Fire area have been burned within 20 years. System equilibrium of carbon and water cycling may be rapid in fire-adapted forests and this equilibrium can be represented through modeling means. A synthesis of the fire severity information with ecological modeling may be used to understand the relationship between fire-return frequency, fire severity, post-fire regeneration, and ecosystem processes.

Development of fire management policies may benefit from using the remote sensing applications outlined here. These technologies are especially important for determining the result of large, severe fires on the landscape structure and nutrient cycling. As managers consider the effects of disturbance on ecosystems at landscape and regional scales, there is a great need to develop models and technology which identify ecosystem processes within the appropriate time and space domains. The approach taken in this study was to define broad descriptions of ecosystem composition and processes. We recognize that these methods have limited appeal for researchers investigating finite spatial and ecological questions. We have outlined the limitations of these methods, but hopefully, have provided a framework for which further research may be founded. For instance, the inclusion of successional models within RHESSys will provide comparative information with field ecological research on the accumulation and allocation of carbon within individual stands. This is related to fire because accumulation of fuels may determine fire frequency, severity, and, ultimately, stand development. Also, by coupling this process with geographic stand age data, we will be able to draw conclusions about the consequences of fire management policy over the past century as a corollary to modeled versions of the same stands using this successional-process modeling system.

LITERATURE CITED

Band, L.E. 1993. Effect of land surface representation on forest water and carbon budgets. *Journal of Hydrology*. 150:749-772.

Band, L.E., D.L. Peterson, S.W. Running, J.C. Coughlan, R. Lammers, J. Dungan, and R. Nemani 1991. Forest ecosystem processes at the watershed scale: basis for distributed simulation. *Ecological Modeling*. 56:171-196.

Benson, A.S., and S.D. DeGloria 1985. Interpretation of Landsat-4 Thematic Mapper and Multispectral Scanner Data for forest surveys. *Photogrammetric Engineering and Remote Sensing*. 51(9):1281-1289.

Beven, K.J. and E.F. Wood 1983. Catchment geomorphology and the dynamics of runoff contributing areas. *Journal of Hydrology*. 65:139-158.

Bolstad, P.V., and T.M. Lillesand 1992. Improved classification of forest vegetation in northern Wisconsin through a rule-based combination of soils, terrain, and Landsat Thematic Mapper data. *Forest Science*. 38(1):5-20.

Bristow, K.L & Campbell G.S. 1984. On the relationship between incoming solar radiation and daily maximum and minimum temperature. *Agricultural and Forest Meteorology*. 31:159-166.

Butera, M.K. 1986. A correlation and regression analysis of percent canopy closure versus TMS spectral response for selected forest sites in the San Juan National Forest, Colorado. *IEEE Transactions on Geoscience and Remote Sensing*. GE-24(1):122-129.

Cibula, W. G. and M.O. Nyquist 1987. Use of topographic and climatological models in a geographical data base to improve Landsat MSS classification for Olympic National Park. *Photogrammetric Engineering and Remote Sensing*. 53(1):67-75.

Conese, C., G. Maracchi, F. Miglietta, F. Maselli, and V.M. Sacco 1988. Forest classification by principal component analyses of TM data. *International Journal of Remote Sensing*. 9(10-11):1597-1612.

Coppin, P.R. and M.E. Bauer 1992. Optimization of the information content of multitemporal Landsat TM data sets for monitoring forest cover disturbance. International Geoscience and Remote Sensing Symposium, May 26-29, 1992, Houston, TX. pp. 983-985.

Dutton, B.L. 1990. Soil map of the Red Bench Fire area, Glacier National Park, Montana. 1:24,000. West Glacier, MT.

Dutton, B.L. and S.B. Cooper 1988. Red Bench Fire intensity mapping and permanent plot installations. Unpublished report to Glacier National Park, West Glacier, MT. 13 p.

Earth Resource Data Analysis System Software. 1991. ERDAS, Inc. 2801 Buford Hwy. Atlanta, GA.

Ezra, C.E., L.R. Tinney, and R.D. Jackson. 1984. Effect of soil background on vegetation discrimination using Landsat data. *Remote Sensing of the Environment*. 16:233-242.

Fetter, C.W. 1988. *Applied Hydrogeology*. Merrill Publishing Co. Columbus, Ohio. 592 pp.

Finklin, A.I. 1986. A climatic handbook for Glacier National Park - with data for Waterton Lakes National Park. USDA Forest Service Gen. Tec. Rep. INT-204. Intermountain Research Station, Ogden, UT.

Fiorella, M. and W.J. Ripple 1993. Analysis of conifer forest regeneration using Landsat Thematic Mapper data. *Photogrammetric Engineering and Remote Sensing*. 59(9):1383-1388.

Fischer, W.C. 1989. The fire effects information system: a comprehensive vegetation knowledge base. P. 107-113, In D.E. Ferguson, P. Morgan, and F.D. Johnson. Comp. USDA Forest Service Gen. Tec. Rep. INT-257. Intermountain Research Station, Ogden UT.

Fischer, W.C. and A.F. Bradley 1987. Fire ecology of western Montana forest habitat types. USDA Forest Service Gen. Tec. Rep. INT-223. Intermountain Research Station, Ogden, UT.

Fleming, M.D., J.S. Berkebile, and R.M. Hoffer 1975. Computer-aided analysis of LANDSAT-1 MSS data: a comparison of three approaches, including a "modified clustering" approach. LARS information note 072475, Laboratory for Applications of Remote Sensing, Purdue University, West Lafayette, Indiana 47906.

Garnier, B.J. & Ohmure, A. 1968. A method of calculating the direct shortwave radiation income of slopes. *Journal of Applied Meteorology*. 7(5):796-800.

Glassy, J.M. & Running, S.W. 1993. Validating diurnal climatology logic of the MT-CLIM model across a climatic gradient in Oregon. *Ecological Applications* (in press).

Gregory, S.V., F.J. Swanson, W.A. McKee, and K.W. Cummins 1991. An ecosystem perspective of riparian zones. *Bioscience*. 41(8):540-5

Hall, D.K., J.P. Ormsby, L. Johnson, amd J. Brown 1980. Landsat digital analysis of the initial recovery of burned tundra at Kokolik River, Alaska. *Remote Sensing of the Environment*. 10:263-272.

Hughes, J.S., D.L. Evans, P.Y. Burns, and J.M. Hill 1986. Identification of two southern pine species in high-resolution aerial MSS data. *Photogrammetric Engineering and Remote Sensing*. 52(8):1175-1180.

Isaaks, E.H. and R.M. Srivastava 1989. *An Introduction to Applied Geostatistics*. Oxford

University Press, New York. 561 p.

Iverson, L.R., R.L. Graham, and E.A. Cook 1989. Applications of satellite remote sensing to forested ecosystems. *Landscape Ecology*. 3(2):131-142.

Jakubauskas, M.E., K.P. Lulla, and P.W. Mausel. 1990. Assessment of vegetation change in a fire altered forest landscape. *Photogrammetric Engineering and Remote Sensing*. 56(3):371-377.

Jensen, J.R. 1986. *Introductory Digital Image Processing*. Prentice-Hall, New Jersey, 379 p.

Kaufmann, M.R., C.B. Edminster, and C.A. Troendle 1982. Leaf area determinations for subalpine tree Species in the central Rocky Mountains. USDA Forest Service Research Paper RM-238. Rocky Mountain Forest and Range Experiment Station.

Keane, R.E., M.E. Jensen, and W.J. Hann. 1990. ECODATA and ECOPAC: analytical tools for integrated resource management. *Compiler*. 8(3):24-37.

Kessell, S.R. 1979. *Gradient modeling*. Springer-Verlag, New York, NY. 432 p.

Key, C. 1988. Map of fire spread over time - Red Bench Fire, Glacier National Park and Flathead National Forest. Glacier National Park Science Center.

Khorram, S. and E.F. Katibah 1984. Vegetation/land cover mapping of the Middle Fork of the Feather River watershed using Landsat digital data. *Forest Science*. 30(1):248-258.

Kleinbaum, D.G., L.L. Kupper, and K.E. Muller 1988. *Applied Regression Analysis and Other Multivariate Methods*. PWS-Kent Publishing Company, Boston. 718 p.

Knapp, A.K., J.T. Fahnestock, S.P. Hamburg, L.B. Statland, T.R. Seastedt, and D.S. Schimel 1993. Landscape patterns in soil-plant water relations and primary production in tallgrass prairie. *Ecology*. 74(2):549-560.

Küchler, A.W. 1967b. Potential natural vegetation of the United States. Washington, DC. USGS National Atlas, pp. 89-90.

Küchler, A.W. 1988. The classification of vegetation. P. 67-80 In A.W. Küchler and I.S. Zonneveld, eds., *Vegetation Mapping*, Kluwer Academic Publishers, Dordrecht, Netherlands.

Leprieur, C.E., J.M. Durand, and J.L Peyron 1988. Influence of topography on forest reflectance using Landsat Thematic Mapper and digital terrain data. *Photogrammetric Engineering and Remote Sensing*. 54(4):491-496.

Likens, W. K. Maw, and D. Sinnott 1982. *Final Report: Landsat Land Cover Analysis Completed for CIRSS/San Bernadino County Project*. NASA Technical Memorandum 84244, 25 p.

Markham, B.L. and J.L Barker 1985. Spectral characterization of the LANDSAT Thematic Mapper sensors. *International Journal of Remote Sensing*. 6(5):697-716.

Mayer, K.E. and L. Fox III 1981. Identification of conifer species groupings from Landsat digital classifications. *Photogrammetric Engineering and Remote Sensing*. 48(11):1607-1614.

McNaughton, K.G. and P.G. Jarvis. 1983. Predicting the effects of vegetation changes on transpiration and evapotranspiration. P. 1-47 In T.T. Kozlowski, ed., *Water Deficits and Plant Growth*, vol. 7, Academic Press, London.

Milne, A.K. 1986. The use of remote sensing in mapping and monitoring vegetational change associated with bushfire events in eastern Australia. *Geocarto International*. 1. pp. 25-32.

Moore, M.M., and M.E. Bauer 1990. Classification of forest vegetation in north-central Minnesota using Landsat Multispectral Scanner and Thematic Mapper data. *Forest Science*. 36(2):330-342.

Morgan, P.M. 1984. Modeling shrub succession following clearcutting and burning. PhD Dissertation, University of Idaho, Moscow, ID, 146 p.

Nemani, R.R. and S.W. Running 1989. Testing a theoretical climate-soil-leaf area hydrologic equilibrium of forests using satellite data and ecological simulation. *Agricultural and Forest Meteorology*. 44:245-260.

Nemani, R.R. and S.W. Running 1991. Applications of ASTER thermal-infrared data in ecological science, unpublished report. Desert Research Institute, University of Nevada, Reno, NV. 55 pp.

Nemani, R., S.W. Running, L.E. Band, and D.L. Peterson. 1993. Regional hydro-ecological simulation system: an illustration of the integration of ecosystem models in a GIS. P. 296, In M. Goodchild, B. Banks, and G. Steyaert, eds., *Integrating GIS and Environmental Modeling*. Oxford, London.

Richards, J.A., D.A. Landgrebe, and P.H. Swain 1982. A means for utilizing ancillary information in multispectral classification. *Remote Sensing of the Environment*. 12:463-477.

Ryan, K.C. and N.V. Noste 1985. Evaluating prescribed fires. P. 230-238, In J.E. Lotan, B.M. Kilgore, W.C. Fischer, and R.W. Mutch, Tec. Coord. Proc. Symposium and Workshop on Wilderness Fire. USDA Forest Service General Tec. Rep. INT-182. Intermountain Forest and Range Experiment Station, Ogden, UT.

Running, S.W. and J.C. Coughlan 1988. A general model of forest ecosytem processes for regional applications I. hydrologic balance, canopy gas exchange, and primary production processes. *Ecological Modelling*. 42:125-154.

Running, S.W. & Gower, S.T. 1991. FOREST-BGC, Ageneral model of forest ecosystem

processes for regional applications. II. Dynamic carbon allocation and ntrogen budgets. *Tree Physiology*. 9:147-160.

Running, S.W. and E.R. Hunt 1993. Generalization of a forest ecosystem process model for other biomes, BIOME-BGC, and an application for global-scale models. P. 141-158 In J.R. Ehleringer and C.B. Field, eds., *Scaling Physiological Processes Leaf to Globe*. Academic Press, San Diego.

Running, S.W., R.R. Nemani, and R.D. Hungerford, R.D. 1987. Extrapolation of synoptic meteorological data in mountainous terrain and its use for simulating forest evapotranspiration and photosynthesis. *Canadian Journal of Forest Research*. 17(6):472-483.

Running, S.W., R.R. Nemani, D.L. Peterson, L.E. Band, D.F. Potts, L.L. Pierce, and M.A. Spanner 1989. Mapping regional forest evapotranspiration and photosynthesis by coupling satellite data with ecosystem simulation. *Ecology*. 70:1090-1101.

Schumucker, K.J 1984. *Fuzzy Sets, Natural Language Computations, and Risk Analysis*. Computer Science Press, Rockville, MD. 192 p.

Shen, S.S., G.D. Badhwar, and J.G. Carnes 1985. Separability of boreal forest species in the Lake Jennette area, Minnesota. *Photogrammetric Engineering and Remote Sensing*. 51(11):1775-1783.

Shovic, H. 1988. Preliminary burned area survey of Yellowstone National Park and adjoining national forests. Unpublished report, Yellowstone National Park, WY. 27 p.

Skidmore, A.K. 1989. An expert system classifies eucalyptus forest types using Thematic Mapper data and a digital terrain model. *Photogrammetric Engineering and Remote Sensing*. 55(10):1449-1464.

Spanner, M.A., L.L. Pierce, D.L. Peterson, and S.W. Running 1990. Remote sensing of coniferous forest leaf area index: the influence of canopy closure understory vegetation and background reflectance. *International Journal of Remote Sensing*. 11(1):95-111.

Walsh, S.J. 1980. Coniferous tree species mapping using Landsat data. *Remote Sensing of the Environment*. 9:11-26.

Weiser, R.L., G. Asrar, and E.T. Kanemasu, 1986. Assessing grassland biophysical characteristics from spectral measurements. *Remote Sensing of the Environment*. 20:141-152.

White, J.D. and S.W. Running *in press*. Testing scale dependent assumptions in regional ecosystem simulations. *Journal of Vegetation Science*.

White, J.D., G.C. Kroh, and J.E. Pinder III. *in press*. Mapping forest species at Lassen Volcanic National Park, California, using Landsat Thematic Mapper data and a geographical information system. *Photogrammetric Engineering and Remote Sensing*.

Wilkinson, L. 1986. *SYSTAT: The System for Statistics*. Evanston, IL: SYSTAT, Inc.

Figure 1 - Spectral reflectance curves of forest groupings for the North Fork of the Flathead River. Spectral data from 1988 Landsat data (Path 41 Row 26) acquired on August 28, 1988. Forest data from ECODATA data from Region 1 of the National Forest Service.

Average Reflectance Value by Group

North Fork ECODATA

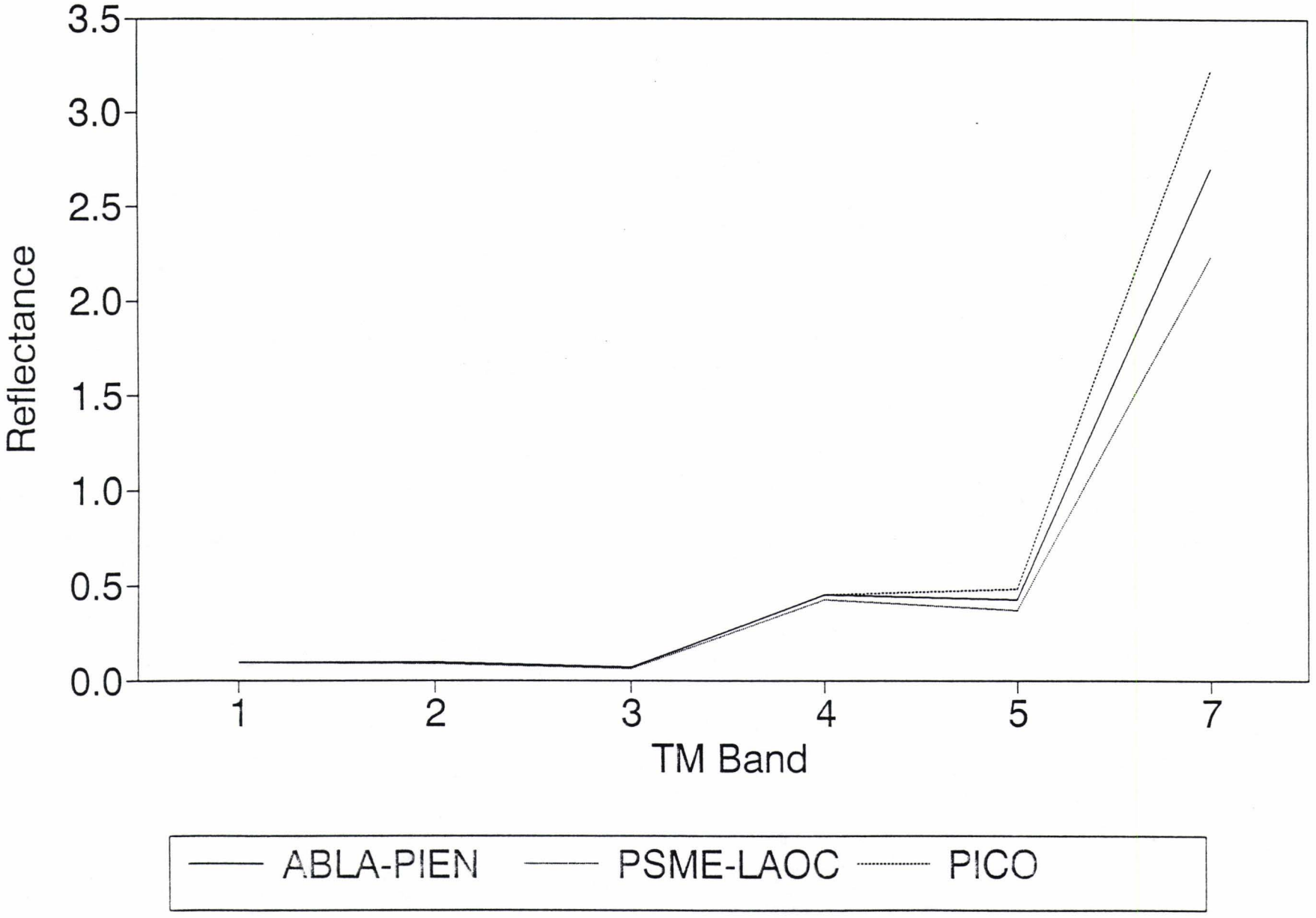

Figure 2 - Graph showing dominant forest species along axes of elevation and slope for north-west aspects of the North Fork.

Elevation v. Slope

NW Aspect

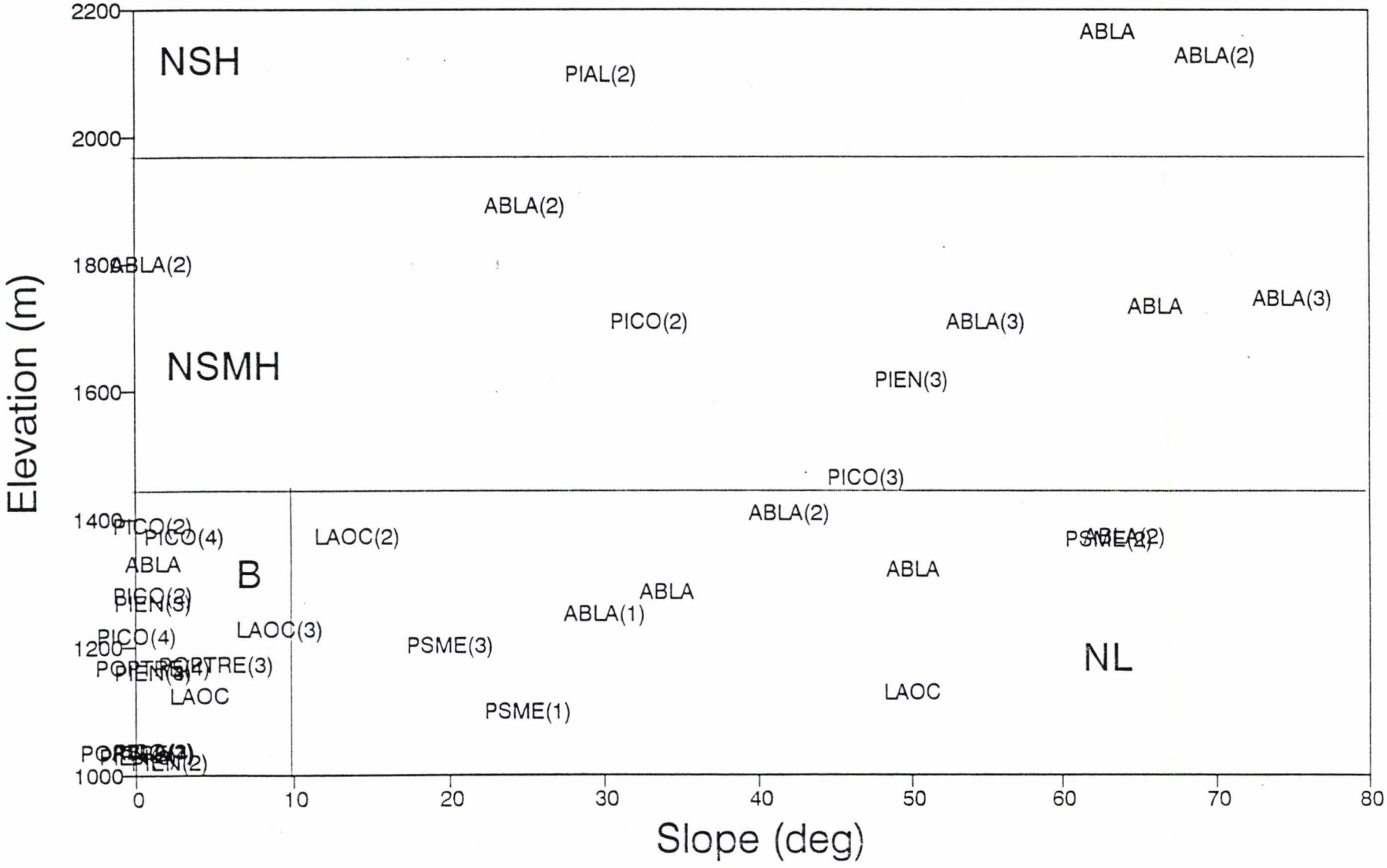

Figure 3 - Graph showing dominant forest species along axes of elevation and slope for south-east aspects of the North Fork.

Elevation v. Slope

SE Aspect

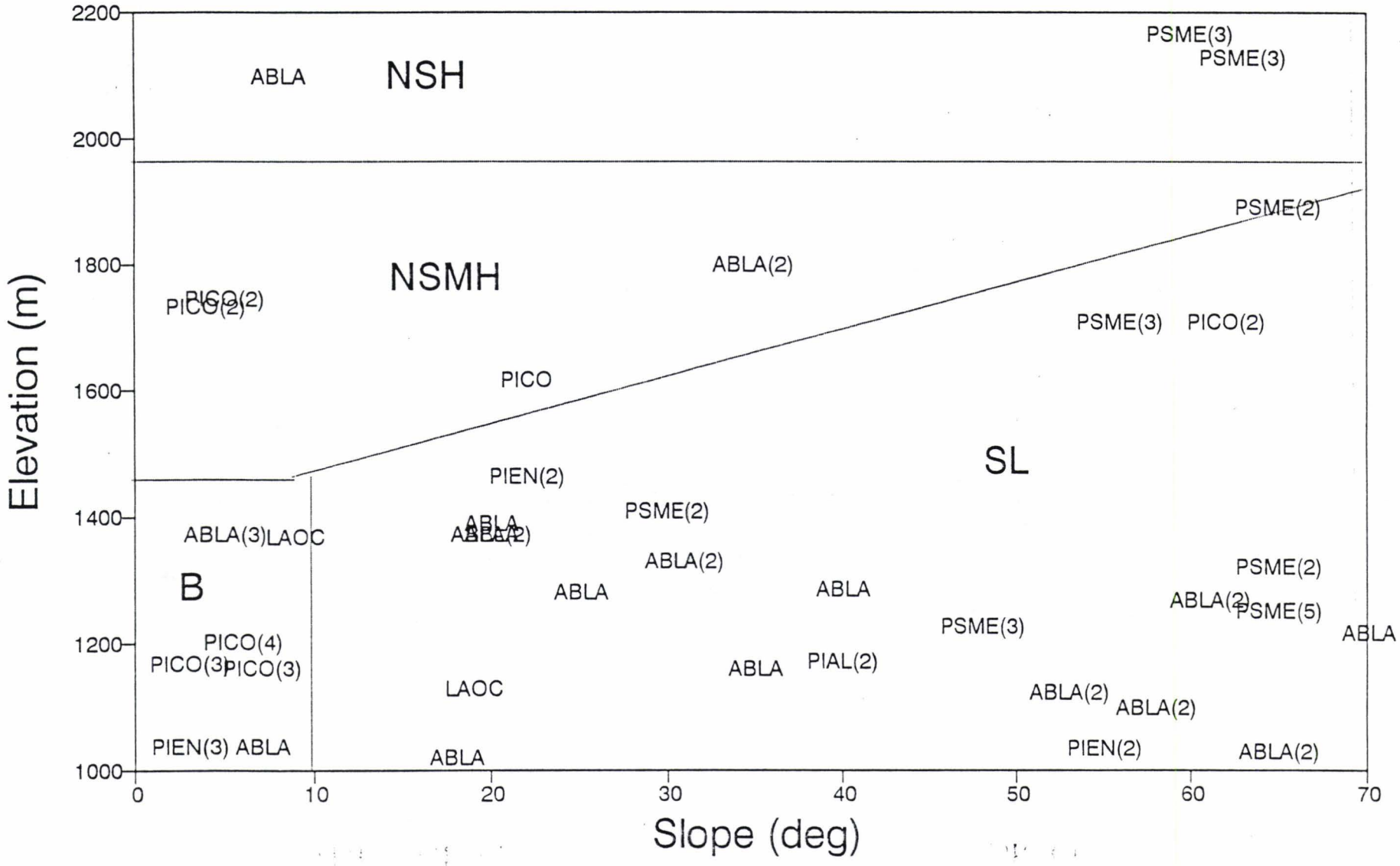

Figure 4 - Image of the vegetation map of the North Fork derived from a combination of spectral classification and topographic analysis.

North Fork of the Flathead River

Vegetation Map

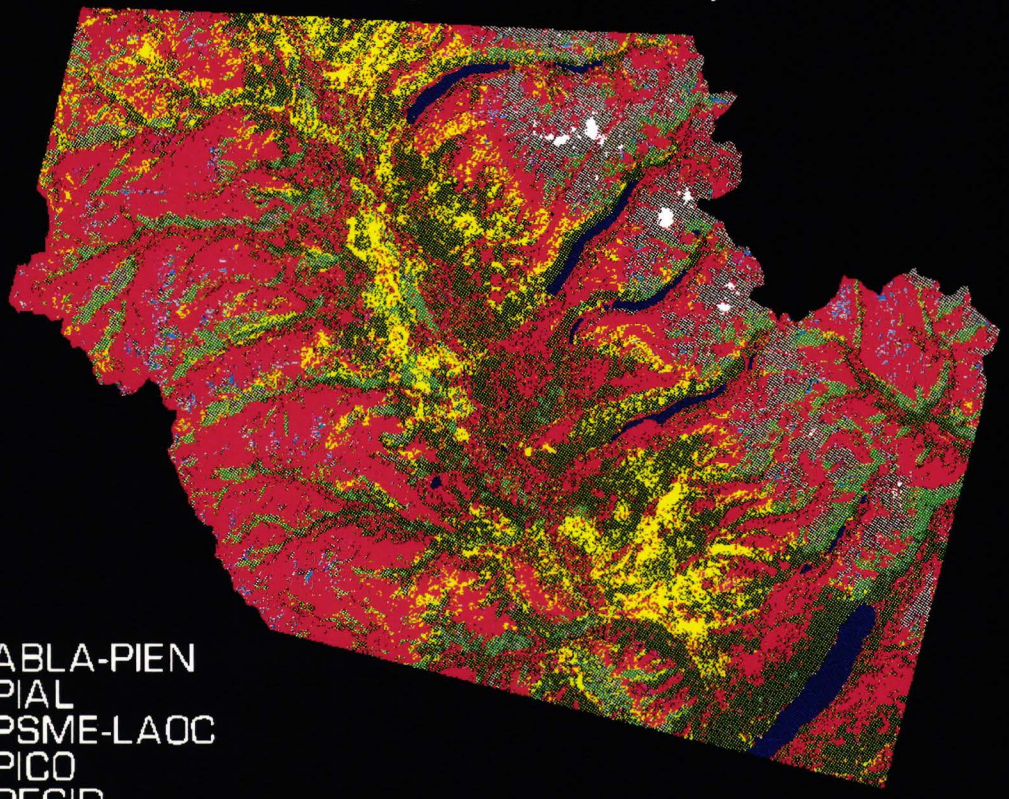

ABLA-PIEN
PIAL
PSME-LAOC
PICO
DECID
MIX
SHRUB/MEAD
BARE GROUND
WATER
SNOW/ICE

0 20 km

white/ryan/running/NTSG

Figure 5 - Classified Landsat TM data (MAX(Band5,7)) for September 20, 1989. Image shows areas in and outside burn area classified same.

Classified September 20, 1989 Landsat TM Data

Red Bench Fire

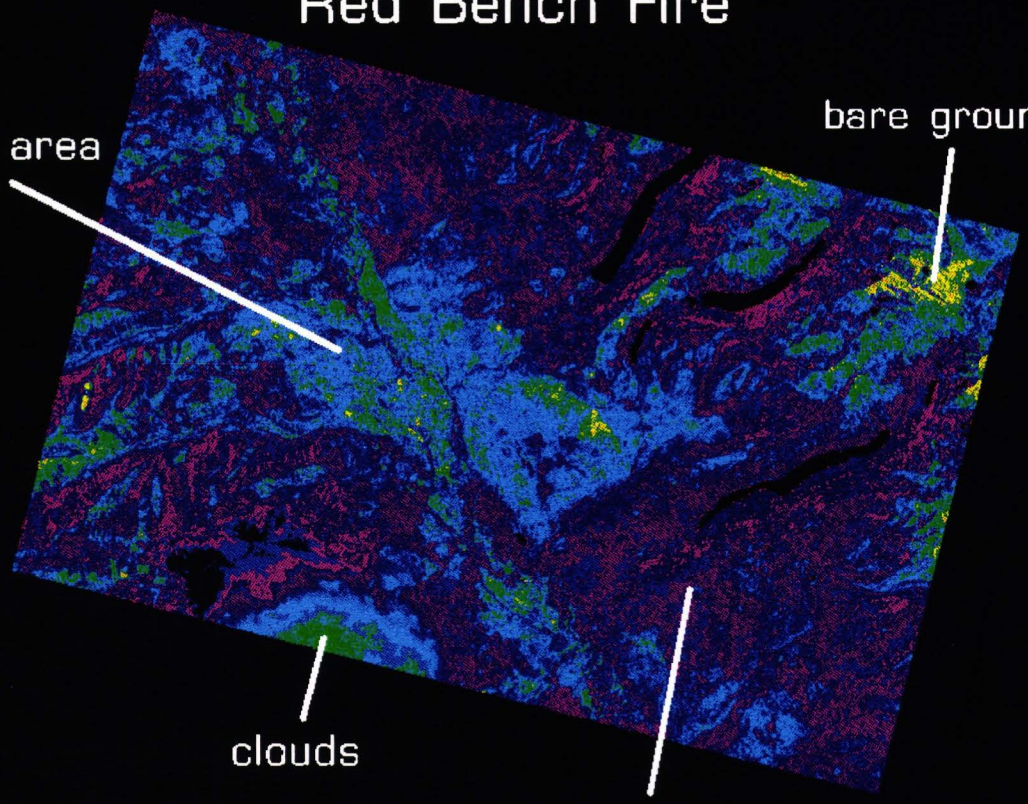

Figure 6 - Image showing final classification of September 20, 1989, Landsat TM data into burn severity classes. Burn perimeter delineated from aerial photograph (Key 1990).

Red Bench Fire Severity Map

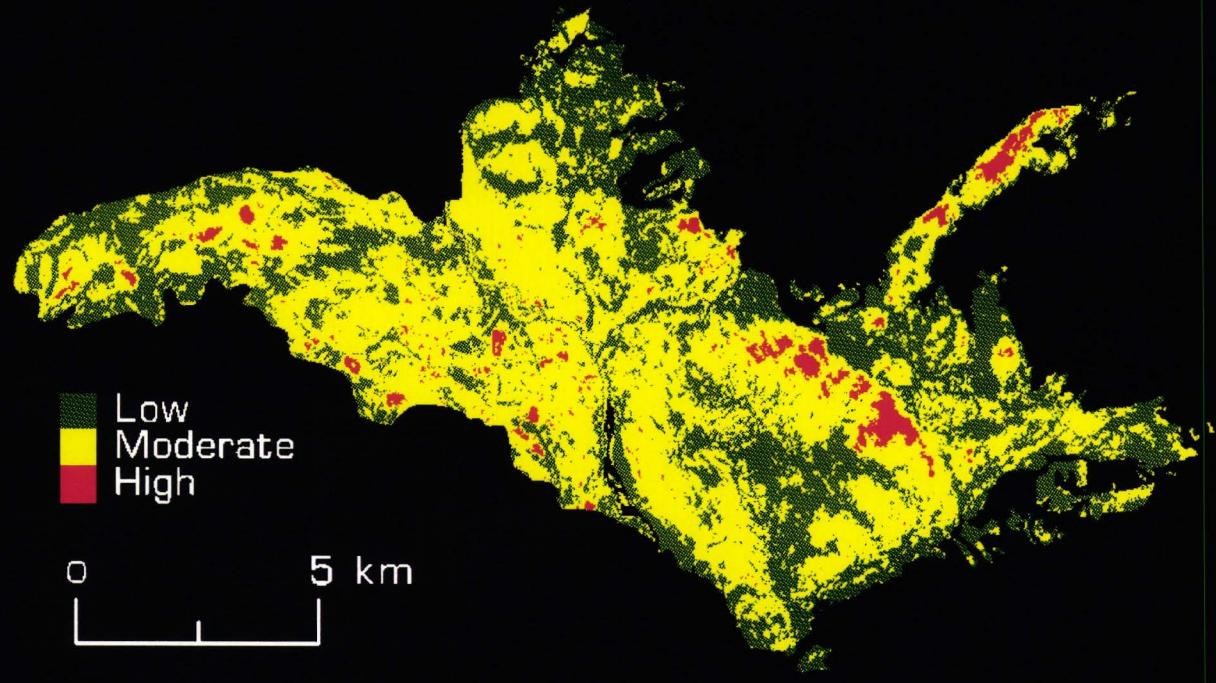

Derived from Landsat TM MAX(Band 5,7) Classification

Figure 7 - Linear regression model of LAI for the re-vegetating grasses and herbaceous vegetation of the burn area versus NDVI values from Landsat TM data, September 3, 1990, for the North Fork area.

1991 LAI v. 1990 NDVI

Red Bench Fire

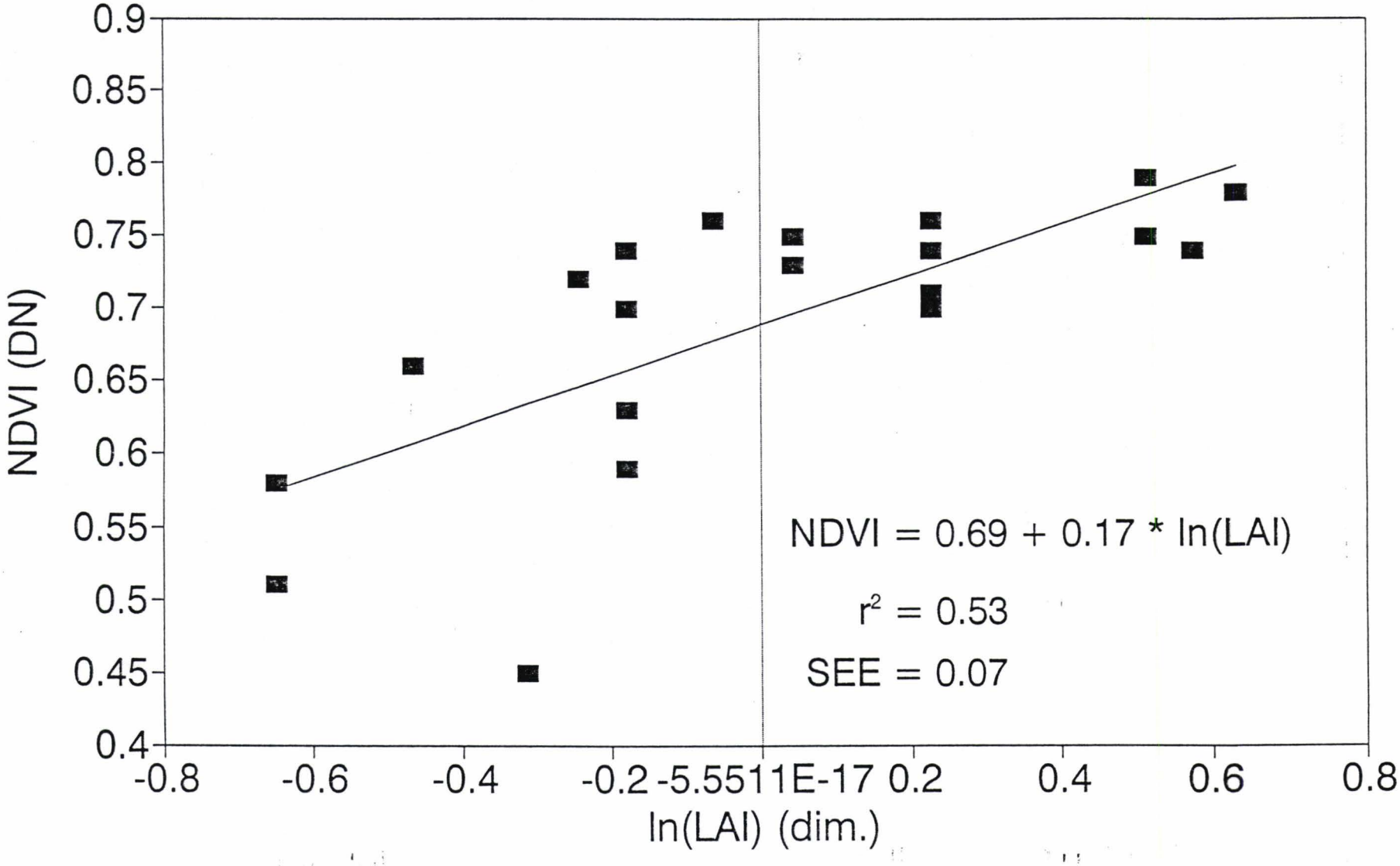

Figure 8 - Differences in spectral reflectance between 1988-89 and 1989-1990 for the three burn severity classes. Burn severity data from Dutton and Cooper field plots (1988).

Difference in Reflectance from 1988-90 between Burn Severity Classes

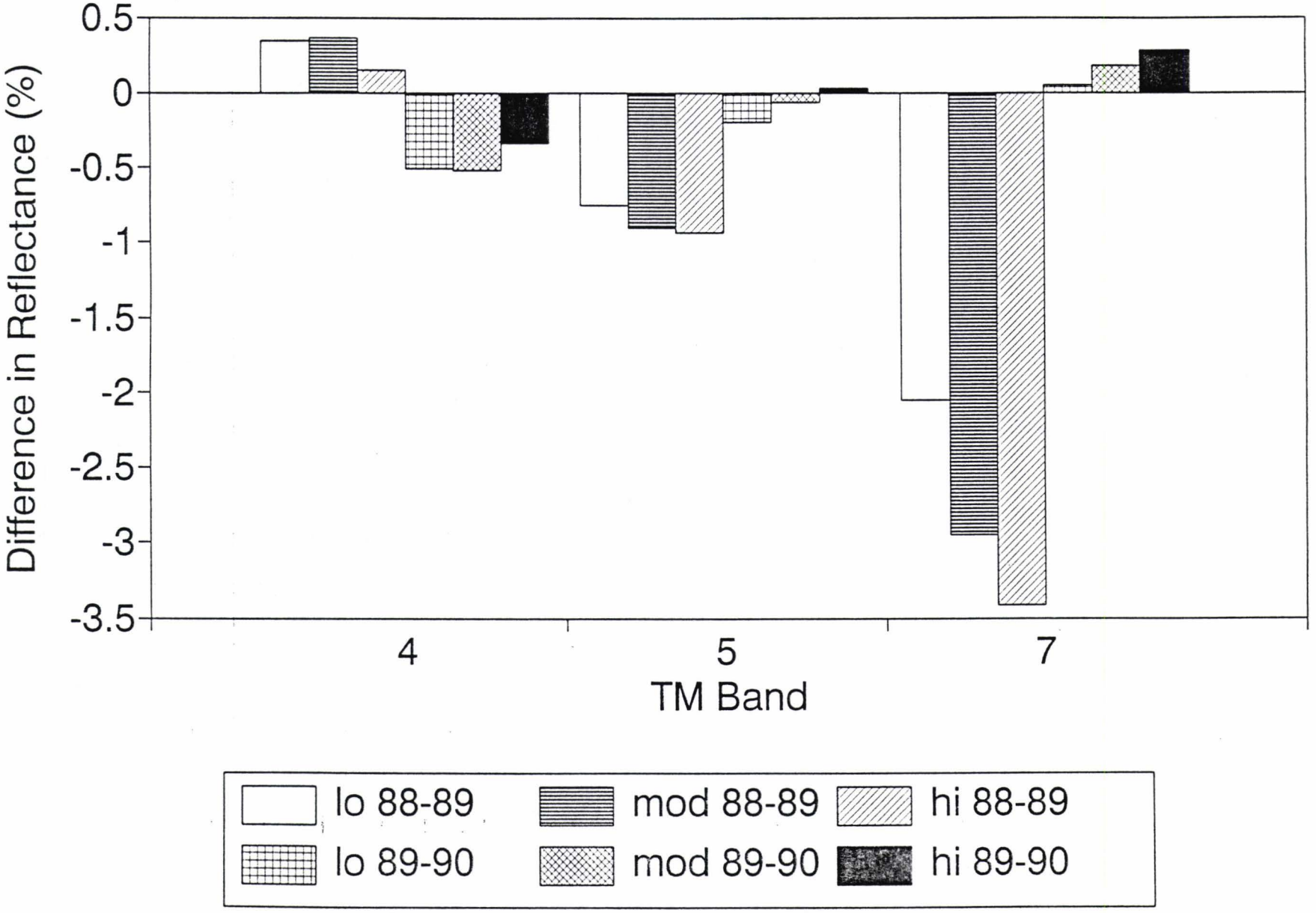

Figure 9 - Flowchart showing breakdown of burn area by vegetation type and burn severity.

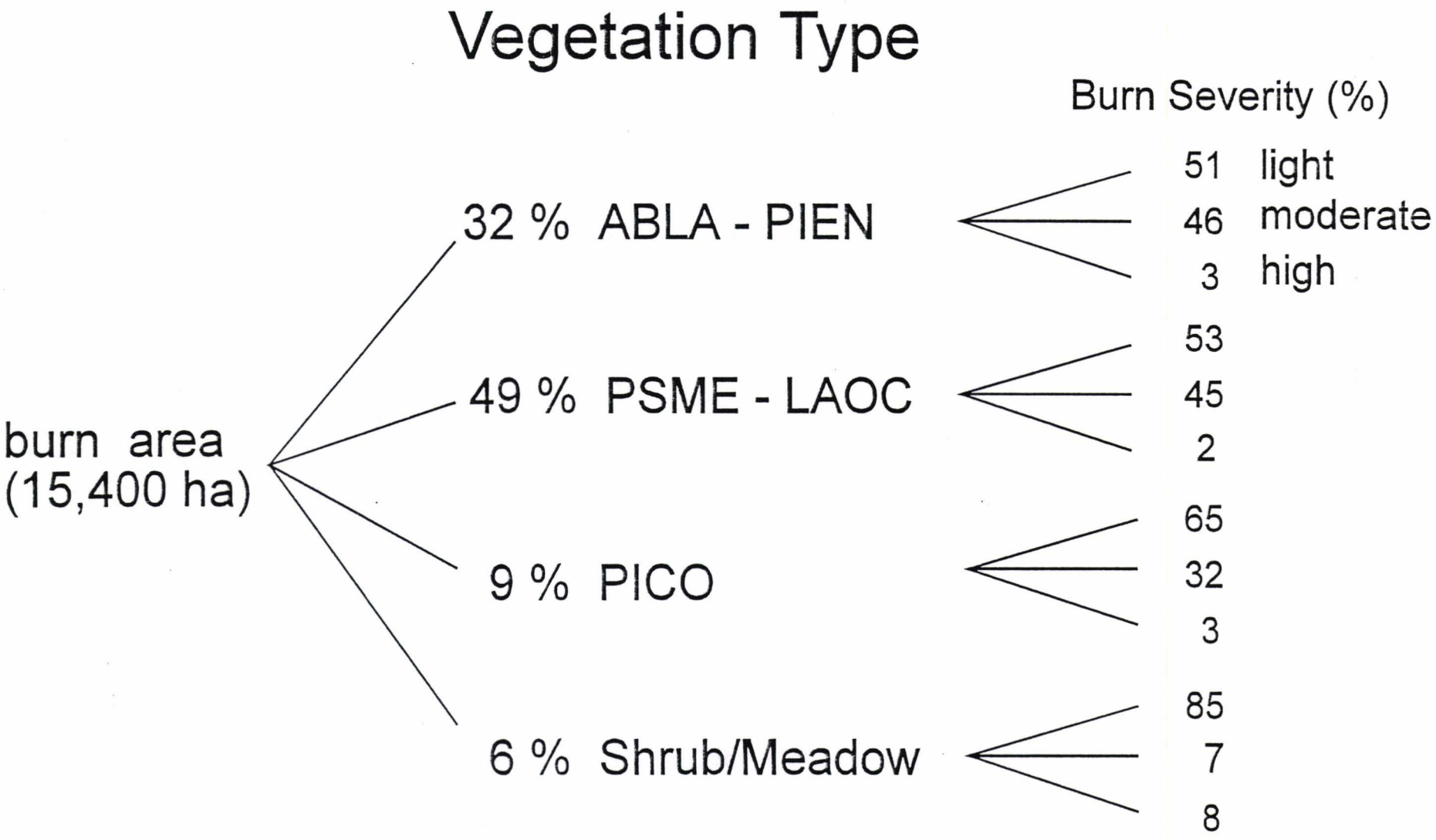
Vegetation Type
Burn Severity (%)
burn area
(15,400 ha)
32 % ABLA - PIEN
51 light
46 moderate
3 high
49 % PSME - LAOC
53
45
2
9 % PICO
65
32
3
6 % Shrub/Meadow
85
7
8

Figure 10 - Outflow hydrograph for the Columbia Falls, MT, and Tuchuck near Flathead, BC, stations and the modeled outflow data.

Hydrologic Outflow

Red Bench Fire

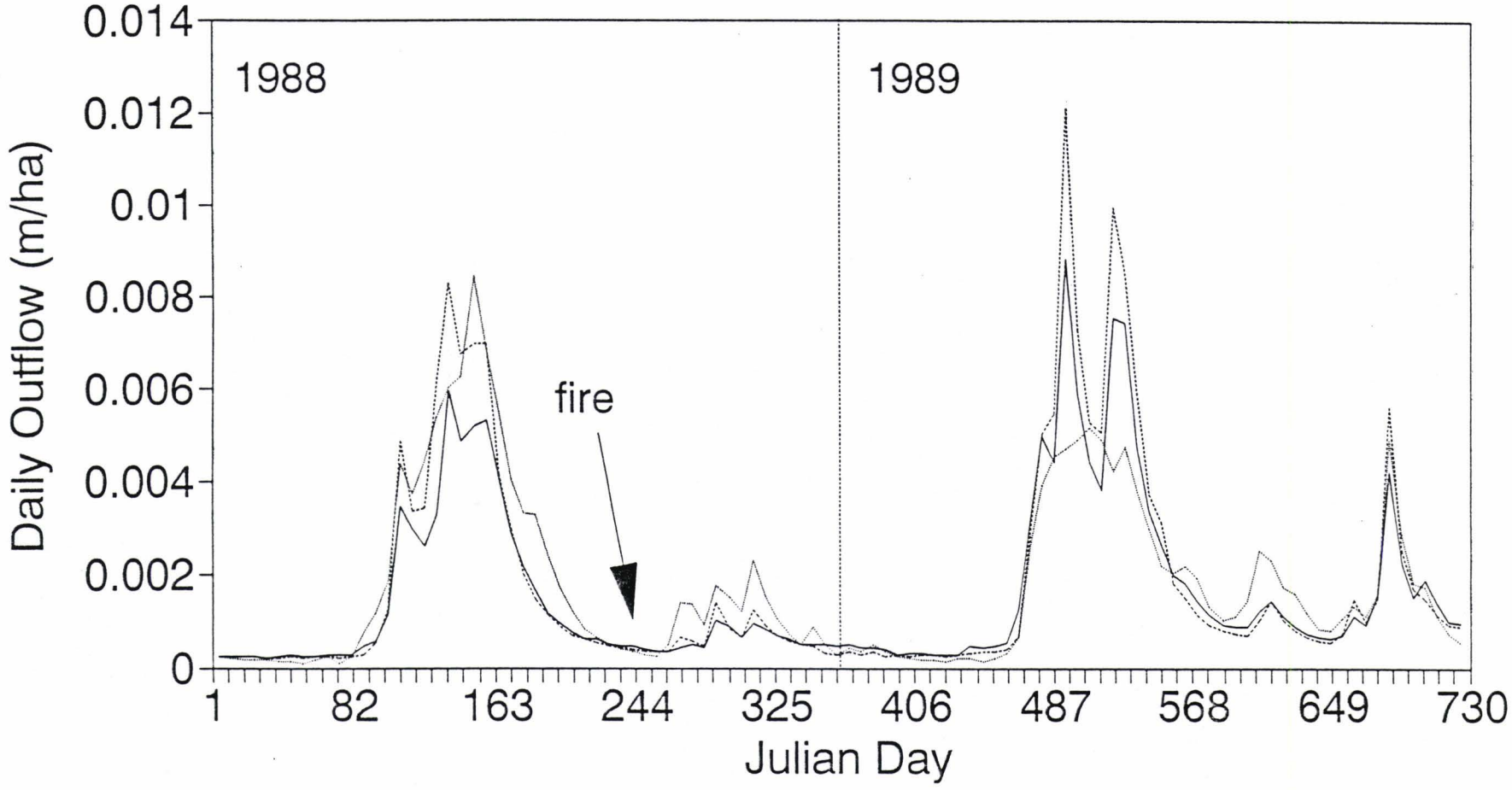

model — Columbia Falls ····· Tuchuck, B.C.

Figure 11 - Residual error ($\hat{E}$) between the Columbia Falls v. model, Tuchuck v. model, and Columbia Falls v. Tuchuck hydrologic outflow data.

Residual Error of Various Outflow Data

Red Bench Fire

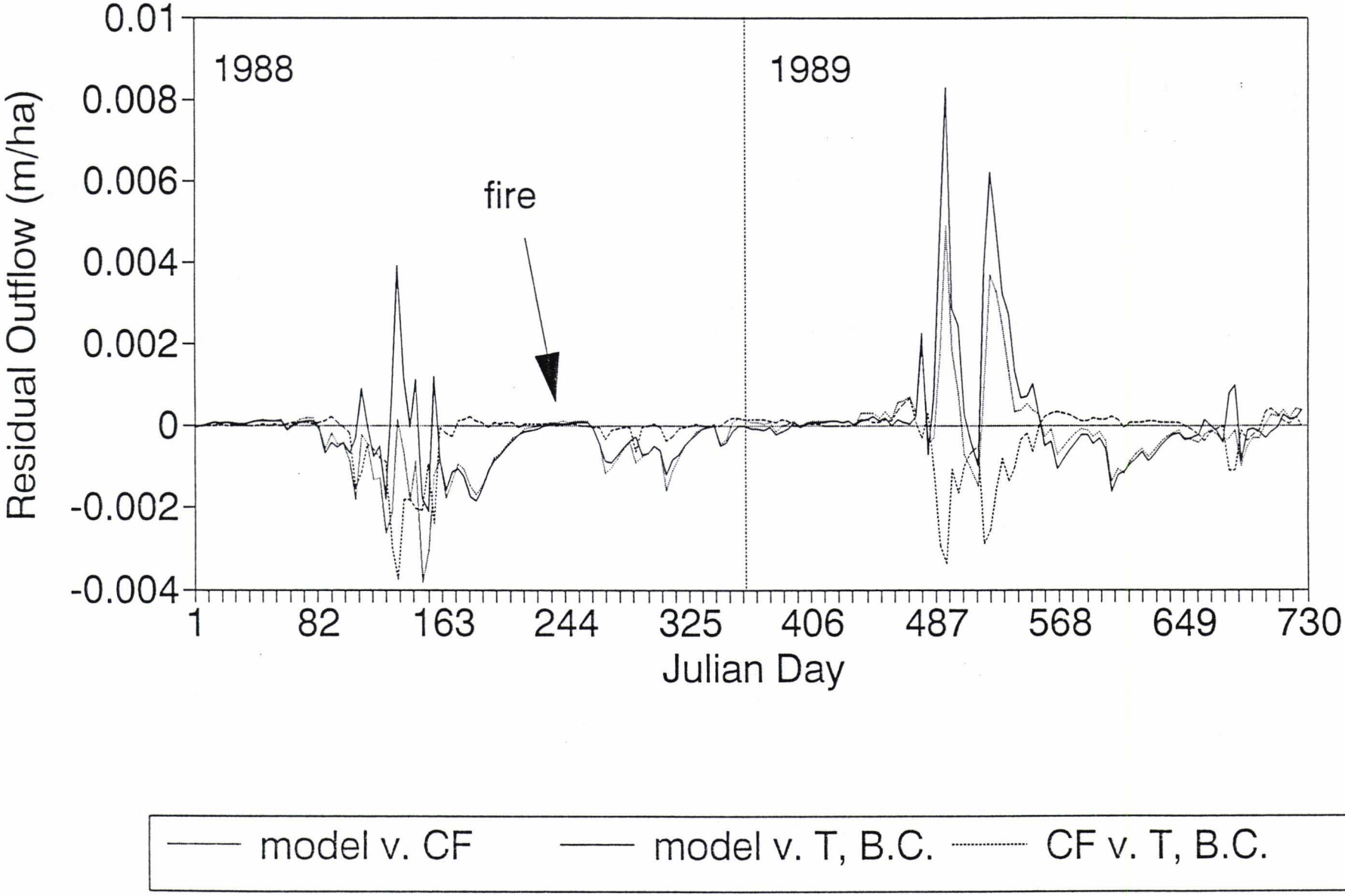

Figure 12 - $\hat{E}$ values between model simulations with and without fire in the North Fork landscape.

Residual Error of Modeled Outflow Data

fire v. no-fire model

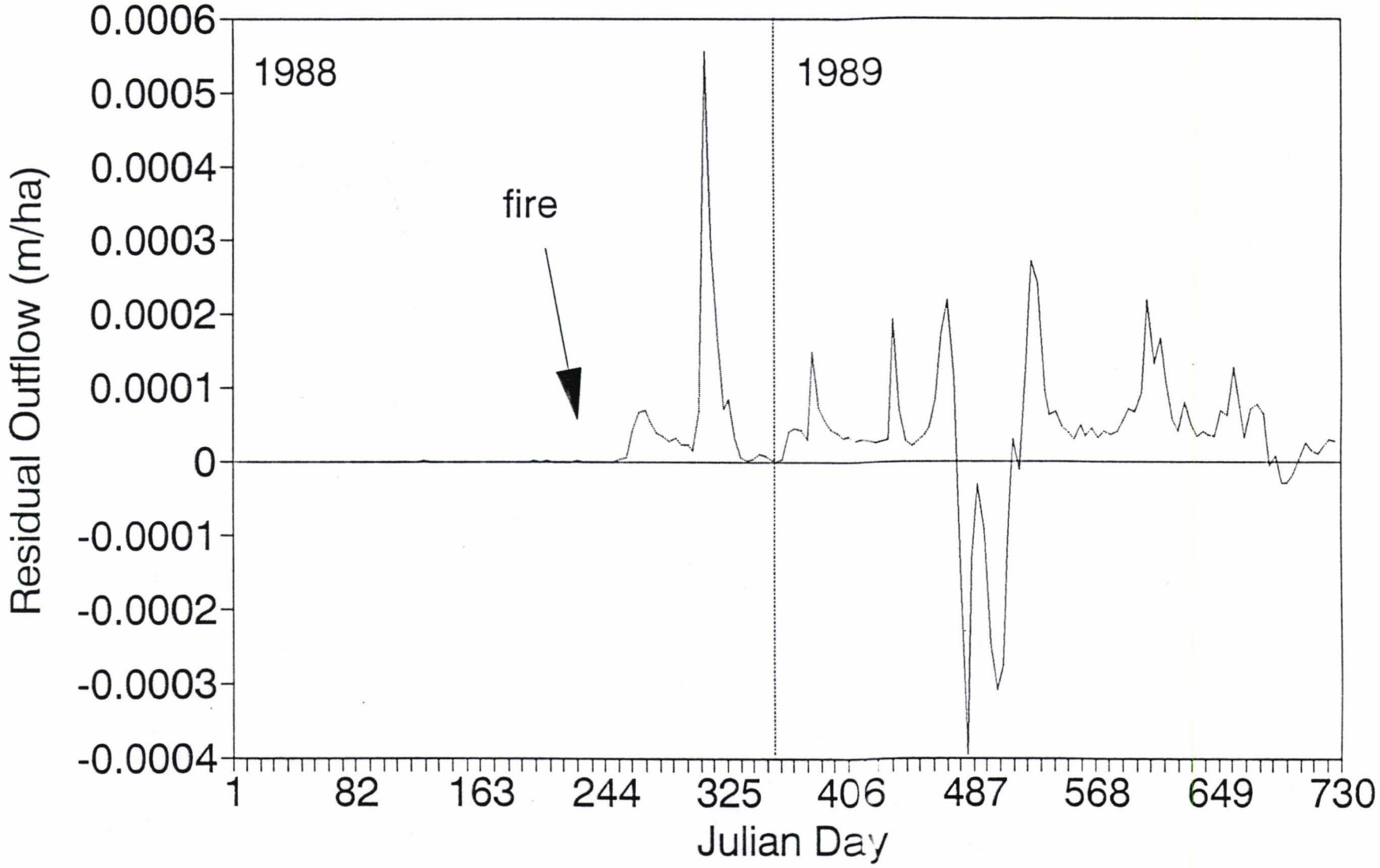

Figure 13 - Cumulative precipitation for the National Weather Station at Polebridge, MT, between JD 100 and 300 for 1988 and 1989.

Cumulative Precipitation 1988 & 1989

Polebridge Weather Station

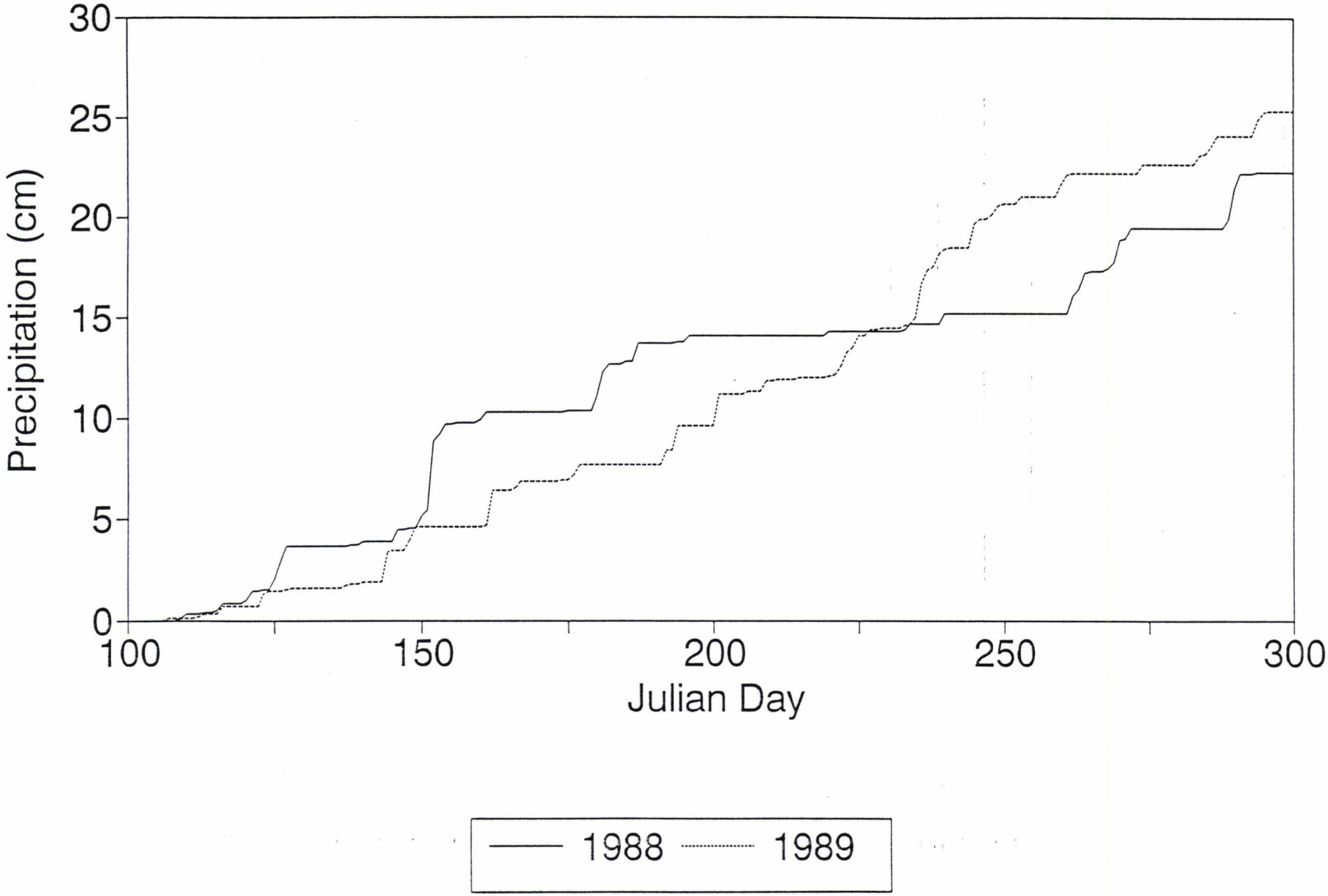

Figure 14 - Distribution of ANPP by area for 1988 and 1989 for the Red Bench Fire ecosystem simulations.

Distribution of Area of ANPP

1988 and 1989 : Red Bench Fire

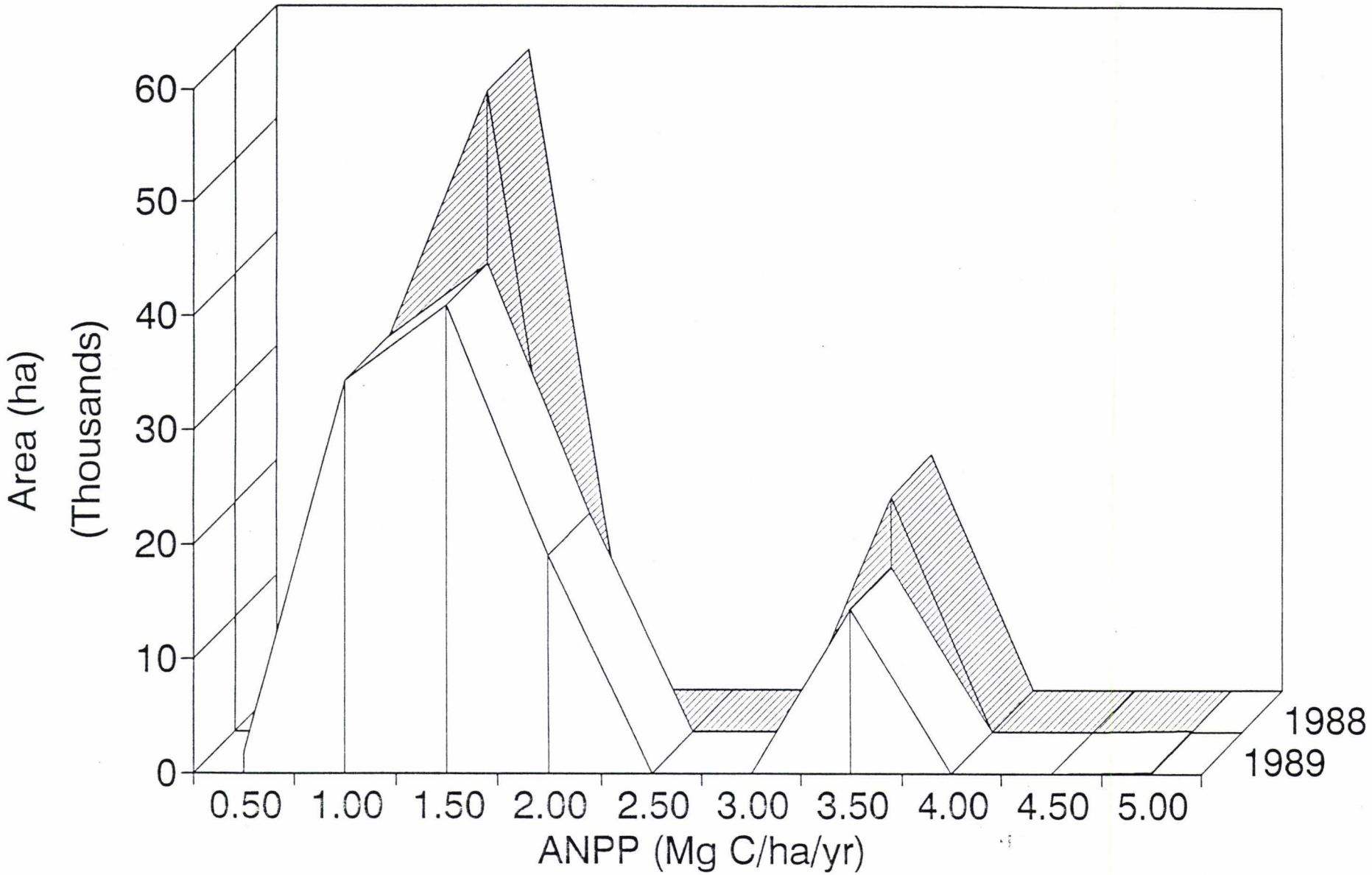

Figure 15 - Image showing spatial distribution of ANPP for the Red Bench Fire area for 1988 and 1989.

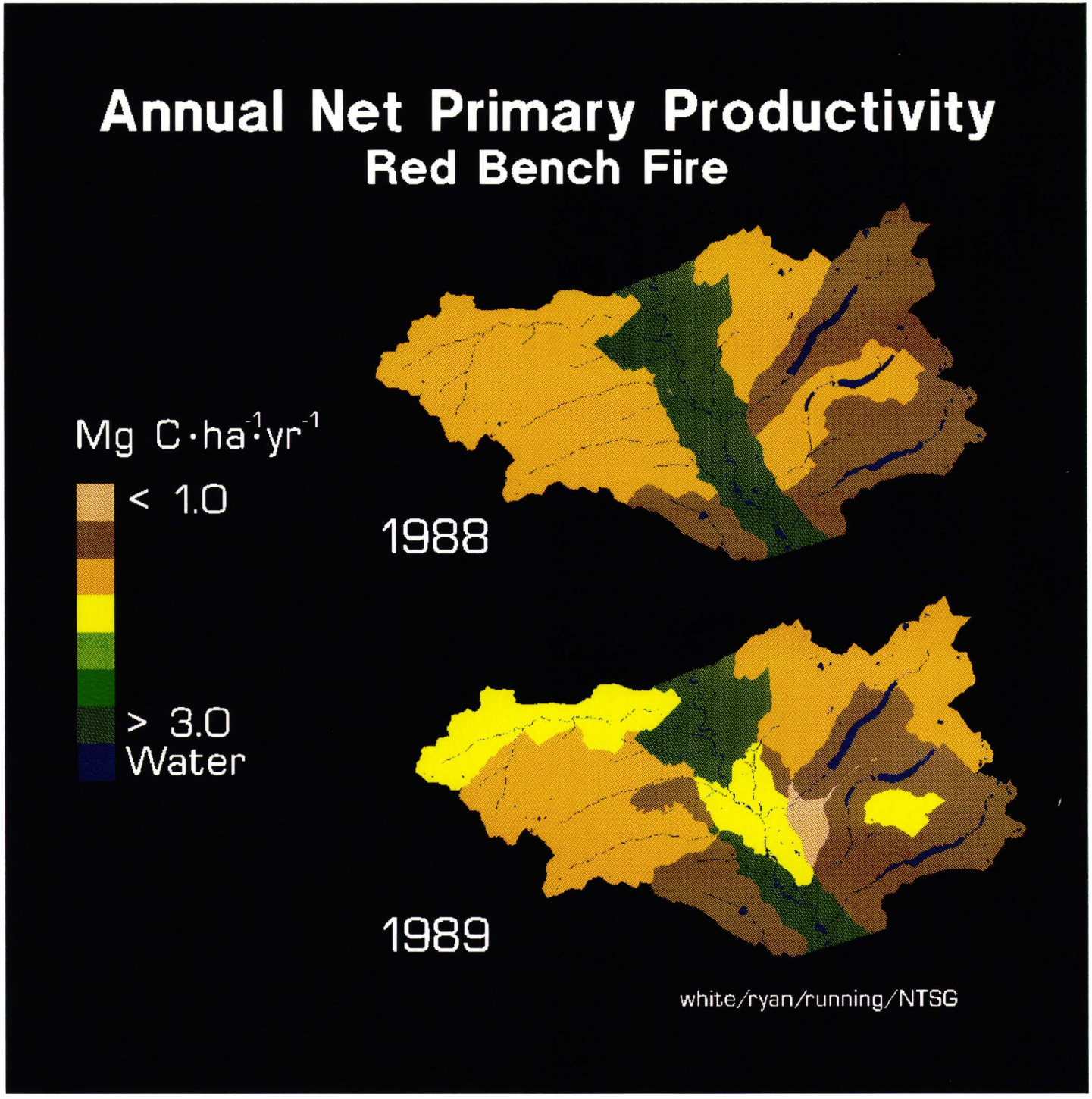
Annual Net Primary Productivity
Red Bench Fire
Mg C·ha-1·yr-1
< 1.0
> 3.0
Water
1988
1989
white/ryan/running/NTSG

Appendix 1 - ECODATA plot summaries for data used in the North Fork vegetation mapping process.

GNP - RED BENCH FIRE ECODATA PLOTS FOR SPECTRAL TRAINING
SELECTED SITES

SPEC SIG ID	PLOT ID	UTM EAST	NORTH	E C	S T	TREE (# denotes cover)						SHRUB/GRASS/FORBS						
36	181G864059	**273040**	**5427770**	C	1							SPBE(1)						
1	181G863046	**272493**	**5427087**	C	1							CAXX	POXX(1)					
95	107L88T302	**255262**	**5392630**	C	1	ABLA	LAOC	PIEN	PSEM	PICO(1)		S(1)	F(1)					
8	107L88L084	**232733**	**5416241**	C	1	ABLA	LAOC	PIEN	PSEM	PICO(1)		S(1)	G(1)	F(1)	G(1)			
11	107L88T301	**254029**	**5393302**	C	1	ABLA	LAOC	PIEN	PSEM	PICO(1)		S(1)						
14	107E89B112	**244412**	**5418560**	C	1	ABLA	PICO(1)					CACA	EPAN(1)					
7	181L872502	**288524**	**5402175**	C	1	ABLA	PIEN(1)					VAGL(1)	G(1)	XETE(2)	F(1)			
51	107E89B108	**234226**	**5416655**	C	1	ABLA	PSME(1)					RUPA(1)	GATR	ANMA(1)				
13	107L88L126	**246410**	**5389638**	C	1	ABLA(1)						CAXX	XETE(1)	ACMI	CACA	EPAN(1)		
27	107G873716	**233531**	**5410731**	C	1	ABLA(1)						XETE	CAGE(1)	ACMI	EPAN	ANMA(1)		
32	181L874544	**286824**	**5401346**	C	1	ABLA(1)						CAGE(3)	POXX(2)	ARLA(2)				
5	181G863058	**282547**	**5411498**	C	1	ABLA(1)						VAGL(1)	CAGE(1)	XETE(4)				
2	181G863047	**272301**	**5427349**	C	1	ABLA(1)						CAXX(1)	SETR(2)					
186	181G862059	**275487**	**5427763**	C	1	ABLA(3)						VAGL(1)	XETE	CAXX(1)	ASER(1)			
9	107L88R019	**243990**	**5410154**	C	1	LAOC	PIEN	PSEM	PICO(1)			S(1)	EPAN(2)	F(1)				
6	181G864065	**276007**	**5428157**	C	1	N	A											
3	107E89B114	**244333**	**5417562**	C	1	PICO	LAOC(1)					FRVI(2)	ACMI(1)					
28	107L88L077	**259175**	**5402965**	C	1	PICO(1)						AMAL	SYAL(1)	F(1)				
29	107L88L076	**259182**	**5403235**	C	1	PICO(1)						SPBE	AMAL	SYAL(1)	G(1)	F(1)		
10	107L88N032	**248220**	**5418804**	C	1	PIEN	PICO(1)					AMAL	SYAL(1)	CACO(1)	FRVI(2)	CISI(		
45	181G862173	**266485**	**5395901**	C	1	PIEN	PSEM	PICO(1)				AMAL	SYAL(1)	G(1)	F(1)			
12	107G863005	**255112**	**5405796**	C	1	PIEN(1)						CACA(2)	ASER	GATR(1)				
44	181G862018	**257788**	**5410712**	C	1	PIEN(1)						SYAL(2)	ACMI	CISI(1)				
98	107G864132	**253238**	**5418595**	C	1	PSME(1)						SYAL(1)	CACO(1)	ASER(1)				
47	181G862039	**268417**	**5397148**	C	1	PSME(2)	LAOC(1)					SPBE(2)	SYAL	AMAL(1)	F(1)	G(1)		
50	107G864164	**243629**	**5404407**	C	2							ALSI(3)	SOSC(2)	S(1)	ABLA(1)	VEVI	F(1)	
40	107G864162	**243225**	**5404901**	C	2	ABLA	PIEN	PSME(1)				ALSI	PAMY	VAGL(1)	EPAN(2)	F(1		
57	181G863024	**270012**	**5386343**	C	2	ABLA	PIEN	PSME(1)				MEFE(3)	VAGL	S(1)	G(1)	XETE	F	
69	107L88R007	**261540**	**5385280**	C	2	ABLA	PIEN	PSME(1)				ALSI	SAXX	S(1)	G(1)	F(1)		
67	107L88T002	**251992**	**5393195**	C	2	ABLA	PIEN(1)					ALSI(3)	S(1)	EPAN	F(1)			
42	107G864093	**248961**	**5389057**	C	2	ABLA	PIEN(1)					MEFE(2)	VAGL	S(1)	CAGE(1)	ARLA(2)		
38	181L872504	**286579**	**5401671**	C	2	ABLA	PIEN(1)					ALSI(4)	S(1)	F(1)				
60	107L88N086	**252542**	**5392893**	C	2	ABLA	PIEN(1)					MEFE	RUPA(2)	ALSI	S(1)	G(1)	F(1)	
102	181G862046	**269109**	**5429359**	C	2	ABLA	PIEN(1)					MEFE(2)	S(1)	GATR(1)				
62	107L88L100	**238824**	**5407412**	C	2	ABLA	PIEN(1)					RUPA(2)	S(1)	G(1)	EPAN	F(1)		
55	107L88R031	**235092**	**5424942**	C	2	ABLA	PSME(1)					ACGL	AMAL	S(1)	F(1)			
58	107G863106	**245065**	**5411330**	C	2	ABLA	PSME(1)					ACGL	VAGL	S(1)	CAGE	G(1)	XETE	F(1)
46	107G863070	**246640**	**5401391**	C	2	ABLA	PSME(1)					AMAL	S(1)	CAGE(1)	F(1)			
41	107G864146	**239844**	**5398986**	C	2	ABLA(1)						VAGL(2)	CAGE(1)	XETE(2)	F(1)			

GNP - RED BENCH FIRE ECODATA PLOTS FOR SPECTRAL TRAINING
SELECTED SITES

SPEC SIG ID	PLOT ID	UTM EAST	NORTH	E C	S T	TREE (# denotes cover)						SHRUB/GRASS/FORBS						
90	107E89B110	**239814**	**5417840**	C	2	ABLA(1)						ANMA	GATR(1)					
63	181G862051	**271000**	**5428180**	C	2	ABLA(1)						RUPA(2)	ACGL	RIXX	S(1)	CACA(1)	THOC	F(1
68	181G862026	**270662**	**5385591**	C	2	ABLA(2)	PIEN(1)					MEFE(4)	VAGL(2)	S(1)	G(1)	F(1)		
65	107L88P080	**252793**	**5392919**	C	2	PIEN(1)						ALSI(2)	RUPA	SAXX	S(1)	CACA(1)	EPAN	F(1
4	107L88L091	**242475**	**5409881**	C	2	PIEN(1)						RUPA	SAXX	S(1)	CACA	G(1)	EPAN(2)	F(1)
64	181G862172	**266576**	**5395655**	C	2	PINE(1)						AMAL(2)	SPBE(1)	G(1)	ACMI	F(1)		
111	181G862089	**286253**	**5391377**	C	2	PSME(2)	ABLA	PIEN(1)				ACGL(2)	RUPA	S(1)	G(1)	F(1		
94	181G862032	**271440**	**5386069**	C	2	PSME(2)	ABLA(1)					VAGL(2)	S(1)	G(1)	XETE(2)	G(1)		
97	107L88H011	**247671**	**5391341**	C	3	ABLA	LAOC	PIEN	POTR(1)			S(1)	G(1)	XETE	F(1)			
91	107L88T102	**252096**	**5398077**	C	3	ABLA	LAOC	PIEN	PICO	POTR	PSME(1)	ALSI	S(1)	F(1)				
158	107L88P017	**247065**	**5415237**	C	3	ABLA	LAOC	PIEN	PICO	POTR(1)		LONU	S(1)	G(1)	F(1)			
99	107L88N023	**244241**	**5417051**	C	3	ABLA	LAOC	PIEN	PSME(1)			RIXX	S(1)	G(1)	EPAN	F(1)		
107	107L88K037	**244820**	**5406222**	C	3	ABLA	LAOC	PIEN	PICO	POTR	PSME(1)	S(1)	G(1)	F(1)				
114	107L88R009	**261440**	**5386919**	C	3	ABLA	LAOC	PIEN	PICO	POTR(1)		MEFE	S(1)	G(1)	F(1)			
105	107G863121	**239990**	**5398330**	C	3	ABLA	PIEN(1)					RUPA	VASC(1)	CAXX(1)				
92	107L88R061	**240446**	**5419716**	C	3	ABLA	POTR(1)					MEFE	PAMY	S(1)	XETE(2)	F(1)		
151	107G873020	**229676**	**5417060**	C	3	ABLA(2)						VAGL	VASC(1)	CAGE	CAXX(1)	XETE(3)		
149	107G863120	**239796**	**5398183**	C	3	ABLA(2)						VASC(1)	CAXX(1)	ARLA(1)				
101	107G864157	**238415**	**5424489**	C	3	ABLA(2)	LAOC	PIEN	POTR	PICO(1)		SAXX(2)	S(1)	F(1				
108	107L88K028	**248800**	**5408120**	C	3	ABLA(2)	PIEN	PICO(1)				MEFE	ALSI	S(1)	CACO	XETE	F	
100	107L88L059	**249518**	**5388754**	C	3	ABLA(2)	PIEN(1)					MEFE(3)	VAGL(1)	XETE(2)	ARLA(1)			
150	107G863072	**246763**	**5401851**	C	3	ABLA(2)	PIEN(1)					VASC	S(1)	CAGE(1)	XETE(3)	F(1)		
116	181G862077	**282024**	**5411554**	C	3	ABLA(3)	PIEN(1)					SYAL	VAGL(1)	CAGE	G(1)	XETE(3)		
104	107G864114	**246840**	**5417365**	C	3	LAOC(2)	ABLA	PIEN	PICO	PSME(1)		ALSI	PAMY	S(1)	F			
152	107G863717	**265201**	**5389957**	C	3	PICO	PSME(2)	ABLA	LAOC	PIEN(1)		ALSI	S(1)	G(1)	F			
115	181G862160	**267159**	**5394907**	C	3	PICO(2)						BERE(2)	SYAL	AMAL(1)	CARU(3)	G(1)	F(1)	
156	107L88R032	**237643**	**5424651**	C	3	PICO(2)	ABLA	PIEN(1)				VASC	S(1)	CARU	G(1)	F(1)		
110	107G863083	**244669**	**5417624**	C	3	PICO(2)	LAOC	PIEN(1)				VASC(2)	S(1)	G(1)	EPAN	F(1		
161	107G863012	**264637**	**5389938**	C	3	PICO(2)	LAOC	PSME(1)				SPBE	S(1)	CARU(1)	F(1)			
125	107G863095	**255040**	**5393419**	C	3	PICO(3)	ABLA	LAOC	PSME(1)			PAMY	S(1)	XETE(1)				
83	181L88N006	**269286**	**5389970**	C	3	PICO(3)	LAOC	PIEN	PSME(1)			SPBE	S(1)	CARU	G(1)	F		
76	107G863138	**251670**	**5418686**	C	3	PICO(4)	ABLA	LAOC	PIEN(1)			PAMY	S(1)	CARU(1)	F(1			
140	107G864112	**245976**	**5416879**	C	3	PICO(4)	ABLA	PSME(1)				PAMY(2)	S(1)	XETE(3)				
70	107L88L030	**258358**	**5388117**	C	3	PSME(1)						SYAL(2)	S(1)	CAGE(1)	EPAN	F(1)		
181	181G862006	**275412**	**5389772**	C	4	ABLA	PIEN	PIAL	PICO	PSME(1)		LIBO(2)	S(1)	G(1)	F			
165	107L88L191	**236795**	**5429690**	C	4	ABLA	PIEN	PIAL	PICO(1)			VASC	S(1)	F(1)				
135	181G864076	**279463**	**5407253**	C	4	ABLA(1)	T(3)											
123	181G862027	**270885**	**5385563**	C	4	ABLA(3)	PIEN(1)					MEFE(4)	VAGL	S(1)	F(1)			
169	107L88L060	**248540**	**5389073**	C	4	ABLA(3)	PIEN(1)					MEFE	VAGL	S(1)	ARCO	F(1)		

GNP - RED BENCH FIRE ECODATA PLOTS FOR SPECTRAL TRAINING
SELECTED SITES

SPEC SIG ID	PLOT ID	UTM EAST	NORTH	E C	S T	TREE (# denotes cover)					SHRUB/GRASS/FORBS						
113	181G863001	**256923**	**5412026**	C	4	LAOC	PIEN	PICO	PSME(1)		LIBO	S(1)	CARU(2)	F(1)			
112	107L88H007	**264654**	**5384554**	C	4	LAOC	PIEN	PICO(1)			PAMY	SAXX	S(1)	G(1)	ARLA	F(1)	
86	182G862078	**293238**	**5394714**	C	4	LAOC	PIEN(1)	T(9)									
180	107L88P030	**250546**	**5418561**	C	4	LAOC(3)	ABLA	PIEN	PICO	PSEM(1)	LIBO(2)	S(1)	G	F			
163	107G863132	**236596**	**5423543**	C	4	PICO(2)	ABLA	LAOC	PIEN	PSME(1)	MEFE(2)	S(1)	F(1				
170	107L88L089	**239814**	**5417856**	C	4	PICO(2)	ABLA	LAOC	PIEN	PSME(1)	LIBO	MEFE(3)	VAGL(1)	ARLA	F(1)		
139	107G864138	**244227**	**5411908**	C	4	PICO(2)	ABLA	PIAL(1)			VAGL	VASC	S(1)	XETE(2)	F(1		
79	107L88H002	**263865**	**5388412**	C	4	PICO(3)	PIEN	PSME(1)			ALSI	RUPA	S(1)	G(1)	F(1)		
182	107G864004	**256094**	**5405294**	C	4	PICO(3)	PIEN(2)				LIBO(2)	S(1)	CARU(3)	ARLA(3)	F(		
72	107G862179	**253251**	**5416514**	C	4	PICO(4)	ABLA	PIEN(1)			VASC	S(1)	CARU(2)	CAGE(1)			
132	181G862159	**266912**	**5395218**	C	4	PICO(4)	ABLA	PIEN(1)			SYAL	LIBO(3)	ROXX(2)	F(1)			
103	181G862016	**257304**	**5410557**	C	4	PIEN	PICO(1)				AMLA	SYAL(1)	THOC	F(1)			
80	107G863008	**254949**	**5405447**	C	4	PIEN(3)					ALSI(1)						
147	181G864154	**255890**	**5428495**	C	4	PSME(3)	PICO(1)				SYAL	SPBE	S(1)	CARU(3)	F(1)		
82	182G862098	**290446**	**5388344**	C	4	PSME(5)	ABLA	PICO(1)			VAGL	S(1)	XETE	F(1)			
109	107G862008	**265297**	**5388567**	C	5	ABLA	LAOC	PIEN	PICO	PSME(1)	S(1)	G(1)	F(1)				
153	107L88N012	**261972**	**5386370**	C	5	ABLA	LAOC	PIEN	PSME(1)		MEFE	PACMY	S(1)	G(1)	F(1		
145	107L88P013	**246328**	**5415060**	C	5	ABLA	LAOC	PIEN	PSME(1)		SPBE	S(1)	F(1)				
144	182G862079	**292309**	**5393918**	C	5	ABLA	LAOC	PIEN	PSME(1)		PAMY	S(1)	XETE(2)	F(1)			
183	181G862094	**285357**	**5391237**	C	5	ABLA	LAOC	PIEN	PICO(1)		LIBO	SPBE	VAGL	S(1)	G(1)		
166	107L88L182	**241059**	**5422162**	C	5	ABLA	PIEN(1)				VAGL(1)	ARLA	XETE(1)				
84	181G863045	**272620**	**5427542**	C	5	ABLA	PIEN(1)				VAGL(1)						
141	107G863081	**245040**	**5417088**	C	5	ABLA(2)	LAOC	PIEN	PSME(1)		PAMY	S(1)	F(1)				
142	181G863142	**270045**	**5403934**	C	5	ABLA(2)	LAOC	PIEN	PSME(1)		PAMY	S(1)	F(1)				
154	107G863123	**246040**	**5411288**	C	5	ABLA(2)	LAOC	PSME(1)			ACGL(2)	PACMY	S(1)	G(1)	F(		
184	181G863036	**267362**	**5398459**	C	5	LAOC	PIEN	PSME(1)			SYAL(2)	RUPA	S(1)	CARU	G(1)	F	
157	181G863127	**254817**	**5427642**	C	5	LAOC	PSME(2)	ABLA	PIEN	PICO(1)	S(1)	CARU(1)	F(1				
85	107L88A082	**245816**	**5398243**	C	5	PIEN(1)											
155	182G862076	**291722**	**5394473**	C	5	PIEN(2)	ABLA(1)				COST	S(1)	G(1)	F(1)			
81	181G863032	**275913**	**5388000**	C	5	PIEN(3)					COST	S(1)	F(1)				
167	107G863084	**245638**	**5417727**	C	5	PIEN(3)	ABLA	LAOC(1)			LONU	S(1)	ARLA	F(1)			
172	181G862174	**265713**	**5395820**	C	5	PIEN(3)	ABLA	PICO(1)			SYAL(3)	S(1)	GATR	THOC	F(1		
143	107G864163	**243156**	**5404280**	C	5	PIEN(3)	ABLA(2)	PSME(1)			MEFE	S(1)	ARLA(2)	F(1)			
174	181G862004	**276156**	**5388306**	C	5	PIEN(4)	ABLA(2)				LIBO	S(1)	F(1)				
179	107G863110	**244673**	**5411510**	C	5	PSEM(2)	ABLA	PICO(1)			VAGL	SPBE	PAMY(1)	G(1)XETE			
160	107G863718	**265304**	**5389930**	C	5	PSME(2)					AMAL	S(1)	CARU(2)	G(1)	XETE	F(1)	
185	107G863013	**264526**	**5390223**	C	5	PSME(2)	ABLA	LAOC	PICO(1)		ACGL(2)	S(1)	CARU(1)				
159	181G863126	**254808**	**5427042**	C	5	PSME(2)	PICO(1)	LAOC			AMAL	BERE	S(1)	CARU(2)	F(1		
71	181G862120	**265729**	**5416928**	C	5	PSME(3)	ABLA	LAOC	PIEN	PICO(1)	VAGL	S(1)	G(1)	F			

GNP - RED BENCH FIRE ECODATA PLOTS FOR SPECTRAL TRAINING
SELECTED SITES

SPEC SIG ID	PLOT ID	UTM EAST	NORTH	E C	S T	TREE (# denotes cover)						SHRUB/GRASS/FORBS				
162	107G864109	**246594**	**5416330**	C	5	PSME(3)	LAOC(1)					AMAL	S(1)	CARU(1)	ASCO	F(1)
173	181G862043	**268370**	**5397537**	C	5	PSME(3)	LOAC	PIEN(1)				RUPA(3)	SYAL(2)	S(1)	THOC	
117	107G863015	**264837**	**5390117**	C	5	PSME(3)	PICO(1)					S(1)	CARU(3)	G(1)	F(1)	
89	107G864022	**266086**	**5389440**	C	5	T(3)										
88	107G864019	**266103**	**5388756**	C	5	T(3)										
130	182G862795	**285915**	**5390147**	C	6	ABLA	LAOC	PICO	PIMO	PSME	TABR(1)	S(1)	F(1)			
131	182G862093	**285254**	**5391518**	C	6	ABLA	LAOC	PIEN	PICO	PIMO	TABR(1)	MEFE	S(1)	F(1)		
171	182G862101	**289590**	**5388770**	C	6	ABLA	LAOC	PIMO	TABR	THPL(1)		VAGL(2)	S(1)	XETE(2		
124	107L88N088	**247462**	**5398761**	C	6	ABLA	PIEN	PIAL	PSME(1)			MEFE(3)	S(1)	F(1)		
122	107L88L210	**250170**	**5395191**	C	6	ABLA	PIEN	PIAL(1)				VASC(2)	VAGL(1)	XETE	F(1)	
136	107L88L072	**249240**	**5394630**	C	6	ABLA	PIEN	PIAL(1)				VAGL	VASC(1)	XETE	F(1)	
87	182G862077	**291945**	**5394280**	C	6	ABLA(1)	T(5)									
137	107L88P077	**241823**	**5397100**	C	6	ABLA(2)	PIEN	PIAL(1)				VAGL(2)	VASC(1)	XETE(2		
118	107L88L184	**240940**	**5422684**	C	6	ABLA(2)	PIEN	PIAL(1)				MEFE(2)	VASC(1)	ARLA	F(1)	
175	107G874006	**234321**	**5412494**	C	6	ABLA(2)	PIEN	TABR(1)				MEFE(3)	S(1)	ARLA(2)	F(1)	
75	182G862095	**288436**	**5388484**	C	6	LAOC(2)	THPL	TSHE	PIMO(1)			S(1)	F(1)			
74	182G862080	**292192**	**5394080**	C	6	LAOC(3)	THPL(2)	PIEN	TSHE(1)			F(1)				
133	181G864155	**255853**	**5427766**	C	6	PIEN(2)						ACGL	RUPA(1)	F(1)		
126	181L874541	**288168**	**5401684**	C	6	PIEN(2)	ABLA					MEFE(2)	S(1)	F(1)		
129	182G862102	**289080**	**5389075**	C	6	PIMO(2)	LAOC	TABR	THPL(1)			ACGL	PAMY(1)	S(1)	F(1	
93	181G862042	**268258**	**5397515**	C	6	PSME(1)						RUPA(2)	CLUN	THOC	F(1)	
134	107L88P022	**244086**	**5418180**	C	6	PSME(4)	PICO(1)					ACGL(3)	S(1)	F(1)		
128	181L874538	**287522**	**5398556**	C	6	TABR(2)	PIEN	PSME(1)	ABLA			SPBE	ACGL	VAGL	S(1)	F
73	181G862088	**286610**	**5390993**	C	6	TSHE(3)	ABLA	LAOC	PIEN	PIMO	TABR(1)	S(1)	F(1)			
78	182G862781	**292403**	**5394587**	C	6	TSHE(3)	PIEN	PIMO	THPL(1)			ACGL(1)	F(1)			
77	182G862092	**285402**	**5391798**	C	6	TSHE(3)	TABR(2)	ABLA	LAOC	PIEN(1)		S(1)	F(1)			
106	107L88Z022	**233252**	**5420421**	C	8	ABLA	PIAL(1)					VAGL	VASC(1)	G(1)	F(1)	
176	107L88Z019	**234468**	**5420482**	C	8	ABLA	PIEN	PIAL(1)				VASC(2)	G(1)	F(1)		
120	107L88Z020	**234675**	**5420490**	C	8	PIAL(2)	ABLA	LAOC	PIEN(1)			VASC(2)	G(1)	F(1)		
121	107L88Z023	**232992**	**5420572**	C	8	PIAL(2)	ABLA	LAOC	PIEN(1)			VASC	VAGL(2)	G(1)	F(1	
178	181G864130	**261890**	**5406430**	E	5	POPTRE(	PIEN(1)					COST	SYAL(2)	S(1)	G(1)	F(1)
148	181G862171	**266540**	**5395676**	E	5	POPTRE(	PIEN	POPTRI(1)				S(3-1)	G(1)	F(1)		
177	181G864127	**262134**	**5405906**	E	5	POPTRE(	PIEN	POPTRI(1)				S(3-1)	G(1)	F(1)		
49	181G864075	**282273**	**5410750**	F	2							S(3)	VIAM(1)			
53	181G862085	**281690**	**5392186**	F	2							SADR(4)	POPR	G(1)		
48	181G862031	**271390**	**5385830**	F	2							S(5)	THOC(1)			
39	107G864167	**252690**	**5416321**	F	2							SADR(1)	FRVI	F(1)		
37	107E89B162	**237736**	**5407095**	F	2							POFR(2)				
52	107E89B097	**237806**	**5406086**	F	2							SADR(3)	G(1)			

GNP - RED BENCH FIRE ECODATA PLOTS FOR SPECTRAL TRAINING
SELECTED SITES

SPEC SIG ID	PLOT ID	UTM EAST	NORTH	E C	S T	TREE (# denotes cover)	SHRUB/GRASS/FORBS					
26	181G862083	**281185**	**5392298**	H	1		POPR(1)	G(1)	ACMI	VIAM	F(1)	ROXX(1)
17	107E89B096	**238006**	**5406070**	H	1		CARO(2)					
16	107E89B178	**250407**	**5391545**	H	1		CARO(1)					
23	181G862014	**268032**	**5397123**	H	1		CAXX(2)	G(1)	F(1)	ROXX(1)		
34	181G863030	**275463**	**5388399**	H	2		SADR(1)	POPR(3)	G(1)	F(1)		
19	181G864029	**282778**	**5411313**	K	1		LUHI	G(1)	ASER	F(1)		
24	181G864073	**282052**	**5411080**	K	1		N	A				
25	181G864061	**275555**	**5428326**	K	1		N	A				
21	181L874545	**286419**	**5401714**	K	2		CAXX(1)	HYFO	F(1)			
22	181G864074	**282127**	**5410655**	K	2		THOC(1)					
15	181G863050	**274868**	**5427756**	L	1		CARNI(3)	G(1)	F(1)	S(1)		
43	181G864072	**281940**	**5411292**	L	1		N	A				
31	181G862053	**273261**	**5428227**	L	1		CANI(2)	LUHI	G(1)	SETR	F(1)	PHEM(1)
30	181G863051	**275034**	**5427827**	L	1		CANI(2)	G(1)	F(1)	S(1)		
33	107G864137	**244217**	**5411698**	N	1		CAGE(2)	G(1)	AMAL(1)	HECY	F(1)	
18	107G864089	**247507**	**5401379**	N	2		N	A				
35	107G864124	**255884**	**5394827**	N	2		AMAL(1)	AGSP	CAGE(2)	CARO(1)	F(1)	

Appendix 2 - Summary of GIS file by class number showing the Kessell model (1979) descriptions and relative cover values used by forest species groups.

Red Bench "Rule" Sheet
Relative Cover Values by Species
from Kessell's Nomograms across Topoelevational Gradients
(burn = time since burn; elev = elevation in m
topo = topographic gradient where B is bottomland etc.)

#	burn	elev	topo	ABLA PIEN	PIAL	PSME LAOC	PICO	DECID
1	20	1250	B	0.26	0.01	0.39	0.18	0.03
2	20	1250	R	0.26	0.01	0.39	0.18	0.03
3	20	1250	D	0.17	0.01	0.50	0.17	0.03
4	20	1250	S-ne	0.16	0.00	0.33	0.16	0.10
5	20	1250	S-sw	0.14	0.00	0.42	0.14	0.09
6	20	1250	O-ne	0.12	0.00	0.35	0.12	0.08
7	20	1250	O-sw	0.09	0.00	0.30	0.24	0.03
8	20	1250	X-ne	0.16	0.01	0.24	0.41	0.02
9	20	1250	X-sw	0.16	0.01	0.24	0.41	0.02
10	20	1500	B	0.40	0.01	0.19	0.25	0.02
11	20	1500	R	0.40	0.01	0.19	0.25	0.02
12	20	1500	D	0.36	0.01	0.26	0.23	0.02
13	20	1500	S-ne	0.24	0.01	0.41	0.21	0.01
14	20	1500	S-sw	0.24	0.01	0.41	0.21	0.01
15	20	1500	O-ne	0.22	0.01	0.37	0.28	0.01
16	20	1500	O-sw	0.15	0.01	0.41	0.30	0.01
17	20	1500	X-ne	0.15	0.01	0.41	0.30	0.01
18	20	1500	X-sw	0.11	0.01	0.43	0.32	0.02
19	20	1750	B	0.56	0.11	0.10	0.01	0.02
20	20	1750	R	0.53	0.19	0.07	0.05	0.02
21	20	1750	D	0.57	0.17	0.06	0.05	0.01
22	20	1750	S-ne	0.43	0.15	0.08	0.21	0.01
23	20	1750	S-sw	0.38	0.17	0.08	0.23	0.02
24	20	1750	O-ne	0.28	0.15	0.15	0.30	0.01
25	20	1750	O-sw	0.31	0.07	0.16	0.33	0.01
26	20	1750	X-ne	0.30	0.01	0.24	0.32	0.01
27	20	1750	X-sw	0.30	0.01	0.24	0.32	0.01
28	20	2000	B	0.54	0.08	0.01	0.01	0.02
29	20	2000	R	0.48	0.17	0.01	0.00	0.02
30	20	2000	D	0.43	0.19	0.01	0.01	0.02
31	20	2000	S-ne	0.39	0.20	0.01	0.01	0.02
32	20	2000	S-sw	0.42	0.22	0.01	0.01	0.02
33	20	2000	O-ne	0.33	0.35	0.01	0.05	0.02

Red Bench "Rule" Sheet
Relative Cover Values by Species
from Kessell's Nomograms across Topoelevational Gradients
(burn = time since burn; elev = elevation in m
topo = topographic gradient where B is bottomland etc.)

#	burn	elev	topo	ABLA PIEN	PIAL	PSME LAOC	PICO	DECID
34	20	2000	O-sw	0.33	0.35	0.01	0.05	0.02
35	20	2000	X-ne	0.28	0.29	0.01	0.20	0.01
36	20	2000	X-sw	0.37	0.09	0.01	0.29	0.02
37	20	2500	B	0.41	0.10	0.02	0.01	0.02
38	20	2500	R	0.32	0.11	0.02	0.01	0.03
39	20	2500	D	0.32	0.11	0.02	0.01	0.03
40	20	2500	S-ne	0.43	0.10	0.02	0.01	0.02
41	20	2500	S-sw	0.34	0.11	0.02	0.01	0.03
42	20	2500	O-ne	0.29	0.24	0.02	0.01	0.02
43	20	2500	O-sw	0.12	0.44	0.01	0.01	0.02
44	20	2500	X-ne	0.23	0.38	0.01	0.01	0.02
45	20	2500	X-sw	0.30	0.35	0.01	0.00	0.02
46	20	3000	B	0.32	0.11	0.02	0.01	0.03
47	20	3000	R	0.32	0.11	0.02	0.01	0.03
48	20	3000	D	0.32	0.11	0.02	0.01	0.03
49	20	3000	S-ne	0.32	0.11	0.02	0.01	0.03
50	20	3000	S-sw	0.32	0.11	0.02	0.01	0.03
51	20	3000	O-ne	0.16	0.14	0.02	0.01	0.04
52	20	3000	O-sw	0.19	0.14	0.02	0.01	0.04
53	20	3000	X-ne	0.19	0.14	0.02	0.01	0.04
54	20	3000	X-sw	0.16	0.14	0.02	0.01	0.04
55	50	1250	B	0.21	0.00	0.32	0.15	0.05
56	50	1250	R	0.21	0.00	0.32	0.15	0.05
57	50	1250	D	0.21	0.00	0.32	0.15	0.05
58	50	1250	S-ne	0.16	0.00	0.18	0.16	0.14
59	50	1250	S-sw	0.13	0.00	0.29	0.13	0.12
60	50	1250	O-ne	0.13	0.00	0.28	0.13	0.09
61	50	1250	O-sw	0.10	0.00	0.35	0.16	0.04
62	50	1250	X-ne	0.15	0.01	0.29	0.39	0.02
63	50	1250	X-sw	0.15	0.01	0.29	0.39	0.02
64	50	1500	B	0.40	0.01	0.19	0.25	0.02
65	50	1500	R	0.40	0.01	0.19	0.25	0.02
66	50	1500	D	0.34	0.01	0.27	0.24	0.02

Red Bench "Rule" Sheet
Relative Cover Values by Species
from Kessell's Nomograms across Topoelevational Gradients
(burn = time since burn; elev = elevation in m
topo = topographic gradient where B is bottomland etc.)

#	burn	elev	topo	ABLA PIEN	PIAL	PSME LAOC	PICO	DECID
67	50	1500	S-ne	0.36	0.01	0.26	0.23	0.02
68	50	1500	S-sw	0.29	0.01	0.28	0.25	0.02
69	50	1500	O-ne	0.19	0.01	0.28	0.37	0.02
70	50	1500	O-sw	0.19	0.01	0.28	0.37	0.02
71	50	1500	X-ne	0.19	0.01	0.28	0.37	0.02
72	50	1500	X-sw	0.13	0.01	0.30	0.39	0.02
73	50	1750	B	0.63	0.09	0.08	0.01	0.02
74	50	1750	R	0.44	0.32	0.06	0.04	0.01
75	50	1750	D	0.48	0.29	0.07	0.04	0.01
76	50	1750	S-ne	0.37	0.27	0.07	0.18	0.01
77	50	1750	S-sw	0.32	0.29	0.07	0.19	0.01
78	50	1750	O-ne	0.27	0.25	0.12	0.25	0.01
79	50	1750	O-sw	0.31	0.07	0.16	0.33	0.01
80	50	1750	X-ne	0.28	0.06	0.23	0.30	0.01
81	50	1750	X-sw	0.23	0.24	0.18	0.24	0.01
82	50	2000	B	0.41	0.30	0.01	0.00	0.01
83	50	2000	R	0.41	0.30	0.01	0.00	0.01
84	50	2000	D	0.36	0.32	0.01	0.00	0.02
85	50	2000	S-ne	0.34	0.36	0.01	0.00	0.02
86	50	2000	S-sw	0.34	0.36	0.01	0.00	0.02
87	50	2000	O-ne	0.33	0.35	0.01	0.05	0.02
88	50	2000	O-sw	0.33	0.35	0.01	0.05	0.02
89	50	2000	X-ne	0.28	0.32	0.01	0.21	0.02
90	50	2000	X-sw	0.37	0.09	0.01	0.29	0.02
91	50	2500	B	0.41	0.10	0.02	0.01	0.02
92	50	2500	R	0.41	0.10	0.02	0.01	0.02
93	50	2500	D	0.41	0.10	0.02	0.01	0.02
94	50	2500	S-ne	0.41	0.10	0.02	0.01	0.02
95	50	2500	S-sw	0.27	0.09	0.01	0.01	0.02
96	50	2500	O-ne	0.19	0.14	0.02	0.01	0.04
97	50	2500	O-sw	0.19	0.14	0.02	0.01	0.04
98	50	2500	X-ne	0.19	0.14	0.02	0.01	0.04
99	50	2500	X-sw	0.36	0.13	0.02	0.01	0.03

Red Bench "Rule" Sheet
Relative Cover Values by Species
from Kessell's Nomograms across Topoelevational Gradients
(burn = time since burn; elev = elevation in m
topo = topographic gradient where B is bottomland etc.)

#	burn	elev	topo	ABLA PIEN	PIAL	PSME LAOC	PICO	DECID
100	50	3000	B	0.44	0.05	0.02	0.01	0.02
101	50	3000	R	0.44	0.05	0.02	0.01	0.02
102	50	3000	D	0.44	0.05	0.02	0.01	0.02
103	50	3000	S-ne	0.44	0.05	0.02	0.01	0.02
104	50	3000	S-sw	0.34	0.06	0.02	0.01	0.03
105	50	3000	O-ne	0.27	0.05	0.02	0.01	0.02
106	50	3000	O-sw	0.15	0.05	0.02	0.01	0.03
107	50	3000	X-ne	0.20	0.07	0.02	0.01	0.04
108	50	3000	X-sw	0.18	0.08	0.03	0.01	0.04
109	90	1250	B	0.47	0.04	0.25	0.06	0.02
110	90	1250	R	0.45	0.04	0.26	0.06	0.02
111	90	1250	D	0.37	0.01	0.42	0.05	0.02
112	90	1250	S-ne	0.32	0.01	0.35	0.20	0.01
113	90	1250	S-sw	0.32	0.01	0.35	0.20	0.01
114	90	1250	O-ne	0.19	0.01	0.29	0.17	0.01
115	90	1250	O-sw	0.17	0.00	0.39	0.14	0.01
116	90	1250	X-ne	0.06	0.01	0.52	0.29	0.01
117	90	1250	X-sw	0.06	0.01	0.52	0.29	0.01
118	90	1500	B	0.49	0.01	0.20	0.05	0.03
119	90	1500	R	0.47	0.01	0.23	0.05	0.02
120	90	1500	D	0.53	0.01	0.20	0.05	0.02
121	90	1500	S-ne	0.32	0.01	0.35	0.20	0.01
122	90	1500	S-sw	0.26	0.00	0.46	0.17	0.01
123	90	1500	O-ne	0.21	0.01	0.49	0.18	0.01
124	90	1500	O-sw	0.13	0.01	0.48	0.26	0.01
125	90	1500	X-ne	0.13	0.01	0.32	0.38	0.02
126	90	1500	X-sw	0.15	0.01	0.20	0.45	0.02
127	90	1750	B	0.56	0.11	0.10	0.01	0.02
128	90	1750	R	0.46	0.33	0.06	0.00	0.02
129	90	1750	D	0.51	0.30	0.06	0.00	0.01
130	90	1750	S-ne	0.53	0.29	0.05	0.00	0.01
131	90	1750	S-sw	0.47	0.30	0.06	0.04	0.01
132	90	1750	O-ne	0.36	0.28	0.05	0.19	0.01

Red Bench "Rule" Sheet
Relative Cover Values by Species
from Kessell's Nomograms across Topoelevational Gradients
(burn = time since burn; elev = elevation in m
topo = topographic gradient where B is bottomland etc.)

#	burn	elev	topo	ABLA PIEN	PIAL	PSME LAOC	PICO	DECID
133	90	1750	O-sw	0.33	0.29	0.05	0.20	0.01
134	90	1750	X-ne	0.34	0.31	0.01	0.21	0.01
135	90	1750	X-sw	0.40	0.07	0.01	0.36	0.02
136	90	2000	B	0.58	0.07	0.01	0.00	0.01
137	90	2000	R	0.41	0.30	0.01	0.00	0.01
138	90	2000	D	0.32	0.34	0.01	0.00	0.02
139	90	2000	S-ne	0.32	0.34	0.01	0.00	0.02
140	90	2000	S-sw	0.36	0.32	0.01	0.00	0.02
141	90	2000	O-ne	0.38	0.34	0.01	0.00	0.02
142	90	2000	O-sw	0.38	0.34	0.01	0.00	0.02
143	90	2000	X-ne	0.38	0.34	0.01	0.00	0.02
144	90	2000	X-sw	0.54	0.11	0.02	0.01	0.03
145	90	2500	B	0.41	0.10	0.02	0.01	0.02
146	90	2500	R	0.41	0.10	0.02	0.01	0.02
147	90	2500	D	0.41	0.10	0.02	0.01	0.02
148	90	2500	S-ne	0.41	0.10	0.02	0.01	0.02
149	90	2500	S-sw	0.41	0.10	0.02	0.01	0.02
150	90	2500	O-ne	0.35	0.08	0.01	0.01	0.02
151	90	2500	O-sw	0.19	0.14	0.02	0.01	0.04
152	90	2500	X-ne	0.34	0.11	0.02	0.01	0.03
153	90	2500	X-sw	0.32	0.11	0.02	0.01	0.03
154	90	3000	B	0.44	0.05	0.02	0.01	0.02
155	90	3000	R	0.44	0.05	0.02	0.01	0.02
156	90	3000	D	0.44	0.05	0.02	0.01	0.02
157	90	3000	S-ne	0.34	0.06	0.02	0.01	0.03
158	90	3000	S-sw	0.34	0.06	0.02	0.01	0.03
159	90	3000	O-ne	0.18	0.08	0.03	0.01	0.04
160	90	3000	O-sw	0.15	0.05	0.02	0.01	0.03
161	90	3000	X-ne	0.15	0.05	0.02	0.01	0.03
162	90	3000	X-sw	0.18	0.08	0.03	0.01	0.04
163	150	1250	B	0.60	0.01	0.17	0.01	0.02
164	150	1250	R	0.63	0.01	0.10	0.01	0.03
165	150	1250	D	0.37	0.01	0.13	0.00	0.09

Red Bench "Rule" Sheet
Relative Cover Values by Species
from Kessell's Nomograms across Topoelevational Gradients
(burn = time since burn; elev = elevation in m
topo = topographic gradient where B is bottomland etc.)

#	burn	elev	topo	ABLA PIEN	PIAL	PSME LAOC	PICO	DECID
166	150	1250	S-ne	0.37	0.01	0.13	0.00	0.09
167	150	1250	S-sw	0.33	0.01	0.14	0.01	0.11
168	150	1250	O-ne	0.33	0.01	0.14	0.01	0.11
169	150	1250	O-sw	0.41	0.01	0.25	0.01	0.04
170	150	1250	X-ne	0.41	0.01	0.25	0.01	0.04
171	150	1250	X-sw	0.41	0.01	0.25	0.01	0.04
172	150	1500	B	0.55	0.01	0.16	0.01	0.03
173	150	1500	R	0.61	0.01	0.14	0.01	0.02
174	150	1500	D	0.67	0.01	0.04	0.01	0.03
175	150	1500	S-ne	0.65	0.01	0.16	0.01	0.02
176	150	1500	S-sw	0.47	0.01	0.12	0.00	0.07
177	150	1500	O-ne	0.45	0.01	0.11	0.00	0.07
178	150	1500	O-sw	0.39	0.01	0.12	0.00	0.09
179	150	1500	X-ne	0.41	0.01	0.25	0.01	0.04
180	150	1500	X-sw	0.41	0.01	0.25	0.01	0.04
181	150	1750	B	0.68	0.09	0.04	0.01	0.02
182	150	1750	R	0.51	0.33	0.01	0.00	0.02
183	150	1750	D	0.53	0.32	0.01	0.00	0.01
184	150	1750	S-ne	0.54	0.30	0.03	0.00	0.01
185	150	1750	S-sw	0.46	0.30	0.10	0.00	0.01
186	150	1750	O-ne	0.46	0.30	0.10	0.00	0.01
187	150	1750	O-sw	0.56	0.09	0.15	0.01	0.02
188	150	1750	X-ne	0.66	0.06	0.02	0.01	0.03
189	150	1750	X-sw	0.69	0.01	0.02	0.01	0.03
190	150	2000	B	0.58	0.07	0.01	0.00	0.01
191	150	2000	R	0.41	0.30	0.01	0.00	0.01
192	150	2000	D	0.36	0.32	0.01	0.00	0.02
193	150	2000	S-ne	0.32	0.34	0.01	0.00	0.02
194	150	2000	S-sw	0.32	0.34	0.01	0.00	0.02
195	150	2000	O-ne	0.38	0.34	0.01	0.00	0.02
196	150	2000	O-sw	0.38	0.34	0.01	0.00	0.02
197	150	2000	X-ne	0.37	0.35	0.01	0.00	0.02
198	150	2000	X-sw	0.56	0.11	0.02	0.01	0.03

Red Bench "Rule" Sheet
Relative Cover Values by Species
from Kessell's Nomograms across Topoelevational Gradients
(burn = time since burn; elev = elevation in m
topo = topographic gradient where B is bottomland etc.)

#	burn	elev	topo	ABLA PIEN	PIAL	PSME LAOC	PICO	DECID
199	150	2500	B	0.41	0.10	0.02	0.01	0.02
200	150	2500	R	0.41	0.10	0.02	0.01	0.02
201	150	2500	D	0.41	0.10	0.02	0.01	0.02
202	150	2500	S-ne	0.41	0.10	0.02	0.01	0.02
203	150	2500	S-sw	0.41	0.10	0.02	0.01	0.02
204	150	2500	O-ne	0.27	0.09	0.01	0.01	0.02
205	150	2500	O-sw	0.19	0.14	0.02	0.01	0.04
206	150	2500	X-ne	0.19	0.14	0.02	0.01	0.04
207	150	2500	X-sw	0.16	0.14	0.02	0.01	0.04
208	150	3000	B	0.44	0.05	0.02	0.01	0.02
209	150	3000	R	0.44	0.05	0.02	0.01	0.02
210	150	3000	D	0.44	0.05	0.02	0.01	0.02
211	150	3000	S-ne	0.44	0.05	0.02	0.01	0.02
212	150	3000	S-sw	0.34	0.06	0.02	0.01	0.03
213	150	3000	O-ne	0.34	0.06	0.02	0.01	0.03
214	150	3000	O-sw	0.13	0.06	0.02	0.01	0.03
215	150	3000	X-ne	0.13	0.06	0.02	0.01	0.03
216	150	3000	X-sw	0.18	0.08	0.03	0.01	0.04

Appendix 3 - Summary of GIS file by class number from the spectral classification showing relative cover values by forest species groups derived from ECODATA plot data.

Red Bench "Rule" Sheet
Relative Cover Values by Species
from ECODATA plot data for each Landsat TM spectral class

#	ABLA PIEN	PIAL	PSME LAOC	PICO	DECID
0	0.00	0.00	0.00	0.00	0.00
1	0.00	0.00	0.00	0.00	0.00
2	0.00	0.00	0.00	0.00	0.00
3	0.00	0.00	0.00	0.00	0.00
4	0.00	0.00	0.00	0.00	0.00
5	0.00	0.00	0.00	0.00	0.00
6	0.00	0.00	0.00	0.00	0.00
7	0.00	0.00	0.00	0.00	0.00
8	0.00	0.00	0.00	0.00	0.00
9	0.00	0.00	0.00	0.00	0.00
10	0.00	0.00	0.00	0.00	0.00
11	0.00	0.00	0.00	0.00	0.00
12	0.38	0.07	0.07	0.00	0.17
13	0.82	0.00	0.33	0.00	0.00
14	0.40	0.00	0.40	0.20	0.00
15	0.75	0.00	0.07	0.00	0.00
16	0.67	0.10	0.00	0.00	0.00
17	0.37	0.10	0.27	0.27	0.00
18	0.83	0.00	0.18	0.00	0.00
19	0.14	0.00	0.29	0.57	0.00
20	0.00	0.00	1.00	0.00	0.00
21	0.67	0.00	0.00	0.07	0.27
22	0.42	0.00	0.17	0.42	0.00
23	1.00	0.00	0.00	0.00	0.00
24	0.20	0.00	0.00	0.00	0.80
25	0.25	0.00	0.58	0.17	0.00
26	0.25	0.00	0.38	0.38	0.00
27	0.13	0.00	0.00	0.50	0.38
28	0.20	0.00	0.10	0.60	0.10
29	1.00	0.00	0.00	0.00	0.00
30	0.57	0.04	0.22	0.00	0.00
31	1.00	0.00	0.00	0.00	0.00
32	0.42	0.19	0.23	0.15	0.03
33	0.71	0.00	0.00	0.00	0.00

Red Bench "Rule" Sheet
Relative Cover Values by Species
from ECODATA plot data for each Landsat TM spectral class

#	ABLA PIEN	PIAL	PSME LAOC	PICO	DECID
34	0.00	0.00	0.00	0.00	0.00
35	0.00	0.00	0.00	0.00	0.00
36	0.00	0.00	0.00	0.00	0.00
37	0.00	0.00	0.00	0.00	0.00
38	0.00	0.00	0.00	0.00	0.00
39	0.00	0.00	0.00	0.00	0.00
40	0.00	0.00	0.00	0.00	0.00
41	0.00	0.00	0.00	0.00	0.00
42	0.00	0.00	0.00	0.00	0.00
43	0.00	0.00	0.00	0.00	0.00
44	0.00	0.00	0.00	0.00	0.00
45	0.38	0.07	0.07	0.00	0.17
46	0.83	0.00	0.33	0.00	0.00
47	0.55	0.00	0.30	0.15	0.00
48	0.75	0.00	0.07	0.00	0.00
49	0.67	0.10	0.00	0.00	0.00
50	0.15	0.04	0.50	0.11	0.00
51	0.51	0.00	0.55	0.10	0.00
52	0.31	0.00	0.29	0.29	0.00
53	0.75	0.00	0.50	0.00	0.00
54	1.00	0.00	0.00	0.00	0.00
55	0.54	0.17	0.08	0.21	0.00
56	0.83	0.00	0.42	0.07	0.07
57	0.21	0.03	0.21	0.17	0.32
58	0.47	0.00	0.55	0.22	0.06
59	0.17	0.00	0.33	0.50	0.00
60	0.53	0.00	0.53	0.10	0.00
61	0.40	0.00	0.40	0.20	0.00
62	0.77	0.00	0.21	0.00	0.01
63	0.50	0.00	0.25	0.00	0.00
64	0.75	0.00	0.00	0.25	0.00
65	0.42	0.19	0.23	0.15	0.03
66	0.74	0.00	0.00	0.00	0.00
67	0.00	0.00	0.00	0.00	0.00

Red Bench "Rule" Sheet
Relative Cover Values by Species
from ECODATA plot data for each Landsat TM spectral class

#	ABLA PIEN	PIAL	PSME LAOC	PICO	DECID
68	0.00	0.00	0.00	0.00	0.00
69	0.00	0.00	0.00	0.00	0.00
70	0.00	0.00	0.00	0.00	0.00
71	0.00	0.00	0.00	0.00	0.00
72	0.00	0.00	0.00	0.00	0.00
73	0.00	0.00	0.00	0.00	0.00
74	0.00	0.00	0.00	0.00	0.00
75	0.00	0.00	0.00	0.00	0.00
76	0.00	0.00	0.00	0.00	0.00
77	0.00	0.00	0.00	0.00	0.00
78	0.38	0.07	0.07	0.00	0.17
79	0.82	0.00	0.33	0.00	0.00
80	0.70	0.00	0.20	0.10	0.00
81	0.76	0.00	0.07	0.00	0.00
82	0.68	0.10	0.00	0.00	0.00
83	0.07	0.02	0.58	0.05	0.00
84	0.33	0.00	0.67	0.14	0.00
85	0.50	0.00	0.00	0.00	0.00
86	0.75	0.00	0.15	0.13	0.04
87	0.17	0.00	0.17	0.67	0.00
88	0.67	0.33	0.00	0.00	0.00
89	0.59	0.00	0.42	0.11	0.03
90	0.22	0.04	0.29	0.23	0.16
91	0.83	0.00	0.08	0.00	0.00
92	0.75	0.00	0.00	0.25	0.00
93	0.57	0.08	0.22	0.03	0.00
94	0.88	0.00	0.00	0.00	0.00
95	0.81	0.00	0.13	0.00	0.03
96	0.60	0.11	0.17	0.00	0.00
97	0.50	0.00	0.00	0.50	0.00
98	0.38	0.38	0.00	0.25	0.00
99	0.78	0.00	0.00	0.00	0.00
100	0.00	0.00	0.00	0.00	0.00
101	0.00	0.00	0.00	0.00	0.00

Red Bench "Rule" Sheet
Relative Cover Values by Species
from ECODATA plot data for each Landsat TM spectral class

#	ABLA PIEN	PIAL	PSME LAOC	PICO	DECID
102	0.00	0.00	0.00	0.00	0.00
103	0.00	0.00	0.00	0.00	0.00
104	0.00	0.00	0.00	0.00	0.00
105	0.00	0.00	0.00	0.00	0.00
106	0.00	0.00	0.00	0.00	0.00
107	0.00	0.00	0.00	0.00	0.00
108	0.00	0.00	0.00	0.00	0.00
109	0.00	0.00	0.00	0.00	0.00
110	0.00	0.00	0.00	0.00	0.00
111	0.38	0.07	0.07	0.00	0.17
112	0.82	0.00	0.33	0.00	0.00
113	0.55	0.00	0.30	0.15	0.00
114	0.75	0.00	0.07	0.00	0.00
115	0.67	0.10	0.00	0.00	0.00
116	0.00	0.00	0.67	0.00	0.00
117	0.36	0.00	0.81	0.15	0.00
118	0.29	0.00	0.58	0.29	0.00
119	0.50	0.00	0.55	0.04	0.01
120	0.19	0.00	0.81	0.13	0.00
121	0.54	0.17	0.08	0.21	0.00
122	0.36	0.00	0.42	0.15	0.00
123	0.23	0.05	0.36	0.29	0.00
124	0.28	0.00	0.43	0.35	0.00
125	0.33	0.00	0.43	0.07	0.00
126	0.67	0.00	0.00	0.00	0.00
127	0.50	0.00	0.50	0.00	0.00
128	0.50	0.00	0.50	0.00	0.00
129	0.63	0.00	0.25	0.00	0.00
130	0.75	0.00	0.00	0.25	0.00
131	0.47	0.00	0.47	0.06	0.06
132	0.72	0.00	0.00	0.00	0.00
133	0.00	0.00	0.00	0.00	0.00
134	0.00	0.00	0.00	0.00	0.00
135	0.00	0.00	0.00	0.00	0.00

Red Bench "Rule" Sheet
Relative Cover Values by Species
from ECODATA plot data for each Landsat TM spectral class

#	ABLA PIEN	PIAL	PSME LAOC	PICO	DECID
136	0.00	0.00	0.00	0.00	0.00
137	0.00	0.00	0.00	0.00	0.00
138	0.00	0.00	0.00	0.00	0.00
139	0.00	0.00	0.00	0.00	0.00
140	0.00	0.00	0.00	0.00	0.00
141	0.00	0.00	0.00	0.00	0.00
142	0.00	0.00	0.00	0.00	0.00
143	0.00	0.00	0.00	0.00	0.00
144	0.38	0.07	0.07	0.00	0.17
145	0.82	0.00	0.33	0.00	0.00
146	1.00	0.00	0.00	0.00	0.00
147	0.75	0.25	0.00	0.00	0.00
148	0.68	0.10	0.00	0.00	0.00
149	0.07	0.02	0.58	0.05	0.00
150	0.33	0.00	0.67	0.14	0.00
151	1.00	0.00	0.00	0.00	0.00
152	0.75	0.00	0.15	0.13	0.04
153	0.17	0.00	0.17	0.67	0.00
154	0.67	0.33	0.00	0.00	0.00
155	0.59	0.00	0.42	0.11	0.03
156	0.22	0.04	0.29	0.23	0.16
157	0.83	0.00	0.08	0.00	0.00
158	0.83	0.00	0.00	0.00	0.00
159	0.50	0.25	0.13	0.00	0.00
160	0.88	0.00	0.00	0.00	0.00
161	0.81	0.00	0.13	0.00	0.03
162	0.67	0.33	0.00	0.00	0.00
163	1.00	0.00	0.00	0.00	0.00
164	0.75	0.25	0.13	0.00	0.00
165	1.00	0.00	0.00	0.00	0.00

Appendix 4 - Fuzzy logic program written for integration of Kessell and spectral data in AIX-based c-language.

```
/*********************************************************************

                                                                FUZZY.C
                        version 0.1


  A program designed to take two images with designated classes
  and determine the dominant class by fuzzy integration based
  on a set of fuzzy rules.

  Built especially for Red Bench Fire pre-fire veg classification.
  Two images are Kessell's topographic model and spectral classification.

  J.D. White 8/18/93
  *********************************************************************/

#include <stdio.h>
#include <stdlib.h>
#include <math.h>
#define MAX(i,j) (i)>(j) ? (i):(j)
#define MIN(i,j) (i)<(j) ? (i):(j)

main()
{
   int row, col, a, b, c, i, j, trash;
   char userin[80], kessell_img, spec_img, veg_class[2000];
   FILE *input1, *input2, *input3, *input4, *output1;
   float kessell[217][5], spectral[166][5], abla_pien_f, pial_f, psme_laoc_f, pico_f, decid_f;
   int abla_pien, pial, psme_laoc, pico, decid;

   /*  Prompt for inputs */

   printf("# cols of images : ");
   gets(userin);
   col = atoi(userin);
   printf("# rows of images : ");
   gets(userin);
   row = atoi(userin);
   printf("Name of Kessell model image : ");
   gets(userin);
   input1 = fopen(userin, "rb");
   printf("Name of Spectral classification image : ");
   gets(userin);
   input2 = fopen(userin, "rb");
   printf("Name of Kessell lookup table : ");
   gets(userin);
   input3 = fopen(userin, "r");
```

```
   printf("Name of Spectral class lookup table : ");
   gets(userin);
   input4 = fopen(userin, "r");

   printf("\n\nName of output image file : ");
   gets(userin);
   output1 = fopen(userin, "wb");

   /* Fill in lookup table matrices */
   printf("\nOpening Kessell lookup ... ");

   for(a=0; a<=216; a++){

      for(b=0; b<5; b++){

         fscanf(input3, "%f", &kessell[a][b]);
         /* printf("\nkess = %f ", kessell[a][b]); */
      }
   }

   printf("\nOpening spectral lookup ... ");
   for(a=0; a<=165; a++){

      for(b=0; b<5; b++){

         fscanf(input4, "%f", &spectral[a][b]);
         /* printf("\nspec = %f", spectral[a][b]); */
      }
   }
   /* Begin fuzzy set compilation */
   printf("\nBeginning computation ... ");

   for(a=0; a<row; a++){

      for(b=0; b<col; b++){

         kessell_img = getc(input1);
         spec_img = getc(input2);
         /* printf("\n kess = %d, spec = %d", kessell_img, spec_img); */

         abla_pien_f = MIN((kessell[kessell_img][0]/1.175),(spectral[spec_img][0]*0.8125));
         pial_f      = MIN(kessell[kessell_img][1],spectral[spec_img][1]);
         psme_laoc_f = MIN((kessell[kessell_img][2]/0.425),(spectral[spec_img][2]*1.575));
         pico_f      = MIN((kessell[kessell_img][3]/0.2),(spectral[spec_img][3]*1.8));
         decid_f     = MIN(kessell[kessell_img][4],spectral[spec_img][4]);

         abla_pien = abla_pien_f*100.0;
```

```
        pial      = pial_f*100.0;
        psme_laoc = psme_laoc_f*100.0;
        pico      = pico_f*100.0;
        decid     = decid_f*100.0;


        if (((abla_pien + pial + psme_laoc + pico + decid) == 0.0) || ((kessell_img == 0) ||
           (spec_img == 0))){
            veg_class[b] = 0;
        }
           else if((abla_pien>pial) && (abla_pien>psme_laoc) && (abla_pien>pico) && (abla_pien>decid)){
              veg_class[b] = 1;
           }
              else if((pial>abla_pien) && (pial>psme_laoc) && (pial>pico) && (pial>decid)){
                 veg_class[b] = 2;
              }
                 else if((psme_laoc>abla_pien) && (psme_laoc>pial) && (psme_laoc>pico) && (psme_laoc>decid)){
                    veg_class[b] = 3;
                 }
                    else if((pico>abla_pien) && (pico>pial) && (pico>psme_laoc) && (pico>decid)){
                       veg_class[b] = 4;
                    }
                       else if((decid>abla_pien) && (decid>pial) && (decid>psme_laoc) && (decid>pico)){
                          veg_class[b] = 5;
                       }
                          else{
                             veg_class[b] = 6;
                          }
     /* printf("\nveg_class = %d,", veg_class[b]); */
     }

     /*printf("\nWriting Row # %d", a); */
     /* Write to ouput file */

     for(c=0; c<col; c++){
        putc(veg_class[c],output1);
     }
  }
}
```

Appendix 5 - Vegetation field data collected by Joseph D. White during the summer of 1992 in the North Fork area.

Field Forms not Copied. Refer to MASTER Copy of Report

Appendix 6 - Vegetation field data collected by Richard V. Ringleb for the North Fork and the Red Bench Fire area during the summer of 1991.

Field Forms Not Copied. Refer To Master Copy of Report

Appendix 7 - Program in AIX c-language used to fill in missing lines in September 20, 1989, Landsat TM data using the weighted inverse distance method.

```
/*****************************************************************************
                                                                        MISSLIN.C
                            ver 0.1

   Program developed to fill missing lines of radiometric data from a
   raster image using a weighted inverse distance algorithm.

   Purposely designed to fill in certain lines missing from the 1989 TM
   data for the North of the Flathead River.

                                                                  2/2/93    J.D. White
 *****************************************************************************/



#include <stdio.h>
#include <stdlib.h>
#include <math.h>

main ()
{
   int cols, rows, fill_row, miss_row, bands, avg_cell, a, b, c, d, e, f, g, h, i, j, k, l, m, n, o, p, q, r;
   int top_row, bottom_row;
   float avg_cell_float_array[1400], bottom_weight, top_weight, t_w[1400], b_w[1400];
   float t_l_w[1400], t_r_w[1400], b_l_w[1400], b_r_w[1400], sum_w_num[1400], sum_wt_dem;
   double top_diag_wt, bottom_diag_wt;
   char userin[80];
   FILE *input1, *output1;
   int good_array [2][1400], out_array[1400], trash_array[1400], avg_cell_array[1400];

   /* user inputs */

   printf("# of columns : ");
   gets(userin);
   cols = atoi(userin);
   printf("# of rows : ");
   gets(userin);
   rows = atoi(userin);
   printf("# of bands : ");
   gets(userin);
   bands = atoi(userin);
   printf("top row # just above missing lines : ");
   gets(userin);
   top_row = atoi(userin);
   printf("bottom row # just below missing lines : ");
   gets(userin);
   bott  ow = atoi(userin);
```

```
   miss_row = (((bottom_row-1)-(top_row-1))-1);
   printf("\n\nMissing rows = %d",miss_row);
   printf("\n\ninput filename TO CORRECT : ");
   gets(userin);
   input1 = fopen(userin, "r");
   printf("input filename FOR OUTPUT : ");
   gets(userin);
   output1 = fopen(userin, "w");

   printf("\nOpening file. Chill out, dude...");

   /* open file, read and write in top of unaffected area */

for (p=0; p<bands; p++)
 {

   for (a=0; a<top_row-1; a++)
   {
      for (b=0; b<cols; b++)
      {
         out_array[b] = getc(input1);
      }
      for (c=0; c<cols; c++)
      {
         putc(out_array[c], output1);
      }
   }

   /* printf("\nTop of file read in O.K., cool..."); */

   /* read top row into good_array */

   for (h=0; h<1; h++)
   {
      for (g=0; g<cols; g++)
      {
         good_array[h][g] = getc(input1);
      }
      for (q=0; q<cols; q++)
      {
         putc(good_array[0][q], output1);
      }
   }
   /* printf("\nTrashing missing rows. Bang your head..."); */

   /* read through and dispose of missing rows */
```

```
   for (d=0; d<miss_row; d++)
   {
      for (e=0; e<cols; e++)
      {
         trash_array[e] = getc(input1);
      }
   }

   /* read in bottom row into good_array */

   for (i=1; i<2; i++)
   {
      for (j=0; j<cols; j++)
      {
         good_array[1][j] = getc(input1);
      }
   }

   /* printf("\nFill er up, dude..."); */

   /* begin averaging using inverse distance averaging technique using
      top and bottom pixel values */

   for (fill_row=0; fill_row<miss_row; fill_row++)
   {
      for (f=0; f<cols; f++)
      {
         top_weight = 1.0/(fill_row+1);
         bottom_weight = 1.0/(miss_row-fill_row);
         top_diag_wt = 1.0/(sqrt(((fill_row+1)*(fill_row+1))+1));
         bottom_diag_wt = 1.0/(sqrt(((miss_row-fill_row)*(miss_row-fill_row))+1));

         if (f == 0 || f == cols-1)
         {
            t_w[f] = (top_weight) * good_array[0][f];
            b_w[f] = (bottom_weight) * good_array[1][f];
            avg_cell_float_array[f] = (t_w[f]+b_w[f])/(top_weight+bottom_weight);
         }
         else
         {
            t_w[f] = top_weight * good_array[0][f];
            b_w[f] = bottom_weight * good_array[1][f];
            t_l_w[f] = top_diag_wt * good_array[0][f-1];
            t_r_w[f] = top_diag_wt * good_array[0][f+1];
            b_l_w[f] = bottom_diag_wt * good_array[1][f-1];
            b_r_w[f] = bottom_diag_wt * good_array[1][f+1];
            sum_w_num[f] = t_w[f]+b_w[f]+t_l_w[f]+t_r_w[f]+b_l_w[f]+b_r_w[f];
```

```
            sum_wt_dem = top_weight+bottom_weight+(2.0*top_diag_wt)+(2.0*bottom_diag_wt);

            avg_cell_float_array[f] = (sum_w_num[f])/(sum_wt_dem);
         }
         sprintf(userin, "%.01f", avg_cell_float_array[f]);
         avg_cell_array[f]=atoi(userin);

      }
      for (r=0; r<cols; r++)
      {
         if (r == 49)
         {
            printf("\navgeraged value for col#50, row# %d",fill_row+1);
            printf(" is = %d",avg_cell_array[49]);
            printf("\ttop weight = %.3f", top_weight);
            printf("\tbottom weight = %.3f", bottom_weight);
            printf("\ttop diag wt = %.3f", top_diag_wt);
            printf("\tbottom diag wt = %.3f", bottom_diag_wt);
         }

         putc(avg_cell_array[r], output1);
      }
   }

   printf("\n\ntop value for column #0 = %d", good_array[0][49]);
   printf("\nbottom value = %d", good_array[1][49]);

   /* printf("\nJust about done, hang loose..."); */

   /* fill in rest of file beginning with bottom row values */

   for (k=1; k<2; k++)
   {
      for (l=0; l<cols; l++)
      {
         putc(good_array[1][l], output1);
      }
   }
   for (m=bottom_row; m<rows; m++)
   {
      for (n=0; n<cols; n++)
      {
         out_array[n] = getc(input1);
      }
       for (o=0; o<cols; o++)
      {
         utc(out_array[o], output1);
```

```
      }
   }

   /* printf("\nAll done! Excellent...");      */
   /* printf("\nOh no, more bands,.. bummer"); */
 }
   /* printf("\nCan I go now?");               */

}
```

PUBLICATIONS

Analysis of Changes in Patterns of a Forested Landscape Following Wildfire Using Landsat Data and Landscape Ecology Methodology

Elizabeth D. Reinhardt
USDA Forest Service
P.O. Box 8089
Missoula, MT 59807

Richard V. Ringleb
School of Forestry
University of Montana
Missoula, MT 59812

ABSTRACT

The September 1988 Red Bench fire burned approximately 38,000 acres of the North Fork of the Flathead River valley, in Glacier National Park and the Flathead National Forest. This study was an attempt to assess the impact of the fire on the structure of the landscape using remotely sensed data. Landsat TM data from August 1988 and July 1989 were used to contrast landscape patterns inside and outside the park, before and after the fire. Landscape ecology techniques were used to quantify aspects of the landscape such as complexity and diversity. Results indicated that landscape diversity was increased by fire, especially inside the park, but the complexity of the shapes of forested areas and openings was unchanged by fire.

INTRODUCTION

The dry summer of 1988 in the northern Rocky Mountains was one of large fires in remote wilderness areas. In the Greater Yellowstone Area 8 fires burned 1.4 million acres. The Canyon Creek and Gates Park fires burned extensive areas in and near of the Bob Marshall Wilderness complex, and the Red Bench fire burned 38,000 acres in and adjacent to Glacier National Park. The extent of these fires and their inaccessible locations made it difficult to document their effects on resource values.

Successful wilderness fire management programs need current data on fuels and vegetation. Managers need information on the extent, location and severity of the current year's fires in order to make decisions on the management of next year's; in part because fires create fuel discontinuities (Martin and others 1989). With knowledge of topography, weather patterns, and location of recent fires, managers can speculate about potential spread and behavior of new fire starts, enabling them to make improved decisions about appropriate fire management. Also, information on the extent, location and severity of wilderness fires is necessary to assess their impact on

such resources as water quality and quantity, and wildlife habitat.

Following the summer of 1988, there was some public sentiment against wilderness fire management policies. We believe, however, that not only are wilderness fires unavoidable (Brown, 1989), but they can be desirable. Fire has been a common historical perturbation in the forests of the northern Rocky Mountains, and many of the plant species in these forest types evolved in the presence of repeated fires (Habeck and Mutch, 1973). One of the benefits that has been ascribed to wilderness fire is its creation or maintenance of a landscape "mosaic" (Kilgore 1987). Spatial heterogeneity and its accompanying ecological diversity can be enhanced by fire.

Landscape ecologists have developed quantitative techniques for assessing landscape characteristics such as complexity and diversity (O'Neill and others 1988). Application of these techniques to prefire and postfire landscapes could allow us to assess the effects of fire on landscape pattern. This paper describes a case study examining, for the 1988 Red Bench fire, the opportunity to use remotely sensed spectral data to map wildfire extent and severity, and using this data to analyze fire-caused changes in landscape pattern.

THE STUDY AREA

The North Fork of the Flathead River flows through a large glacial valley, and divides Glacier National Park on the east from the Flathead National Forest and private land on the west. The valley is densely forested primarily with lodgepole pine, and also contains areas of prairie, sedge meadows and riparian bottomland.

The Red Bench fire burned on both sides of the North Fork of the Flathead River. It was started by lightning on the Flathead National Forest on the west side of the North Fork on August 17 (Bushey 1990). The fire smoldered undetected until September 6th, when it was reported by a logging crew. Its size at that time was about 1/4 acre. Pushed by high winds during the course of the next 2 days the fire grew to a size of 15,000 acres, exhibiting extreme fire behavior, burning fifteen homes and five outbuildings in the community of Polebridge, crossing the North Fork of the Flathead River, and penetrating 6 miles into Glacier Park. The fire continued to burn throughout September, eventually reaching a size of 38,000 acres.

Although the North Fork is an area of generally short, moist summers (Bushey 1990), fires such as the Red Bench fire may not be uncharacteristic. Barrett (1983) studied the fire history of the area and described it as one of occasional severe stand-replacing fires, with frequent understory fires. In a detailed analysis of a 60,000 acre study area on the west side of the North Fork, he found a mean fire interval of 39 years between fires that burned at least 10,000 acres. The large fires were not evenly distributed over time however. Most of the study area

burned in large fires in the late 1600's, and again in the late 1800's and early 1900's. There had been no large fires since the advent of fire suppression in the 1930's; however, since much of the area had burned shortly before that, fuel accumulations may not have been unnaturally high. Barrett concluded his report by noting that "most stands are now approaching the maximum fire intervals that existed in presettlement times. . . .evidently the stage is now being set for major fires in the North Fork valley in the coming decades."

METHODS

Image Processing

Landsat Thematic Mapper (TM) data were acquired for August 31, 1988, (one week before the fire), and July 30, 1989, (10 months postfire). Defense mapping agency digital elevation data were also acquired for the study area. ERDAS image processing software and a COMPAQ 386 microcomputer were used for the analysis. The three data sets were georeferenced and an area of approximately 220,000 acres surrounding the burn was extracted for further analysis. The Landsat data has a pixel size of 30 meters square. To make the data sets a more manageable size, pixels were grouped to a size of 90 meters square.

An unsupervised clustering technique using a minimum spectral distance classifier was used to classify the prefire spectral data. Bands 3 (red), 4 (near infrared), 5 (mid range infrared), 6 (thermal infrared) and elevation were used to develop the classification. Thirteen classes resulted (Figure 1). Most of the pixels were classified as either dense conifer stands, sedge meadows, grass or low shrubs, south facing scree slopes, high elevation beargrass with scattered timber, lakes, or snow fields. Following the initial unsupervised clustering, these classes were grouped, resulting in three classifications: forest, clearings, and other. The third category included lakes and high elevation areas not impacted by fire, so the remainder of the analysis focused only on the effects of the fire in converting forested area to clearings.

A fire map was generated from the postfire TM scene by dividing the data values for Band 4 by the average of Bands 3, 6 and 7, and multiplying the resulting ratio by 64. This manipulation of data resulted in a postfire image in which the burned area had low data values. Preliminary field validation suggested that lower values were associated with more severe fire treatment; this correlation will be field tested in the summer of 1991. The postfire classified data were then overlaid on the prefire scene, creating a composite image (Figure 2) in which all values were taken from the prefire scene except those pixels that had been classified as burned in the post-fire TM scene. This procedure was used instead of repeating the clustering technique on the postfire scene in order to reduce sources of variability other than the fire, such as differences in atmospheric conditions between the dates of the two scenes. By overlaying only the burned pixels on the prefire scene, we insured that the landscape

Figure 1. Classified Landsat TM scene of the North Fork area on August 31, 1988. The North Fork flows from the northwest to the southeast corner of the area. Light colored patches along the river are open areas. The dark area is closed canopy forests. Upper elevation areas of a variety of land types are also light in color.

changes we found were fire caused. Burned pixels were taken to represent open or unforested areas in the new postfire scene.

Landscape Ecology

Both the prefire and the postfire scenes were divided along the North Fork, creating separate data sets for inside and outside Glacier National Park. For each of the resulting four data sets, four indices of landscape characteristics were computed, using the program SPAN (Turner and Ruscher 1988).

Diversity, dominance and contagion are indices developed from information theory (O'Neill and other 1988, Turner and Ruscher 1988). They were computed for the scenes using individual pixels as data.

Diversity was computed as:

$$\sum_{k=1}^{m} (P_k)\log(P_k),$$

where P_k is the proportion of the landscape in land type k, and m is the number of land types present. Larger values indicate more diversity in the landscape. Largest values result when equal areas are in each land type. Dominance was computed as the deviation from maximum possible diversity, and used to indicate the extent to which the landscape was dominated by a land type.

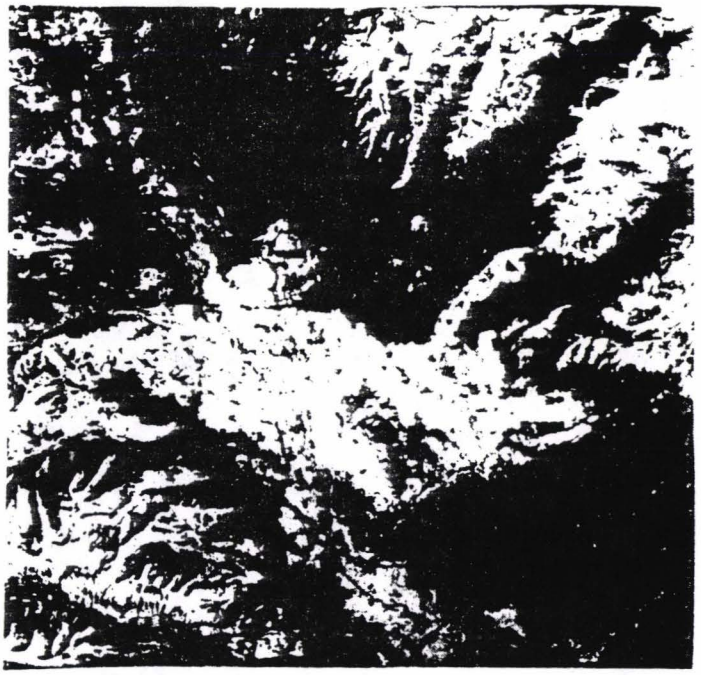

Figure 2. The August 1988 scene overlaid with the fire area from the July 1989 scene.

Contagion was computed as

$$2m \log(m) + \sum_{i=1}^{m} \sum_{j=1}^{m} (Q_{i,j}) \log(Q_{i,j}),$$

where $Q_{i,j}$ is the proportion of pixels of land type i that are adjacent to pixels of land type j, and m is the number of land types present. Contagion was used as a measure of the extent to which land types were clumped. Lower values mean that the different land types are broken up and distributed over the landscape, large values mean that land types are aggregated: a given area, or in this case pixel, is more likely to be near other similar areas than expected if land types were randomly distributed.

Patches of contiguous pixels of each land type were identified, and the size and perimeter of each was calculated. Fractal dimension was used as a measure of the complexity of shapes in the landscape. The concept of fractal geometry was introduced by Mandelbrot (1977), and

has been developed as a mathematical model of spatial phenomena. It has been used by landscape ecologists to indicate landscape complexity (Krummel and others 1987, Turner 1987). It was computed as 2 (ln(perimeter/4))/ln(size)) for each individual patch. Fractal dimension of the landscape as a whole was computed by regressing ln(perimeter/4) against ln(size). The fractal dimension was twice the slope of the regression line. In addition, summaries of patch size distributions by land type were developed.

RESULTS AND DISCUSSION

Fire mapping

Visual examination of images for each Thematic Mapper band showed the fire perimeter was barely visible in bands 3 and 4, and somewhat more visible in bands 6 and 7. By combining these four bands in the combination $(B_4/((B_3+B_6+B_7)/3))*64$ the burned area was strikingly evident (Figure 3). It appeared from preliminary field verification that this combination was successful at delineating fire perimeters, and also was correlated with fire severity, with lower data values representing more severely burned areas. Statistical validation of this correlation will be conducted in the 1991 field season.

Thematic mapper band 3 measures the radiance of red light as reflected from the earth's surface (Table 1). Areas with green, living biomass absorb red light, resulting in low digital values. Burned areas reflected more red light because the green canopy cover was removed.

Band 4 measures radiance of near infrared radiation. It has been found to correlate well with amount of green biomass because the cell structure of green leaves reflects near infrared energy (Lillesand and Kiefer 1987). Unlike band 3, it showed less reflectance in the burned areas.

Data values in band 6 represent thermal emissions. Higher temperatures show up as higher data numbers. Values are higher in burned areas, presumably due to reduction in vegetative cover and associated cooling by evapotranspiration.

Band 7 (mid infrared) has data values that are inversely correlated to moisture. Burned areas had high values. Burned areas were probably drier than surrounding areas because removal of plant cover and shading allowed for soil drying, and also because leafy biomass is itself moist and had been removed.

Since band 4 had lower values in burned areas, while bands 3,6 and 7 had higher values, the ratio of $(B_4/((B_3+B_6+B_7)/3))*64$ had much lower values in the burned areas than unburned areas. The Red Bench fire was primarily a crown fire. Near 100% tree mortality occurred within burned areas, and foliage and small branches were consumed by fire. A less severe fire might not be as easily delineated using spectral data. The data

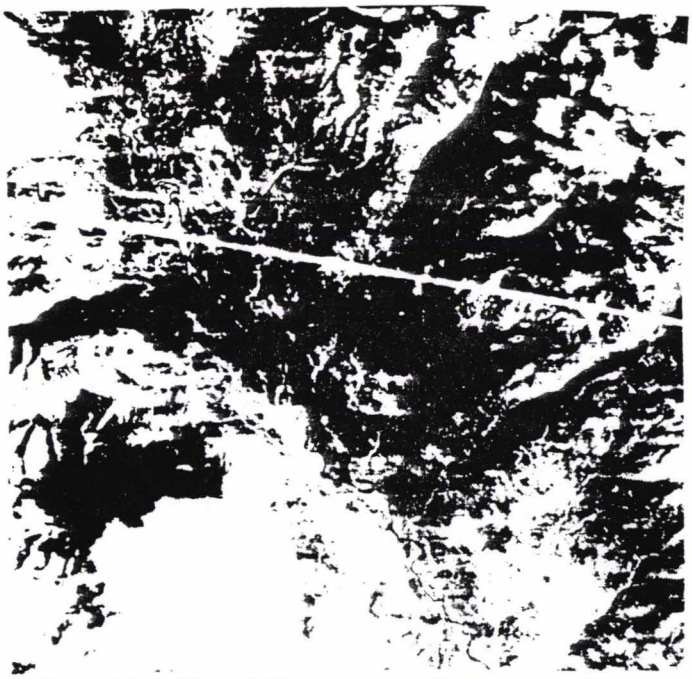

Figure 3. July 30, 1989 Landsat TM scene. Data shown is $(B_4/((B_3+B_6+B_7)/3))*64$. The diagonal line is a 7 pixel wide band of missing data. There is a cloud and its shadow in the lower left corner of the image.

Table 1. Characteristics of Thematic Mapper bands used in classifying burned areas and prefire vegetation.

Band		Wavelength micrometers	Response to increasing coniferous vegetation
3	red	0.63 - 0.69	decrease
4	near infrared	0.76 - 0.90	increase
5	mid infrared	1.55 - 1.75	decrease
6	thermal infrared	10.40 - 12.5	decrease
7	mid infrared	2.08 - 2.35	decrease

transformation used here should be tested on other fires of varying severity and vegetation type to assess its broader usefulness.

Landscape ecology indices

Allocation of land area by land type and patch size is summarized in Table 2. Both inside and outside the park the proportion of forested land area decreased following

the fire, as expected. The relative reduction was less outside the park, where there was more open area before the fire. Before and after fire, smaller patches were mostly openings, while large patches (1000+ acres) were forest. Postfire scenes inside and outside the park had more coverage, both forested and open, in small (< 1000 acre) patches, indicating that the fire resulted in a more broken up landscape.

Landscape ecology indices for the prefire and postfire scenes inside and outside the park are summarized in Table 3. As expected, diversity increased inside and outside the park following fire, while dominance decreased. Prefire and postfire diversity were greater outside the park than inside, presumably due to land use practices such as logging. Contagion was greater inside the park than outside, and was almost unchanged by fire.

Fractal dimension of the landscape was essentially the same for the four scenes. Fractal dimension is a measure of how complex the perimeters of land types are. Square patches have a fractal dimension of 1, while very irregular patches have a fractal dimension approaching 2. Similarly, landscapes composed of very simple patches have a fractal

Table 2. Proportion of area in patches of different sizes and land types. Patch Sizes are 1 = 2 acres, 2 = 3-10 acres, 3 = 11-100 acres, 4 = 101-1000 acres, 5 = 1001+ acres.

	Patch Size					
	1	2	3	4	5	F/O[1]
	---------Forested----------					
Prefire NF[2]	.005	.007	.020	.015	.743	3.8
Postfire NF	.007	.010	.031	.025	.656	2.7
Prefire NP[3]	.002	.002	.006	.004	.943	22.3
Postfire NP	.004	.005	.012	.007	.827	6.0
	----------Open----------					
Prefire NF[2]	.008	.012	.038	.106	.047	
Postfire NF	.013	.021	.071	.123	.041	
Prefire NP[3]	.004	.006	.010	.010	.013	
Postfire NP	.011	.017	.044	.071	.000	

[1] F/O = ratio of acres in forest / acres in openings.

[2] NF = West side of the North Fork, primarily National Forest land with some private land.

[3] NP = East side of the North Fork, Glacier National Park.

Table 3. Landscape ecology indices applied to the classified TM scenes.

Scene	Diversity	Dominance	Contagion	Fractal Dimension
Prefire NF[1]	.879	.219	.749	1.37
Postfire NF	.936	.163	.748	1.37
Prefire NP[2]	.617	.482	.804	1.36
Postfire NP	.805	.293	.821	1.37

[1] NF = West side of the North Fork, primarily National Forest land with some private land.

[2] NP = East side of the North Fork, Glacier National Park.

dimension near 1, while landscapes formed of complex shapes have dimensions near 2. Results of the study showed that while patch size and composition were impacted by fire, patch shape was not. The landscape, both before and after fire, inside and outside the park, was formed of fairly simple shapes with fairly low edge/area ratios.

Our estimate of fractal dimension may have been influenced by the nature of our data: square pixels of a fairly coarse resolution. Table 4 shows that the average fractal dimension increased with patch size. Perimeters of small patches may actually have been more irregular than they appeared, but resolution was lost at the small scales.

Table 4. Average fractal dimension for patches[1] of different sizes.

Patch size (acres)	Average fractal dimension
2	1.00
3-10	1.22
11-100	1.33
101-1000	1.41
1001+	1.49

[1] Open and forested patches from all four data sets are included in these averages, however, similar trends can be seen in each class and in each data set.

CONCLUSIONS

Broadly applicable techniques for mapping fire extent and severity from remotely sensed spectral data should be developed to allow wilderness managers to update vegetation maps or geographic information systems on an annual basis. The preliminary methodology developed here needs to be statistically verified for the Red Bench fire, and then tested on other fires, particularly less severe fires and fires in other vegetation types.

Results of this study indicated that landscape diversity was increased by the Red Bench fire, while distribution of landtypes and the complexity of the landscape was unchanged. This was true in both the managed landscape (National Forest) and the natural landscape (Glacier National Park). Whether this is typical of large scale wildfires is as yet unknown.

Landscape indices serve as indicators of trend or as quantitative tools for comparing landscapes. Their values are not intrinsically meaningful however. A challange for resource managers and researchers is to relate the indices to other resource values. What kind of values for contagion, for example, will best result in habitat usage by big game? What were the landscape characteristics of historical natural landscapes? If we can identify these, we will be able to compare them to managed landscapes to provide a quantitative method of assessing alternative management choices. This could allow managers to set goals of maintaining natural landscape characteristics through management practices such as timber harvest or prescribed burning.

REFERENCES

Barrett, S.W. 1983. Fire History of Glacier National Park: North Fork Flathead River Drainage. Final Report. Cooperative Agreement 22-C-2-INT. Intermountain Fire Sciences Laboratory, Missoula, MT and Systems for Environmental Management, Missoula, MT. Copy on file at the Intermountain Fire Sciences Laboratory, Missoula, MT.

Brown, J.K. 1989. Could the 1988 Fires in Yellowstone have been avoided through prescribed burning? Fire Management Notes 50(3), pp. 7-13.

Bushey, C. L. 1990. The 1988 Red Bench Fire: Documentation of Fire Behavior, Fire Weather, and Preburn Fuel Conditions in the North Fork Flathead River Valley. Cooperative Agreement INT-89439-RJVA. Intermountain Fire Sciences Laboratory, Missoula, MT and Systems for Environmental Management, Missoula, MT. Copy on file at the Intermountain Fire Sciences Laboratory, Missoula, MT.

Habeck, J.R. and R.W. Mutch. 1973. Fire-dependent forests in the northern Rocky Mountains. Quaternary Research 3, pp. 408-424.

Kilgore, B.M. 1987. The role of fire in wilderness: a state-of-knowledge review. In: Proceedings-National Wilderness Research Conference: Issues, State-of-Knowledge, Future Directions; July 23-26, 1985; Fort Collins, CO. General Technical Report INT-220. USDA For. Serv., Intermountain Research Station, pp. 70-103.

Krummel, J.R., R.H. Gardner, G. Sugihara and others. 1987. Landscape patterns in a disturbed environment. OIKOS 48, pp. 321-324.

Lillesand, T.M. and R.W. Kiefer. 1987. Remote Sensing and Image Interpretation. 2nd Ed. John Wiley and Sons.

Mandelbrot, B.B. 1977. Fractals, form, chance and dimension. W.H. Freeman and Co.

Martin, R.E., J.B. Kauffman, and J.D. Landsberg. 1989. Use of prescribed fire to reduce wildfire potential. In: Proceedings of the symposium on fire and watershed management; Oct 16-28, 1988, Sacramento, CA. General Technical Report PSW-109, USDA For. Serv. Pacific Southwest Forest and Range Experiment Station, pp. 17-22.

O'Neill, R.V., J.R. Krummel, R.H. Gardner and others. 1988. Indices of landscape pattern. Landscape Ecology. 1(3), pp. 153-162.

Turner, M.G. 1987. Spatial simulation of landscape changes in Georgia a comparison of 3 transition models. Landscape Ecology 1(1), pp. 29-36.

Turner, M.G. and C.L. Ruscher. 1988. Changes in landscape patterns in Georgia, USA. Landscape Ecology. 1(4), pp. 241-251.

REMOTE SENSING AND ECOLOGICAL MODELING OF THE 1988 RED BENCH FIRE[1]

Joseph D. White[2], Kevin C. Ryan[3], and Steven W. Running[2]

ABSTRACT: In September of 1988, the Red Bench Fire burned over 15,400 hectares of vegetation on the Flathead National Forest and Glacier National Park. Pre- and post-fire Landsat Thematic Mapper (TM) data were acquired to investigate: a) the composition and structure of the vegetation communities before and after the fire, b) the relationship of fire severity to pre-fire communities and post-fire spectral characteristics, and c) the changes in carbon and water cycling in the burned watersheds using TM data as input into a regional ecosystem model. TM and topographic data in a geographic information system (GIS) were used to map pre-fire vegetation communities. Burn severity classes derived from post-fire spectral analysis and ground data were compared with pre-fire communities. Hydrologic outflow and net primary productivity (NPP) were modeled for pre- and post-fire conditions to demonstrate differences in carbon and water flux associated with changes in remotely sensed data.
KEYWORDS: Landsat TM, vegetation mapping, fire severity, ecological modeling

INTRODUCTION

Remote sensing tools are well suited for investigating the effects of large natural fires. The combination of repeated observations, enhanced spectral information, and fine spatial resolution of current satellite sensors make them an important means of studying fire effects on forested areas. This is especially true in cases where little field data on pre-fire conditions are known and where the size of the fire precludes field sampling as an efficient means of providing a comprehensive view of fire effects on the landscape.

Satellite data has been used as a fairly reliable data source for vegetation mapping (Mayer and Fox 1981, Benson and DeGloria 1985). The power of satellite data for mapping purposes can be increased if topographic data is used to provide ecological definition of probable locations of vegetation types (Cibula and Nyquist 1987, White *et al. in press*). Mapping vegetation by enhanced spectral/GIS methods is useful for providing information about forested areas previous to removal due to destructive

---

[1]A paper presented at the 12th Conference on Fire and Forest Meteorology, October 26-28, 1993, Jekyll Island, Georgia.

[2]Joseph D. White and Steven W. Running, University of Montana, School of Forestry, Missoula, MT, USA, 59812.

[3]Kevin C. Ryan, Intermountain Research Station, Forest Service, U.S. Department of Agriculture, Intermountain Fire Sciences Laboratory, P.O. Box 8089, Missoula, MT, USA, 59807.

fire. Fire can have a significant effect on the reflective properties of the land surface due to vegetation removal, soil exposure, and soil color alteration making the observation of fire severity by spectral data possible (Jakubauskas *et al.* 1990, Milne, 1986). Finally, spectral data is useful for providing information about ecosystem processes through correlation of certain spectral bands with important vegetation parameters such as leaf area index (LAI) (Spanner *et al.* 1990). This study seeks to outline three different uses of satellite spectral data for the purpose of investigating fire effects on a forested landscape. In this paper, we outline the use of remote sensing data for 1) determining pre-fire vegetation communities, 2) developing a spectral model which differentiates burn severity classes, 3) input into an ecosystem model for understanding the effects of a fire on regional estimates of net primary productivity (NPP) and hydrologic outflow.

METHODS

Study Area

Our study area is the United States portion of the North Fork drainage of the Flathead River, Montana. The drainage is oriented north-south with the Glacier View Ranger District of the Flathead National Forest comprising the western side and Glacier National Park forming the eastern side. The Red Bench Fire burned an area of approximately 15,400 ha in the Flathead National Forest and Glacier National Park between September 6 and 17, 1988. The fire was ignited by a lightning strike at around 2:30 p.m. on the 6th and consumed roughly 10,100 ha by the 8th (Key 1988). The fire burned for 9 more days and was extinguished by manned fire-intervention.

Pre-Fire Vegetation Map

We produced a pre-fire vegetation map using a merger of multi-spectral classification and topographic gradient analysis. This method was chosen to resolve the forest vegetation classes to a pre-determined level. Neither the spectral data nor the topographic analysis alone provided sufficient information for differentiating these pre-determined forest vegetation classes. An August 28, 1988 Landsat Thematic Mapper (TM) scene (Path 41, Row 26) was obtained which included the North Fork drainage area. These data were georectified to a Universal Transverse Mercator (UTM) coordinate system using ground control points derived from landmarks on USGS 7½′ topographic maps. The reflective TM bands (1-5,7) were converted to radiance values and atmospheric haze influence in the data were reduced using the "clear-lake" strategy (Jensen, 1986).

Merger of the classified Landsat data with the topographic gradient model was accomplished using a fuzzy logic approach. In fuzzy logic, objects are assigned to a set in partial quantities. The "fraction of membership" to which an object belongs to a set can be based on some *a priori* relationship that the object has with the set. In our model, we used relative cover as a measure of the degree to which our spectral classes and topographic gradient classes belonged to the pre-determined vegetation categories. These vegetation categories were *Abla lasiocarpa - Picea spp.* mix (subalpine fir - spruce, ABLA-PIEN), *Pinus albicaulis* (white-bark pine, PIAL), *Pseudotsuga menziesii - Larix occidentalis* mix (Douglas fir - western larch, PSME-LAOC), *P. contorta* (lodgepole pine, PICO), deciduous mix (*Populus spp., Betula paperifera*), and shrub-meadow.

Spectral classification of the Landsat TM scene was produced using the Earth Resources Data Analysis System (ERDAS 1991) series of programs. The spectral classification procedure was composed of two parts: a) identification of the natural spectral classes using the ISODATA program and b) maximum likelihood classification (MAXCLAS) of topographically defined subsets of the TM data

using summary statistics of the ISODATA classification. Using ECODATA plot data (Keane *et al.* 1990) provided by the Region 1 office of the National Forest Service, the results of the ISODATA spectral classification indicated broad overlap of forest species within each spectral class. To resolve this ambiguity, the spectral data were stratified into topographic regions based on field observation of the overall topographic distribution of forest species. Ideally, spectral identification of species would increase by limiting the number of species within each region. The product of this two-step classification provided a better, though incomplete, resolution of the pre-requisite forest categories. Using the ECODATA information, relative cover values of the vegetation categories were assigned for each spectral class for the entire drainage.

The topographic gradient model developed by Kessell (1979) provided a summary of relative cover values for species of the North Fork region based on axes of increasing potential topographic moisture, elevation, and time since last stand-replacing fire. Using digital elevation data and maps of fire history, a map of the Kessell model was produced for the drainage with the associative relative cover values for the defined vegetation groups.

The final vegetation map was produced joining the spectral classification and topographic gradient maps as a function of the intersection of these two maps. An intersection of two groups in a fuzzy operation can be defined as the minimum value of membership of an object in either set (Schumucker 1984). An example of this operation is:

$$\text{ABLA-PIEN} = \text{SPEC} \cap \text{TOPO} = \text{MIN(SPEC,TOPO)}$$

where ABLA-PIEN is the final set membership value for the subalpine fir-spruce group based on the minimum relative cover value from the spectral (SPEC) and topographic (TOPO) data. This operation was calculated for each of the 6 vegetation groups for the entire drainage. Dominant vegetation was assigned for 50 by 50m polygons based on the maximum final set membership between the six vegetation categories. Where no maximum occurred, i.e. the final membership value between two groups was equal, the polygon was assigned as mixed. Non-vegetation categories such as water, bare ground, etc., were derived exclusively from the spectral classification.

Mapping accuracy was calculated based on an error matrix using field samples acquired in 1991 and 1992 of area outside the burn area. Some vegetation communities and non-vegetated areas such as *P. albicaulis*, deciduous, mixed, bare ground, and water were not sampled and were not included in our accuracy assessment.

Fire Severity Map

A map of fire severity was produced by using field plots within the burn area as a reference to understand the relationship between fire effects on landcover characteristics and satellite spectral data.

In October of 1988, Barry Dutton and Steve Cooper were contracted by Glacier National Park to establish plots within the burn area. They established 36 permanent plots, sampling for pre-fire vegetation, habitat type, age class, and burn severity. Burn severity was derived from Ryan and Noste (1983) which Dutton and Cooper condensed into three main categories: light, moderate, and high (Table 1). Dutton and Cooper produced a map of burn severity by interpolating the results of their field sampling and some aerial photographic interpretation onto USGS 7½′ topographic maps.

Carl Key, Geographer for Glacier National Park, also produced a burn severity map of the park side of the burn using aerial photos obtained shortly after the fire in 1988. Key interpreted severity similar to Dutton and Cooper with the exception that severity was determined based solely on fire effects in the vegetation canopy.

Table 1 - Dutton and Cooper fire severity classification scheme (after Ryan and Noste 1983).

Burn Severity	Litter	Soil	Fuel	Vegetation
light	not consumed	not altered	few small fuels consumed	some scorch, esp. shrubs
moderate	completely consumed	darkened w/ white ash	small fuels consumed	small diameter trees and shrubs killed
high	completely consumed	stability lost, reddish w/ white ash	small and medium fuels consumed	all vegetation killed, incl. rhizomes

September 20, 1989 Landsat TM data were obtained and processed in the same manner as the 1988 TM data. In addition, these data were converted into reflectance values. Five pixels surrounding and including the Dutton and Cooper field sites were extracted from the 1989 TM data for statistical analysis. Important in this analysis was determining which TM bands contained the most information regarding burn severity. Student's *t*-tests were used to determine the significant difference in reflectance value populations between burn severity classes. The TM bands which demonstrated meaningful separability between severity classes were used in a spectral classification (ERDAS CLUSTR program).

Agreement between Dutton and Cooper's, Key's, and our fire severity map was assessed by comparing randomly selected points between their maps and our own to assess overall percent map-to-map correspondence.

Ecosystem Modeling

The Regional Hydro-Ecological Simulation System (RHESSys) (Nemani *et al.* 1992) was used to simulate NPP and hydrologic outflow for the area centered around the Red Bench Fire. RHESSys is a process model which simulates climate, hydrologic balance, and biogeochemical cycling within a GIS. Primary geographic database inputs for RHESSys are climate, vegetation, soils, and topography. Remote sensing data is used for determining regional vegetation characteristics, especially, lifeform and leaf area index (LAI). Lifeform, e.g. needle-leaf evergreen, needle-leaf deciduous, etc. is important for parameterizing the certain plant physiological variables, while LAI is important for modeling the rate of plant processes such as evapotranspiration, photosynthesis, and respiration. LAI may be derived from satellite data by correlating ground measurements of LAI with a ratio of near infrared to red wavelengths referred to as the normalized difference vegetation index (NDVI). The 1988 Landsat data were used to derive LAI values for forested areas using correlation coefficients previously derived for the area (Spanner *et al.* 1990). To simulate the occurrence of the fire during 1988, a fire progression map produced by Carl Key of Glacier National Park was used to remove LAI over the days of burning. In 1989, the burn areas were assumed to have converted from a forested lifeform to a grassland. As a best guess LAI for the burned area was derived from correlating 1990 NDVI data with 1991 field estimates of biomass. LAI outside the burn area was assumed to have remained constant or at least changed very little, therefore, 1988 LAI values were re-used for 1989 simulations of forested areas.

NPP values for the region were calculated from the model outputs of photosynthesis and respiration. Also, hydrologic outflow was calculated by the model. The outflow data were compared with USGS North Fork stream gauge data which is located approximately 30 km downstream of the study area. These streamflow data were used because no other data were available for this area.

RESULTS

The results of our analysis of the pre-fire vegetation map indicate an overall mapping accuracy of 70% percent of selected communities. Table 2 illustrates that a wide range of accuracy exists among different communities.

Table 2 - Error matrix with ground versus classified data for pre-fire vegetation map.

	GROUND DATA			
CLASSIFIED DATA	A-P	P-L	P	S/m
ABLA-PIEN (**A-P**)	31	5	4	1
PSME-LAOC (**P-L**)	11	29	11	0
PICO (**P**)	0	6	20	1
Shrub/meadow (**S/m**)	1	2	0	16
Accuracy (%)	72	69	57	89

Analysis of the post-fire TM data indicated that the maximum reflectance value of either TM band 5 and 7 (MAX(band 5,7)) were useful for separating areas of different burn severity. This difference is illustrated by comparing the frequency distribution of MAX(band 5,7) within the different burn severity classes (Figure 1). Results of the *t*-test indicate that these populations of reflectance values are significantly different ($P < 0.01$).

A comparison of randomly selected points from the Dutton and Cooper and Key fire severity maps with our classified map produced from the MAX(band 5,7) data indicate that there is a 68% percent agreement among fire severity classification between our map and Dutton and Cooper's and a 70% agreement between our map and Key's map.

There is an overall shift in NPP from 1988 to 1989 with more areas having less productivity in 1989 than in 1988 (Figure 2). Also, the regional average of NPP dropped from 2.71 ± 0.69 Mg C $\cdot$ ha$^{-1} \cdot$ yr^{-1} to 2.54 ± 0.60 Mg C $\cdot$ ha$^{-1} \cdot$ yr^{-1}. Comparison of the modeled and observed outflow data illustrate an overall agreement for the timing and magnitude of outflow events (Figure 3). The Mean Average Percent Error (MAPE) (Pankratz 1983), a measure of relative residual error between observed and expected data, demonstrated that the model had percent residual error of 12.16 percent.

DISCUSSION

This study demonstrated that remote sensing provides a powerful information base for understanding the effects of fire on the structure and ecology of a forested landscape. The reliability

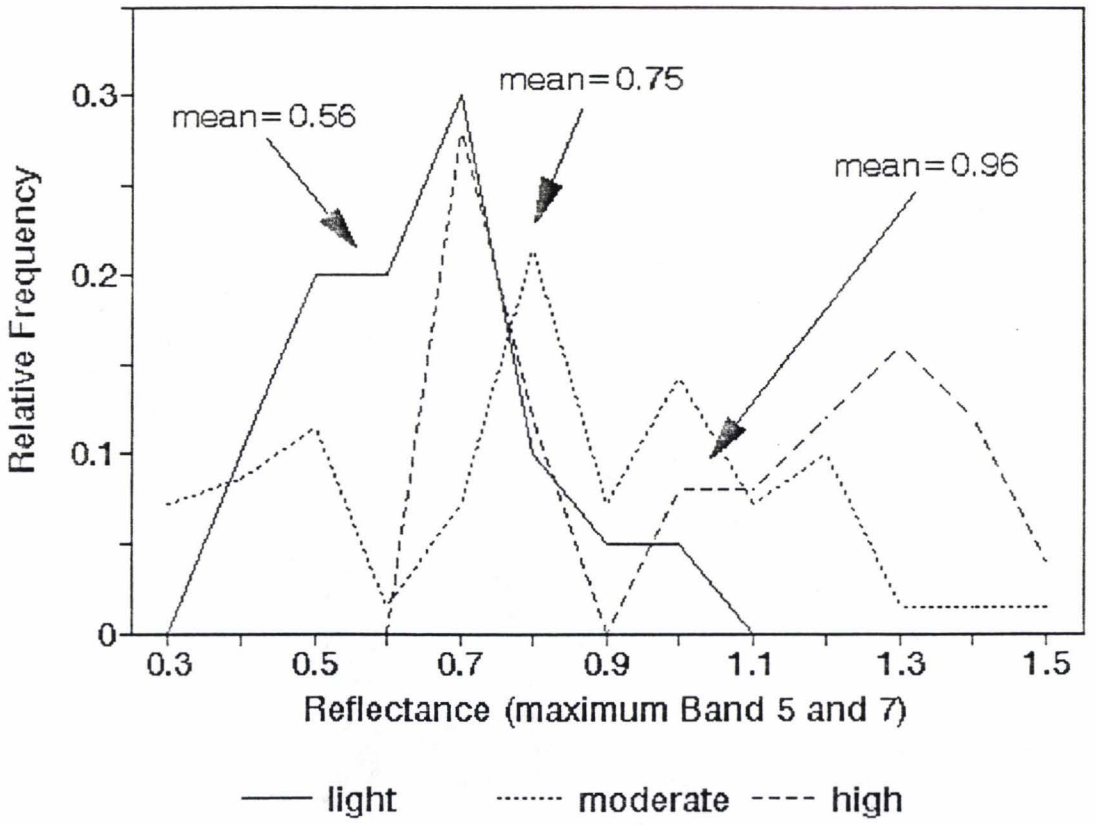

Figure 1 - Relative frequency of MAX(band5,7) values by fire severity class. Mean reflectance values indicated.

and accuracy these data provide are subject to certain limitations. As we have stated, the spectral data could not produce the vegetation map in the desired detail without the combination of a topographic component. The overall mapping accuracy of 70% may be low for some application standards, however, little information was known about the spatial distribution of these forest types. Therefore, while our mapping accuracy is low, our knowledge base about the spatial distribution of these forests has increased.

Satellite data are useful for understanding what effect fire has on a forest because certain spectral wavelengths are more sensitive to the degree of landcover changes outlined in Table 1. The relationship we established between TM bands 5 and 7 and fire severity was expected given that these bands have been shown to be sensitive to sparse vegetation cover (Butera 1986), soil exposure (Ezra *et al.* 1984), and geochemical alteration of soils (Jensen 1986). We anticipated that this relationship was based solely on the immediate effects of the fire on the vegetation communities, however, a full year passed between the fire and the date of the satellite data used for this analysis. During this period, vegetative regeneration occurred which must be included in our evaluation of the relationship between the spectral and severity data. Fire severity greatly influenced the plant communities ability to resprout or seed, degree of canopy degeneration due to cambium and crown scorch, and biophysical environment for plants to re-establish. As a result, the spectral response to fire severity is partly based on the effect of

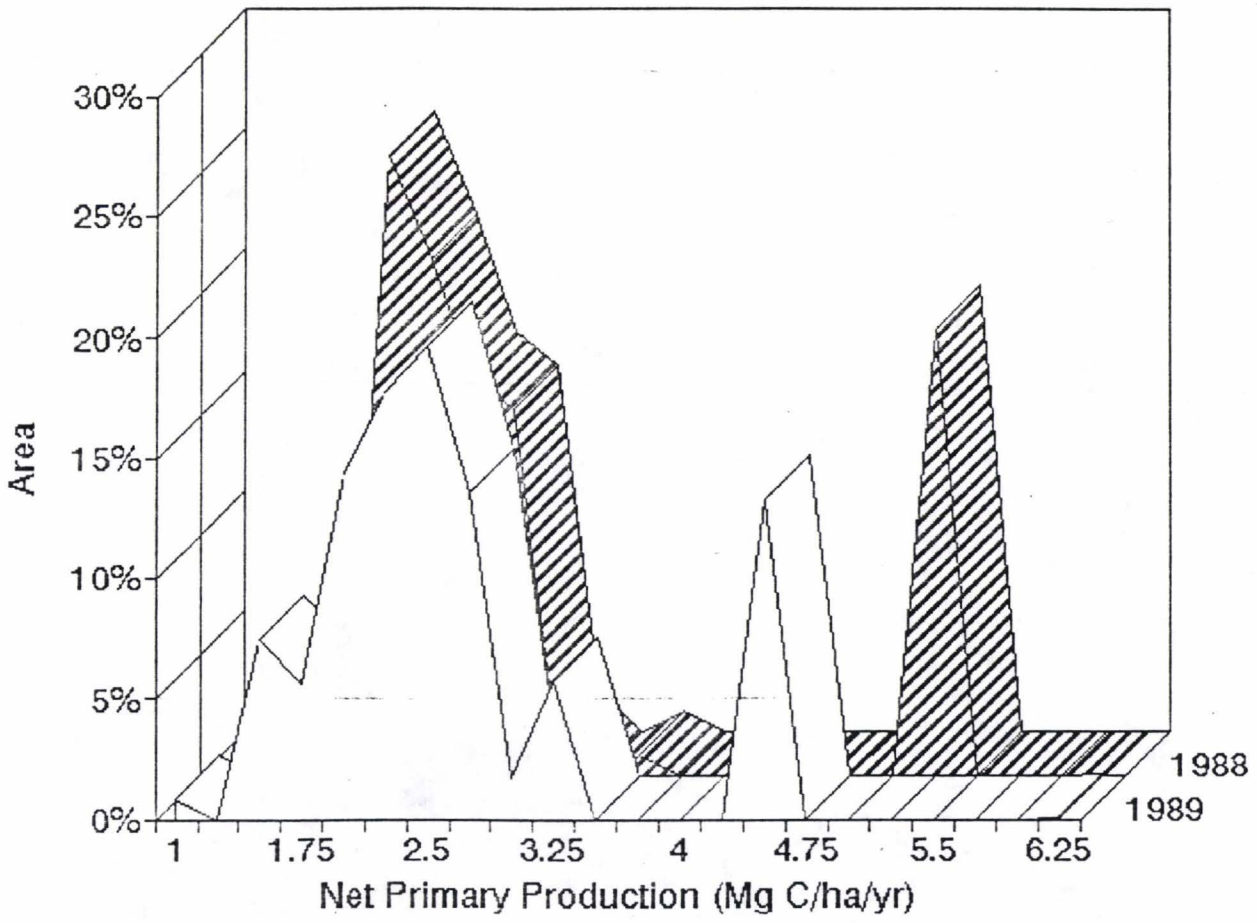

Figure 2 - NPP by percentage of study area for 1988 and 1989 simulations.

the fire on plant regeneration. The spectral response is related to the fire effects on fuels, soils, litter, and vegetation in as much as these characteristics relate to post-fire regeneration. It would be useful to analyze later TM data to understand how this relationship develops with post-fire succession.

The correspondence of the different fire severity maps demonstrates that the spectral mapping procedure presented here is a valuable tool for post-fire analysis of fire severity. The mapping process is an important step for understanding the size and distribution of fire effects. The real significance of this information is realized when it is integrated with other information sources such as the pre-fire vegetation map. This integration reveals broader ecological implications of the fire (Figure 4). This illustrates that most of the forested communities were lightly or moderately burned. The PICO community appears to have more light burn than the other forested areas (65%) which is inconsistent with field observations by Dutton and Cooper. They observed that PICO communities dominated the burn area and that these communities had the most severe burn. The low mapping accuracy of PICO stands (57%) in our pre-fire classification may indicate that we have underestimated the extent of these communities in the burn area. Likewise, the moderate agreement between fire severity maps (68-70%) indicates that size of severely burned forest may be misrepresented. Alternatively, Dutton and Cooper sampled a limited area of the entire burn which could have biased their perception of the overall characteristic of the burn. In this case, the map integration refutes the field observation. In reality, the effect of fire on the Red Bench Fire forests may be represented by an combination of the remotely

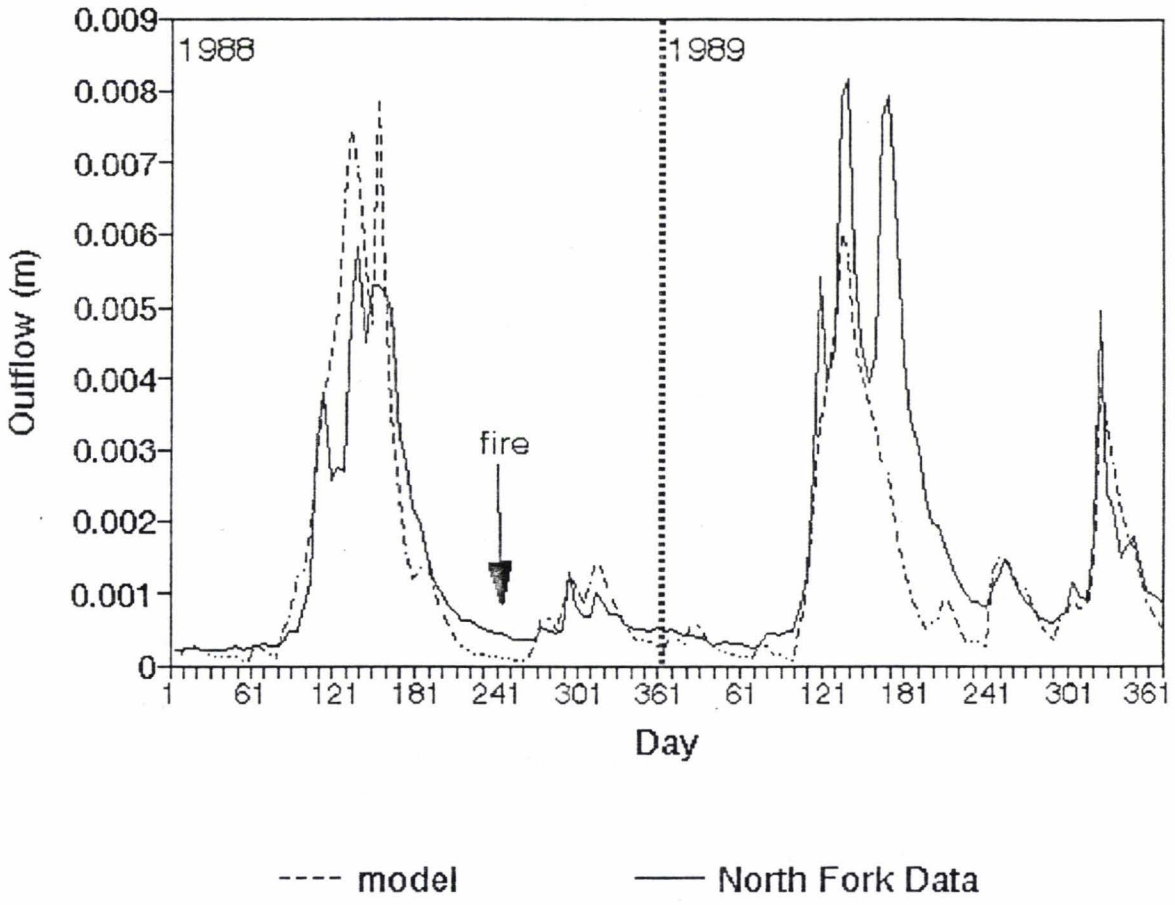

Figure 3 - Modeled and North Fork hydrologic outflow data for 1988 and 1989.

sensed and field information.

Up to this point, we have discussed the use of remote sensing for understanding the effect of fire on the structure and composition of a forested landscape. We used an ecosystem model to assess what effects fire has on the processing of carbon and water within the landscape. As evapotranspiration is in part directly correlated with LAI (McNaughton and Jarvis 1983), hydrologic outflow is inversely related to LAI. By comparing the outflow data from the model with the North Fork stream gauging data, it is possible to understand what effect LAI may have. Following the fire in 1988, three surge events occurred which illustrate that the model overestimated outflow. LAI was assumed to have been completely removed from the burn area during the fire in the model. We cannot determine if the model is representative of the "true" outflow event using our limited observed data. We can assume, however, that the model best represents the change in the landscape and that differences between the model and gauging data are due to other modeling parameterization factors such as climatology or hydrology (Band *et al.* 1991). In 1989, the modeled versus observed outflow data showed a trend on underestimation. This difference may be caused by phenological differences defined in the models. Leaf-on dates in the grassy, burned areas were arbitrarily set to begin on Julian day 120 and quit on day 240 (Running and Hunt 1993). The forested areas remained in leaf throughout the year. Phenology determined the magnitude of outflow as a function of the presence and absence of evapotranspiring leaf area. Between days 100 and 170 in 1989, the model underestimated outflow. The artificial modeled leaf display date

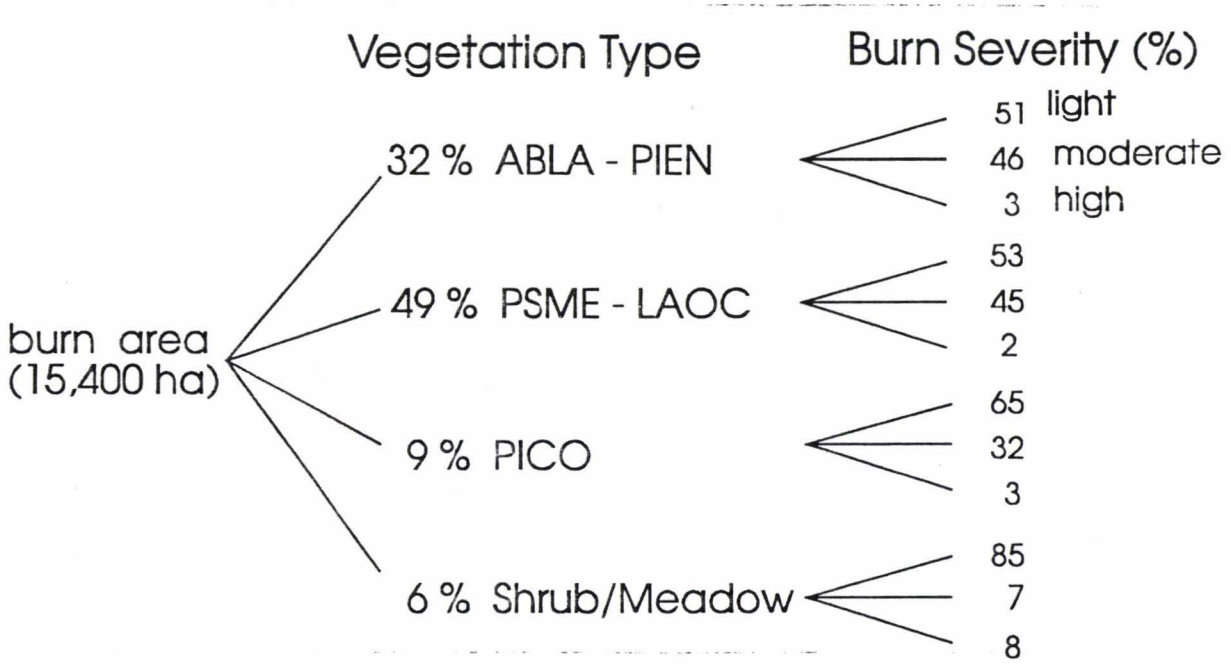

Figure 4 - Definition of burn area by vegetation type and burn severity.

caused leaf area to appear and function before the observed, natural leaf-out of the burned area vegetation. In contrast, between days 315 and 330 of 1989, the model had high correlation with a surge event recorded in the gauging data. During this period, we can assume our judgement about the absence of non-forest leaf area caused an increase in the modeled outflow which is similar to the observed outflow. From this, it is apparent that our model should include a leaf display control as a function of biophysical parameters such as soil temperature and water stress.

Despite differences between the modeled and observed outflow data, our model represents a best guess of the ecological process of water and carbon cycling. This is supported by the MAPE score in which the residual error of the model was only 12.16 percent. From this, we believe our basic assumptions about the burn area which were a) conversion to a grassland in 1989, b) LAI for the grassland derived from NDVI, c) LAI outside the burn area remaining constant between 1988 and 1989 were reasonable. Parameterization of plant physiology and hydrologic components of the model are also important and are affected to the relationship between LAI and outflow.

Coupling remote sensing data and modeling can be used to understand the dynamic relationship between fire and ecological function in this landscape. The minor changes in modeled NPP from 1988 to 1989 despite major changes in vegetation cover demonstrate just how adapted these communities are to fire. Historical records indicate that parts of the Red Bench Fire area have been burned within 20 years. System equilibrium of carbon and water cycling may be rapid in fire-adapted forests and this equilibrium can be represented through modeling means. A synthesis of the fire severity information with ecological modeling may be used to understand the relationship between fire-return frequency, fire severity, post-fire regeneration, and ecosystem processes. Fire management policies may benefit from

evaluation using the remote sensing applications outlined here to determine the result of large, severe fires on the landscape structure and nutrient cycling.

Acknowledgements

The authors of this paper would like express our deep appreciation to the following persons for their expertise and work on this project: Richard Ringleb, Elizabeth Reinhardt, Barry Dutton, Steve Cooper, and Carl Key. We would also like to thank Glacier National Park for their cooperation and logistical help in collecting data. This research was funded in part by an interagency research agreement between the USDA Forest Service, Intermountain Research Laboratory, the National Park Service, and the University of Montana, INT-89440-RJVA.

Literature Cited

Band, L.E., Peterson, D.L., Running, S.W., Coughlan, J.C., Lammers, R., Dungan, J. & Nemani, R. 1991. Forest ecosystem processes at the watershed scale: basis for distributed simulation. Ecological Modeling. 56:171-196.

Benson, A.S., and S.D. DeGloria. 1985. Interpretation of Landsat-4 Thematic Mapper and Multispectral Scanner data for forest surveys. Photogrammetric Engineering and Remote Sensing. 51(9):1281-1289.

Butera, M.K. 1986. A correlation and regression analysis of percent canopy closure versus TMS spectral response for selected forest sites in the San Juan National Forest, Colorado. IEEE Transactions on Geoscience and Remote Sensing. GE-24(1):122-129.

Cibula, W. G. and M.O. Nyquist. 1987. Use of topographic and climatological Models in a geographical data base to improve Landsat MSS classification for Olympic National Park. Photogrammetric Engineering and Remote Sensing. 53(1):67-75.

Earth Resource Data Analysis System Software. 1991. ERDAS, Inc. 2801 Buford Hwy. Atlanta, GA.

Ezra, C.E., L.R. Tinney, and R.D. Jackson. 1984. Effect of soil background on vegetation discrimination using Landsat data. Remote Sensing of the Environment. 16:233-242.

Jakubauskas, M.E., K.P. Lulla, and P.W. Mausel. 1990. Assessment of vegetation change in a fire altered forest landscape. Photogrammetric Engineering and Remote Sensing. 56(3):371-377.

Jensen, J.R. 1986. Introductory digital image processing. Prentice-Hall, New Jersey. 379 p.

Keane, R.E., M.E. Jensen, and W.J. Hann. 1990. ECODATA and ECOPAC: analytical tools for integrated resource management. Compiler. 8(3):24-37.

Kessell, S.R. 1979. Gradient modeling. Springer-Verlag, New York, NY. 432 p.

Key, C. 1988. Map of fire spread over time - Red Bench Fire, Glacier National Park and Flathead National Forest. Glacier National Park Science Center.

Mayer, K.E. and L. Fox III. 1981. Identification of conifer species groupings from Landsat digital classifications. Photogrammetric Engineering and Remote Sensing. 48(11):1607-1614.

McNaughton, K.G. and P.G. Jarvis. 1983. Predicting the effects of vegetation changes on transpiration and evapotranspiration. P. 1-47 In T.T. Kozlowski, ed., Water deficits and plant growth, vol. 7, Academic Press, London.

Milne, A.K. 1986. The use of remote sensing in mapping and monitoring vegetational change associated with bushfire events in eastern Australia. Geocarto International 1. pp. 25-32.

Nemani, R., S.W. Running, L.E. Band, and D.L. Peterson. 1993. Regional hydroecological simulation system: an illustration of the integration of ecosystem models in a GIS. P. 296-304, In M. Goodchild, B. Banks, and G. Steyaert, eds., Integrating GIS and environmental modeling. Oxford, London.

Pankratz, A. 1983. Forecasting with univariate Box-Jenkins models. John Wiley and Sons, New York, NY. 562 p.

Ryan, K.C. and N.V. Noste. 1983. Evaluating prescribed fires. P. 230-238 in Wilderness Fire Symposium, Missoula, MT, Nov. 15-18, 1983. USDA For. Serv. Gen. Tech. Rep. INT-182.

Running, S.W. and E.R. Hunt. 1993. Generalization of a forest ecosystem process model for other biomes, BIOME-BGC, and an application for global-scale models. P. 141-158 In J.R. Ehleringer and C.B. Field, eds., Scaling physiological processes leaf to globe. Academic Press, San Diego.

Schumucker, K.J. 1984. Fuzzy sets, natural language computations, and risk analysis. Computer Science Press, Rockville, MD. 192 p.

Spanner, M.A., L.L. Pierce, D.L. Peterson, and S.W. Running. 1990. Remote sensing of coniferous forest leaf area index the influence of canopy closure understory vegetation and background reflectance. International Journal of Remote Sensing. 11(1):95-111.

White, J.D., G.C. Kroh, and J.E. Pinder III. in press. Mapping forest species at Lassen Volcanic National Park, California, using Landsat Thematic Mapper data and a geographical information system. Photogrammetric Engineering and Remote Sensing.